Development of conformation specific Amyloid-β antibodies

Von der Fakultät für Lebenswissenschaften
der Technischen Universität Carolo-Wilhelmina zu Braunschweig

zur Erlangung des Grades eines
Doktors der Naturwissenschaften
(Dr. rer. nat.)

genehmigte

D i s s e r t a t i o n

von Patrick Bernhard Herbert Droste
aus Haselünne

1. Referent: Professor Dr. Stefan Dübel
2. Referent: Privatdozent Dr. Florian Bittner
eingereicht am: 23.06.2014
mündliche Prüfung (Disputation) am: 24.10.2014

Druckjahr 2014

Table of contents

Table of contents

Table of contents

Summary

Alzheimer's Disease (AD) is the major cause of dementia in the elderly with over 35 million people suffering as of 2012. The total annual costs generated by dementia exceed 600 billion $ and are expected to rise to more than 1,100 billion $ within the next 15 years. The main cause of neurodegeneration in AD is believed to be due to a shift in the equilibrium between production and clearance of amyloid-β (Aβ), a cleavage product of the APP transmembrane protein. When produced in excess, Aβ aggregates to amyloid plaques and causes neuronal dysfunction.

The current diagnosis of AD is performed by cognitive function tests and imaging methods that can only detect advanced neuronal degradation. For an accurate identification of the disease at an early stage it is essential to get a deeper insight view on the biological processes in the brain of Alzheimer patients and monitor the aggregation of Aβ under physiological conditions. Highly selective antibodies that can distinguish between the different forms of Aβ monomers, oligomers and mature fibrils are thought to fill the gap that still exists in the current understanding of AD.

The objective of this work was to generate conformational specific antibodies that fulfill these goals and characterize their biochemical and biophysical properties.

For this, two Aβ42 specific immune phage display libraries were constructed from an immunized macaque (*Macaca fascicularis*) and screened together with two established naive human libraries for selective binders. 8 individual scFvs were obtained, transferred into the scFv-Fc format and produced in mammalian cell culture. 5 antibodies were produced in high enough concentrations for further assay. These scFvs detected different epitopes in Aβ42 and exhibited affinities to various aggregates in the micromolar to nanomolar range. While three of the five antibodies investigated demonstrated a general specificity towards β-amyloid, PaD213-A5 and PaD233-E5 presented a tendency to certain forms of Aβ42. PaD213-A5 is highly specific for mature Aβ42 fibrils and was able to distinguish between various fibrillar structures depending on the acidity of the surrounding milieu during fibrillogenesis while PaD233-E5, albeit

binding also oligomers and fibrils, showed a 100fold increased affinity towards monomers. Further assessment of the impact on aggregation and toxicity *in vitro* determined that PaD97-D6, PaD233-E5 and PaD236-H2 are able to inhibit the formation of Aβ42 fibrils from monomers in a concentration dependent manner and all antibodies were able to rescue the negative effect of Aβ42 on the metabolism of SH-SY5Y cells.

The antibodies generated in this work can be used to examine Aβ42 *in vitro* and show promising potential for further application as therapeutic and diagnostic tools.

1. Introduction

1.1 Antibodies

Antibodies, also termed Immunoglobulins (Ig), are part of the immune system of jawed vertebrates (lat. *gnasthostomata*, subclass of vertebrates) and play an essential role as key modulators in the adaptive immune system.

Synthesized by B-lymphocytes and secreted into the blood plasma during an infection, Immunoglobulins feature two distinct functions: First is the recognition of exogenous, potentially pathogenic substances (termed antigens) with high specificity and affinity and second the activation of other components of the immune system to eliminate these pathogens. Both functions are separated structurally, with the antigen binding by the variable regions at the amino-terminal end of the antibody and the activation of the immune system by the constant regions at the carboxy-terminal end.

All antibodies are heterotetramers and exhibit a conserved basic structure, consisting of two identical heavy (H) and two identical light (L) chains. According to the subtypes of their heavy chain (α, δ, ε, γ and μ) they are divided into 5 classes (isotypes): IgA (α), IgD (δ), IgE (ε), IgG (γ) and IgM (μ). The isotype differ in their effector functions with e.g. activation of the complement system, opsonization or neutralization of toxins. The IgG isotype (figure 1.1) is the predominant form with a content of 80 % of the antibodies in the human blood serum. It has a relative molecular mass (M_r) of appr. 150 kDa with 25 kDa for each light chain and a combined M_r of 100 kDa for the heavy chains. Each heavy chains consist of four different regions: a variable domain V_H and a constant part with three domains C_H1, C_H2 and C_H3 (the isotypes IgE and IgM have an additional C_H4 domain) (Edelman, 1973). The light chain consist as well of one variable domain (V_L) and one constant domain (C_L) and is linked to the heavy chain by a disulfide bond. The light chains are divided into two subgroups, lambda (λ) and kappa (κ), with a ratio of 2:3 (λ:κ) in humans (Abbas, 2007).

Together, the variable domains at the amino-terminal end of the light and heavy chain compose the Fv (fragment variable) region that is the essential part in antibody binding. Both variable domains are composed of four framework and three complementarity determining regions (CDRs). The framework regions span a β-barrel structure, stabilizing the CDRs that make up the paratope of the antibody (Wu and Kabat, 1970). The first constant domains C_L and C_H1 of the light and heavy chain and the Fv-region compose the Fab-fragment (fragment antigen binding) which is connected by the hinge-region to the Fc-part (fragment crystallizable). This section of the IgG consists of the constant domains C_H2 and C_H3 and is essential for the activation of the complement system and in the binding of several other plasma proteins.

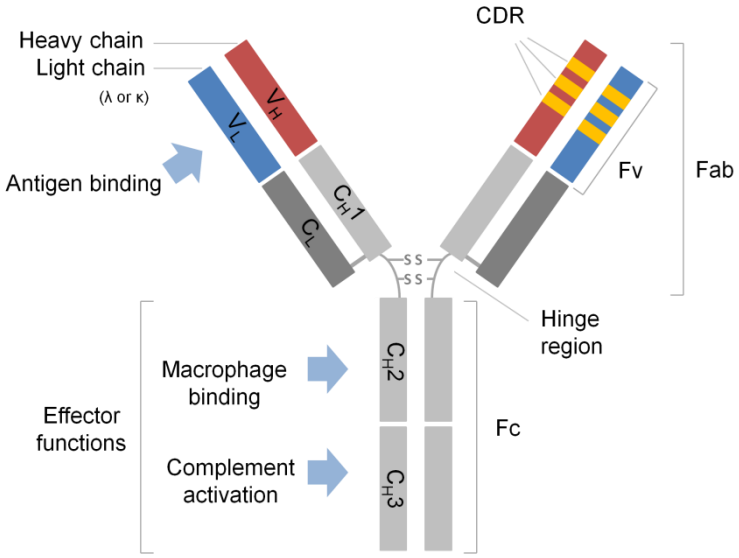

figure 1.1: **schematic illustration of an IgG antibody**
CDR: complementarity determining region, Fab: fragment antigen binding, Fv: fragment variable, Fc: fragment chrystallizable, C_L: constant domain light chain, C_H1-3: constant domains 1-3 heavy chain, V_L: variable domain light chain, V_H: variable domain heavy chain

1.1.1 Recombinant antibody formats

Recombinant antibody formats play a vital role in modern day biotechnology. They are easily produced in prokaryotic hosts and can provide benefits in certain areas of research and therapy due to their smaller size compared to full size Immunoglobulins.
The smallest binding recombinant antibody fragment is the Fv fragment (fragment variable) consisting of the variable domains of the heavy and light chain (V_H and V_L).

The antibody chains are not connected by disulfide bridges or any other covalent bond hence Fv fragments lack stability. This drawback is circumvented in the most frequently used antibody format, the scFv (single chain fragment variable, figure 1.2). Here the variable domains are connected by a 15 - 20 amino acid long, hydrophilic peptide linker (Bird et al., 1988; Huston et al., 1988). The linker most commonly connects the carboxy-terminal end of the V_H with the amino-terminal end of the V_L domain. An arrangement with the connection of the C-terminal end of the V_L with the N-terminal end of the V_H domain is also possible and influences the steric configuration positively (Schmiedl et al., 2000).

Equally essential in this work is another recombinant antibody format, the scFv-Fc format (figure 1.2). Two identical scFvs are connected via the hinge-region to the species-specific Fc-part of an Immunoglobulin, in this work to the Fc-part of a human IgG1, resulting in a bivalent antibody (Moutel et al., 2009). Attributed to the dimerization the scFv-Fc format bears significant advantages regarding a higher stability and apparent affinity.

With a relative molecular mass of 100 kDa scFv-Fc antibodies are smaller than a full size IgG (appr. 150 kDa) but exceed scFvs with a mass of 25 - 30 kDa considerably.

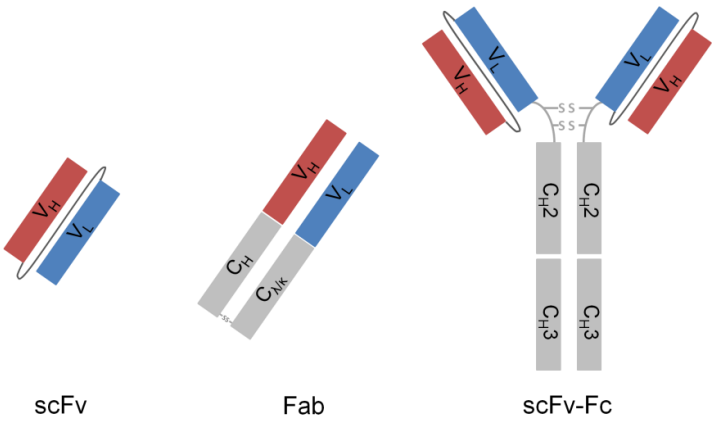

figure 1.2: **schematic illustrations of various antibody fragments**
scFv: single chain fragment variable, monovalent, V_L and V_H connected by peptide linker, Fab: fragment antigen binding, monovalent, light chain is connected to heavy chain by disulfide bonds, scFv-Fc: single chain fragment variable-fragment chrystallizable, bivalent, two scFvs are connected by the hinge region to the Fc-part of an IgG

1.2 Antibody phage display technology

Besides immunization (Behring and Kitasato, 1980) and the hybridoma technology (Köhler and Milstein, 1975), antibody phage display represents an additional robust and effective system for the *in vitro* selection and isolation of recombinant antibodies (Dübel et al., 2010; Hust et al., 2011; Schofield et al., 2007).

Antibody fragments are presented on the surface of filamentous phage coupled to one of the coat proteins and their genetic information is integrated in the phage genome. This physical link of the phenotype and genotype together with the subsequent selection of specific antibodies resembles the natural occurring clonal selection of B-lymphocytes. It allows for the amplification of selective antibodies out of very large antibody gene libraries (Breitling et al., 1991; Clackson et al., 1991)

1.2.1 M13 phage

Bacteriophage, or phage in short, were first described in 1917 by Felix D'Herelle (D'Herelle, 1917) and are viruses that solely infect bacteria. The filamentous phage M13, f1 and fd are bacteriophage belonging to the family of Inoviridae with a genome composed of single strand, circular DNA (ssDNA) (Ray et al., 1966). The M13 phage (figure 1.3) used in this work is approximately 600 - 2000 nm in length, 8 nm wide (Marvin, 1998) and is resistant to high temperatures and proteolytic digestion with trypsin (Breitling and Dübel, 1997).

The genome of the M13 phage has a size of 6.5 kb and codes for a total of 11 genes. Three of these are necessary for DNA replication and the assembling of the phage particles respectively while the remaining five genes code for the phage proteins. With around 2700 copies the pVIII is the main coat protein and is makes up the tubular structure. The minor coat protein pIII is at the front-end of the phage and facilitates the binding of the phage particle to the f-pilus of *E. coli* (Henry and Pratt, 1969). Because the infection is f-pilus driven only bacteria carrying an f-plasmid are infected. The host cell then releases ca. 200 phage particles per cell cycle, limiting its growth by up to 50 % but not being destroyed by the phage (Barbas et al., 1991).

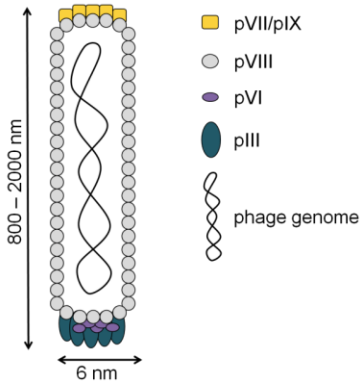

figure 1.3: **schematic illustration of an M13 phage**
pIII, pVI, pVII, pVIII and pIX are phage proteins

1.2.2 Antibody phage display

The main principle of phage display is the presentation of a protein or peptide on the phage surface by fusing the heterologous molecule to a coat protein (Smith, 1985). In this work scFvs were linked to the minor coat protein pIII at the front-end of the phage. Linkage to other phage proteins is also possible.

The genetic information of this antibody phage particle fusion protein is integrated into the phage genome (McCafferty et al., 1990) or coded on a phagemid (Barbas et al., 1991; Breitling et al., 1991; Hoogenboom et al., 1991) (figure 1.4). Next to the gene for the antibody-pIII fusion protein, these phagemids contain the genetic information for the replication and selection in *E. coli* as well as an origin of replication that enables the packaging of the phagemid (Hust and Dübel, 2005). All other proteins that are essential for the packaging process are encoded in the genome of a helperphage. Another important aspect is the signal peptide which facilitates the secretion of the antibody to the periplasm of the bacteria. The oxidative milieu allows for the generation of disulfide bonds which are important for the proper folding of the scFv (Thie et al., 2008). The expression of the scFv-pIII fusion protein is not consecutive but regulated by an inducible *lac*-promoter (Breitling and Dübel, 1997).

The wildtype pIII of the helperphage and the antibody-pIII fusion protein compete for the integration onto the phage surface which results statistically in one scFv being presented on the phage (Chasteen et al., 2006). This monovalent display can be circumvented by using modified helperphage (e.g. Hyperphage) that carry a partially

deleted gIII (codes for the pIII protein) (Rondot et al., 2001; Soltes et al., 2007). Hence the antibody-pIII fusion protein is the sole source for the pIII during phage assembly which results ultimately in a polyvalent display.

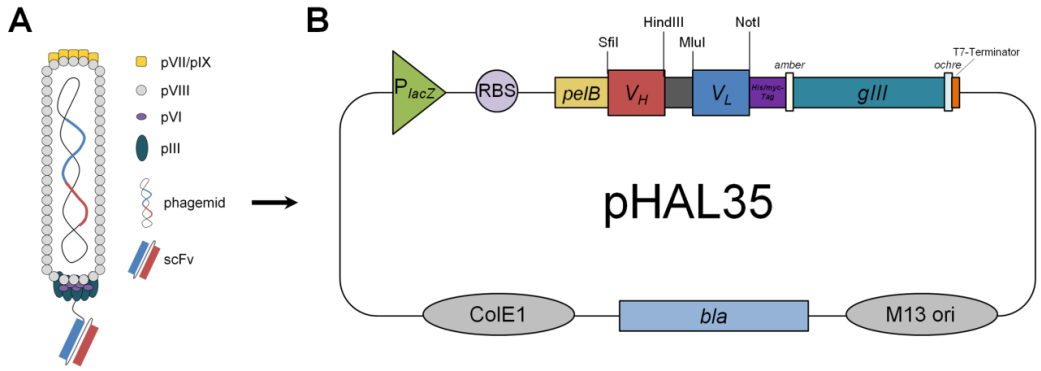

figure 1.4: **schematic illustration of an M13 phage and the pHAL35 phagemid**
(A) M13 phage with scFv fused to the pIII minor coat protein, pIII, pVI, pVII, pVIII and pIX are phage proteins, **(B)** pHAL35 phagemid, PlacZ: inducible *lacZ*-promoter, RBS: ribosomal binding site, pelB: gene of the signal peptide, V_H: gene of the variablke domain of the heavy chain, V_L: gene of the variable domain of the light chain, HIS- and Myc-TAG for purification and detection of the scFv, amber: stop codon UAG, ochre: stop codon UAA, gIII: gene for pIII, M13 ori: phage packaging signal, bla: gene for β-lactamase (marker for selecion), ColE1: origin of replication for *E. coli*

1.2.3 Antibody gene libraries

Antibody gene libraries are collections of phage that comprise the genetic information of a vast variety of different antibodies and present the proteins on their surface. They are established by extraction of the genetic information for the antibodies from B-lymphocytes of host organisms by PCR amplification and subsequent integration into a phagemid system (figure 1.5). These libraries can be divided into two main groups: immune and universal antibody gene libraries.

Immune antibody phage display libraries are derived from the IgG repertoire of immunized hosts that already underwent a primary and secondary immune response. This guarantees for the presence of a large number of specific and affinity matured antibodies against a certain antigen while on the other hand antibodies targeting antigens not utilized during the immunization process are very limited in the library. The restriction to the solely amplification of IgGs results in a lower diversity of 10^6 - 10^7 individual antibodies (Clackson et al., 1991).

Universal antibody gene libraries are based on the gene repertoire of IgM antibodies of non immunized hosts and have a diversity of 10^8 - 10^{10} individual antibodies (Vaughan et al., 1996; de Haard et al., 1999; Hust et al., 2011). Due to the involvement of the IgM molecules in the primary immune response and the resulting extremely large diversity of the libraries it is theoretically possible to obtain antibodies targeting nearly any antigen (Marks et al., 1991; Griffiths et al., 1993). Universal antibody gene libraries can be subdivided into three groups: synthetic, semi-synthetic and naive libraries. While naive libraries consist of the original host antibodies with a rearranged combination of the V_L and V_H domains, semi-synthetic libraries include artificial sequences, e.g. alterations in CDR3 (Hoogenboom and Winter, 1992; Pini et al., 1998; Goletz et al., 2002; Hoet et al., 2005). Synthetic libraries include fully randomized CDRs with defined framework regions resulting in very high diversities of 10^{10} - 10^{11} individual clones (Hayashi et al., 1994; Knappik et al., 2000; Tiller et al., 2013).

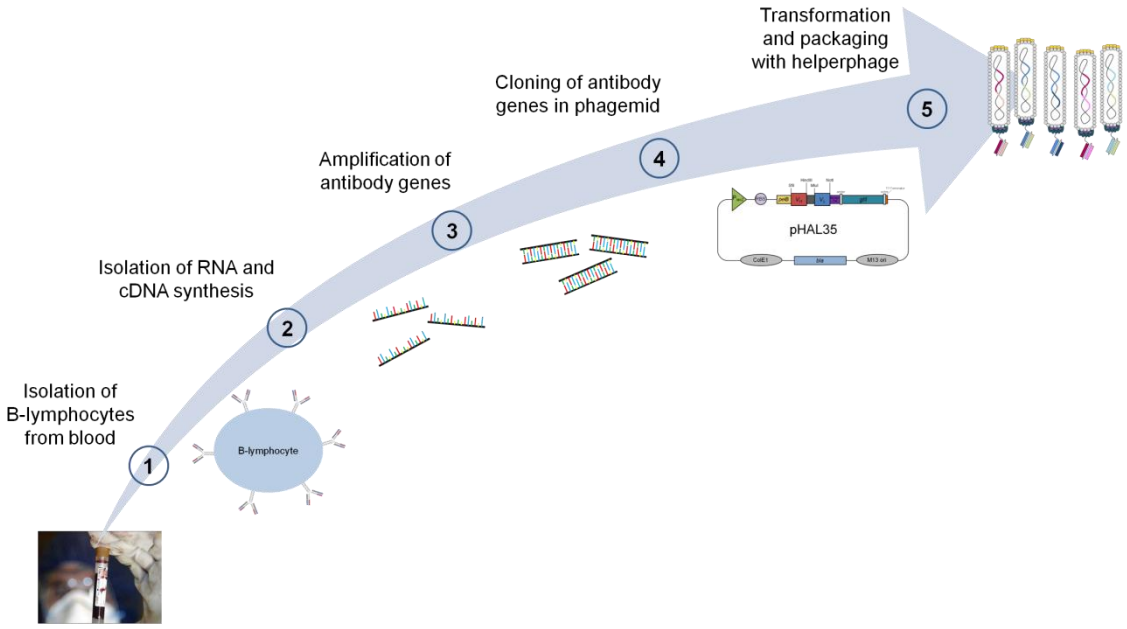

figure 1.5: schematic overview of the generation of antibody gene libraries

1.2.4 Antibody phage selection ("panning")

The phage display technology represents a powerful tool for the *in vitro* selection of highly specific antibodies from complex antibody gene libraries. The name "panning" derives from the gold panners process of washing out gold nuggets from the river bed gravel.

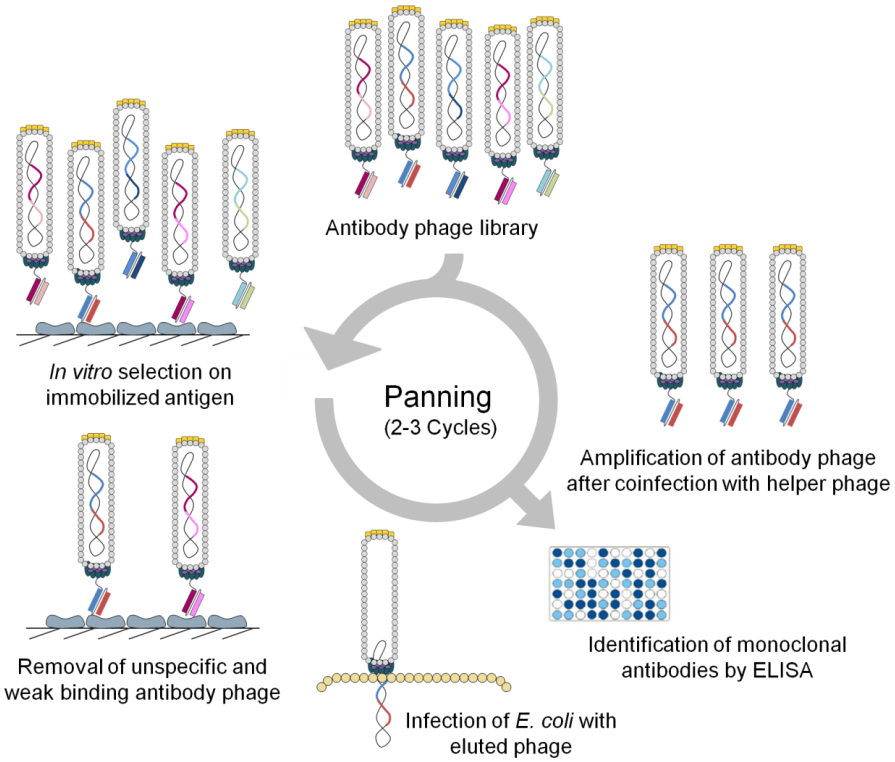

figure 1.6: **schematic illustration of the antibody selection process ("panning")** generally after 3 rounds potential binders are identified by ELISA

For the antibody selection process (figure 1.6) the target antigen is either immobilized on a stationary phase like immunotubes (Hust et al., 2002), micro titre plates (Barbas et al., 1991) or magnetic beads (Hawkins et al., 1992) or it is in solution during the incubation and subsequently being separated by a pull down (Schütte et al., 2009). During the following incubation of the antibody phage library on the antigen, adjusting parameters like pH or temperature, or competition with unwanted proteins and peptides lead to antibodies with the desired biochemical characteristics. Unspecific phage are removed by washing and the antibody phage that detected the target antigen properly are eluted either enzymatical with trypsin or by shifting the pH (Barbas et al., 1991).

These eluted phage can be used for an infection of *E. coli* cells. Addition of helperphage to the infected bacteria facilitates the amplification of antibody phage which then can be used for continuous panning rounds. Usually, this "panning process" is repeated 2-3 times to accumulate specific binders which are being identified after soluble production by ELISA.

1.3 Alzheimer's Disease

Alzheimer's Disease (AD) is a slowly progressing, irreversible neurodegenerative disorder and the most common form of dementia in the elderly today. In 2012, 35.6 million people worldwide and 1.4 million in Germany alone suffered from dementia with between 60 - 80 % of these cases being attributed to AD. With 7.7 million new cases every year and a survival time after diagnose of 7.1 years (Fitzpatrick et al., 2005) these numbers will most likely more than triple with 115 million people by 2050. The total costs of dementia currently exceed 600 billion $ and are estimated to rise to 1,117 billion $ as early as 2030 (www.who.int, www.deutsche-alzheimer.de, world alzheimer report 2013). These number set the ground for the urgent need of diagnostic and therapeutic tools in AD that target the disease progression at an early stage.

The symptoms were first described by Alois Alzheimer with his patient Auguste Deter in the early years of the last century (Alzheimer, 1907). He was also the first who detected the lesions in the brain that are still today the histological hallmarks of AD: amyloid (senile) plaques and neurofibrillary tangles (NFTs). It took almost 80 years of advancement in biological methods to learn about the composition of these accumulations, with intracellular NFTs being aggregates of hyperphosphorylated Tau (Goedert et al., 1988; Kosik et al., 1986) and the extracellular amyloid plaques consisting of Aβ peptides (Glenner and Wong, 1984; Masters et al., 1985; Selkoe et al., 1986).

Modern diagnosis of AD is based on a combination of cognitive tests and imaging techniques like x-ray computed tomography (CT), positron emission tomography (PET), or magnetic resonance tomography (MRT) that together with dyes like Pittsburg compound B (PIB) can detect amyloid fibrils in the brain. Since there is no definite

correlation between the amount of amyloid plaques and memory impairment (Rowe and Villemagne, 2011) more precise diagnostic tools are highly desirable.

Currently, there are no techniques to detect AD before neuronal impairment sets in and *post mortem* investigations of brain matter with NFTs and senile plaques are today the only method to identify AD with 100 % accuracy (Ballard et al., 2011).

The key challenge is to detect AD at a presymptomatic stage to be able to slow down or even stop the disease's progression. Conformational antibodies that target biomarkers such as Aβ oligomers or phosphorylated Tau protein with high specificity and selectivity in cerebrospinal fluid (CSF) or plasma can be a giant leap forward in the fight against AD.

1.3.1 APP processing and amyloid-β production

Amyloid-β peptides are the result of a sequential processing of the amyloid precursor protein (APP). The genetic information for APP is located on the long arm of chromosome 21 and due to alternative splicing the protein exists in nine different isoforms with APP695 being the one predominantly expressed in neurons (Zheng and Koo, 2006).

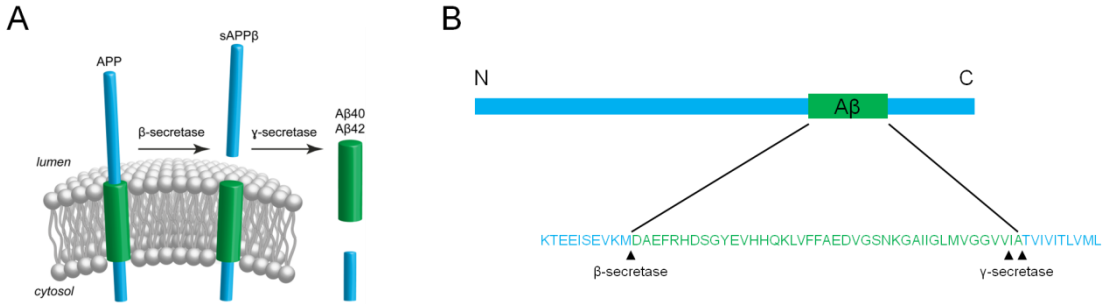

figure 1.7: **processing of APP to amyloid-β**
(A) schematic illustration of the cleavage of APP (Bereza, 2013), **(B)** overview of β- and γ-secretase cleavage sites in the sequence

APP is a type I transmembrane protein that consists of a large ectodomain at the N-terminal end, a transmembrane domain (TMD), and a small cytoplasmic domain at the C-terminal end and is cleaved by three different proteinases located in the membrane termed α-, β- and γ-secretase. The initial cleavage by α- or β-secretase discards nearly the whole ectodomain and leaves a carboxy-terminal fragment (CTF) in the membrane

that is further processed by the γ-secretase and released from the membrane as p3 or Aβ. Depending on the secretases APP is processed either in a non-amyloidogenic or an amyloidogenic manner. With regards to AD the amyloidogenic pathway is of main interest since it results in the production of Aβ40 and Aβ42 (figure 1.7), the peptides considered to be causing the neuropathology of AD.

Here, the initial cleavage is carried out by the β-secretase (β-site APP cleaving enzyme, BACE1) between the amino acids M596 and D597 (isoform APP695) (Sinha et al., 1999) resulting in the soluble ectodomain sAPPβ and the cell associated β-C-terminal fragment with a size of 99 amino acids, hence the term β-CTF or C99.

The γ-secretase is involved in the next processing steps, cleaving the C99 stepwise to the amyloid-β peptide. These peptides are various in length with the majority being either 40 or 42 amino acids long. The heterologous outcome is due to various neighboring cleavage sites for the γ-secretase. Nearly 90 % of the generated Aβ peptides are Aβ40 and about 5 - 10 % are Aβ42 (Jakob-Roetne and Jacobsen, 2009). After γ-secretase cleavage the intracellular domain of APP (APP intracellular C-terminal domain, AICD) is discharged into the cytosol and the 4.5 kDa Aβ peptide is secreted into the extracellular space.

1.3.2 The amyloid cascade hypothesis and aggregation of amyloid-β

The amyloid cascade hypothesis is an approach to combine the diverse findings along the way from Aβ production to the clinical symptoms in the end (figure 1.8). It was first described in the early 1990s that the accumulation of amyloid-β is the causative agent of the pathology in Alzheimer's Disease (Hardy and Higgins, 1992).

Changes in the Aβ metabolism lead to an imbalance between elevated production and decreased clearance and a concentration shift that facilitates self aggregation of β-amyloid. These events trigger molecular and cellular alterations that lead to synaptic failure and neuronal injury which precede formation of amyloid plaques and neurofibrillary tangles (NFTs) and ultimately dementia.

While plaques and β-amyloid fibrils were regarded as the cause for neuronal dysfunction in AD in the beginning, the hypothesis was later revised to implicate

soluble Aβ oligomers as the main neurotoxic form (Haass and Selkoe, 2007; Selkoe, 2008).

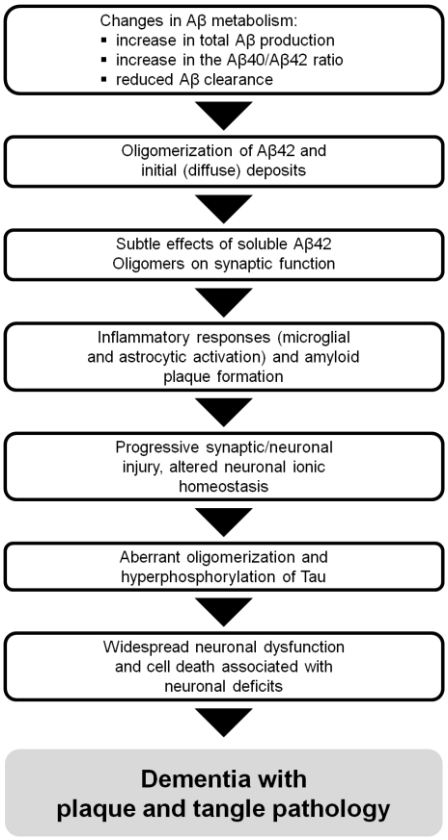

figure 1.8: the amyloid cascade hypothesis of AD
(Haass and Selkoe, 2007)

Once a critical concentration is surpassed, amyloid-β aggregation follows a nucleation-dependent polymerization process (figure 1.9, A) (Harper and Lansbury, 1997; Jarrett et al., 1993) . This process can be divided into three distinct stages:

1. lag phase: Aβ monomers interact to form small Oligomer assemblies/seeds termed "nuclei" which serve as starting points for fibrillization. These clusters are thermodynamically unstable and disintegrate rapidly
2. growth phase: Addition of free monomers to the growth end of the Oligomer "nuclei" results in a rapid elongation into Aβ fibrils
3. steady state phase: Aβ fibrils are in an equilibrium with the remaining Aβ monomers (which don't exceed the critical concentration)

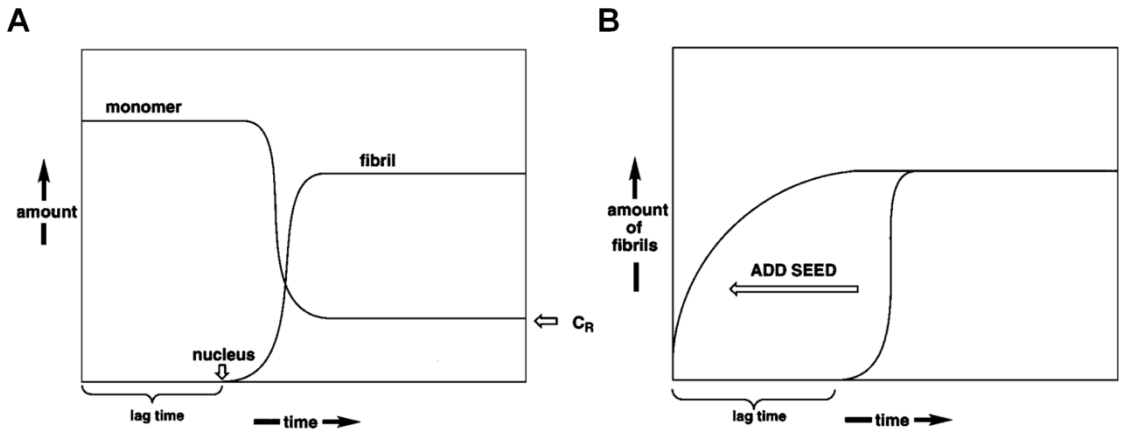

figure 1.9: **nucleation-dependent polymerization process**
(A) after the initial lag time rapid aggregation occurs until fibrils and monomers are in an equilibrium and monomer concentration is below the critical concentration (C_R), **(B)** addition of seeds eliminates lag time, (Harper and Lansbury, 1997)

The rate limiting step during Aβ aggregation *in vitro* is the formation of the nuclei or seeds. Addition of seeds in the form of stable β-amyloid aggregates (e.g. fibrils) it completely eliminates the lag time and induces Fibril formation immediately (figure 1.9, B) (Harper and Lansbury, 1997).

1.3.3 Morphology of amyloid-β aggregates

There are a multitude of different Aβ aggregates that have been identified so far (figure 1.10). The smallest occurring forms are monomers. Aβ40 and Aβ42 are 40 and 42 amino acids in length with Aβ42 having two additional amino acids at the C-terminus. These amino acids (isoleucine and alanine) contribute to the hydrophobic character of the carboxy-terminal end of Aβ42. On the other hand, the N-terminal segment is hydrophilic giving the peptide an amphipatic character all together. These segments are consistent with the predicted distribution with $Aβ_{1-28}$ being part of the extracellular APP domain whereas $Aβ_{29-42}$ is part of the TMD (Finder and Glockshuber, 2007).

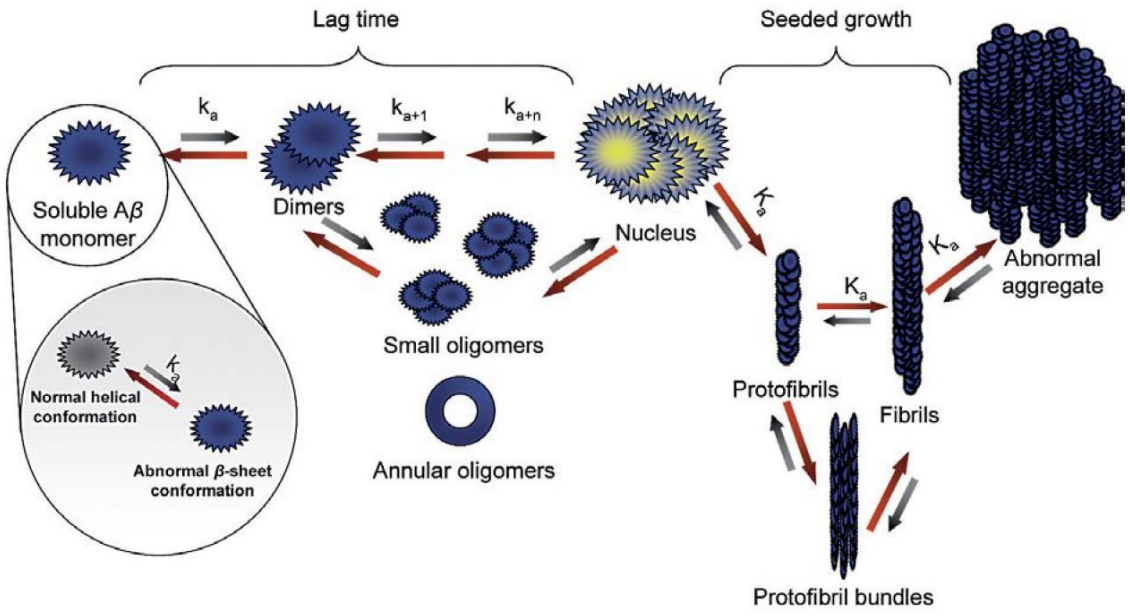

figure 1.10: **schematic illustration of amyloid-β aggregation**
Aβ monomers aggregate to form Nuclei including small oligomers and Annular oligomers during the lag-phase, followed by a rapid transition into protofibrils and mature fibrils, (Finder and Glockshuber, 2007)

The next larger aggregate are Dimers (Garzon-Rodriguez et al., 1997; Roher et al., 1996), followed by oligomers that differ greatly in their structural appearance and size. Ranging from 3 - 50 monomers, oligomers occurring *in vivo* exhibit a heteromorphous, transient, and unstable nature and are in the center of investigation on being the most cytotoxic type of β-amyloid aggregates (Bitan et al., 2005; Cleary et al., 2005; Dahlgren, 2002; Lesné et al., 2006; Walsh et al., 2002). Another form of small oligomers are Aβ-derived diffusible ligands (ADDLs). These nonfibrillar, neurotoxic 3 - 24mers have been observed in murine and human brain extracts (Klein, 2002; Lambert et al., 1998) and morphologically resemble ring shaped protofibrils (Harper et al., 1999). Other aggregates include protofibrils and annular, pore-like oligomers. Annular oligomers have been observed *in vitro* and are being hypothesized to deliver their pathogenicity by membrane disruption (Lashuel et al., 2002). Protofibrils are the last stage before the final transition into mature fibrils and are ordered structures between 8 - 200 nm in length. This rod-shaped specie was observed *in vitro* and *in vivo* in AD patients and mice, can be stained by congo red and thioflavin T suggesting a high β-sheet content (Harper and Lansbury, 1997; Walsh et al., 1997) and displays toxicity (Hartley et al., 1999; Jan et al., 2010a). Protofibrils seem to be in an equilibrium with

smaller oligomers and monomers (Jan et al., 2008) and can be converted into mature fibrils by addition of monomers at the growth ends (Harper and Lansbury, 1997). The next stage in β-amyloid aggregation are fibrils later accumulating into amyloid plaques (Müller-Hill and Beyreuther, 1989). Aβ fibrils were detected in AD patients and mouse models as well as *in vitro* (Klunk et al., 2004) and are insoluble, thermodynamically stable entities composed of an ordered set of Aβ monomers (Ross and Poirier, 2005). Like protofibrils mature fibrils can also being stained by congo red or thioflavin T (Klunk et al., 1999; LeVine, 1999) due to the cross β-sheet structure that all amyloid fibrils share (Fändrich, 2007).

1.3.4 Conformation specific antibodies in AD

To differentiate between diverse Oligomer intermediates along the fibrillization pathway of Aβ it is essential to apply highly selective methods. Conformation specific antibodies that can distinguish between e.g. small oligomers and protofibrils are able to fill this existing gap. These antibodies do not detect a distinct sequence of amino acids but rather tertiary and quaternary structures.

So far there have been described a couple of antibodies that bind only to certain forms of Aβ aggregates, among others A11 and A-887755 detecting oligomers (Hillen et al., 2010; Kayed et al., 2003), mAb158 detecting protofibrils and fibrils (Englund et al., 2007), OC detecting oligomers and fibrils (Kayed et al., 2007) and WO1 and WO2 detecting fibrils (O'Nuallain and Wetzel, 2002). Some antibodies, while being specific only for fibrils with Aβ aggregates, detect fibrils of other amyloid proteins as well (O'Nuallain and Wetzel, 2002). This was also found for amyloid-β Oligomer specific antibodies that stained oligomers of α-synuclein and IAPP (Kayed et al., 2007). Sometimes, antibodies while binding all forms of Aβ, exhibit a stronger affinity towards certain aggregates (Habicht et al., 2007; Lafaye et al., 2009; Zameer et al., 2008). Such findings gave rise to the idea that oligomers and fibrils of amyloidogenic peptides expose a generic structural motif like the cross β-sheet structure in fibrils that is detected by amyloid specific antibodies (Dumoulin and Dobson, 2004; Glabe and Kayed, 2006; O'Nuallain and Wetzel, 2002).

Antibodies that exhibit high selectivity for defined Oligomer aggregates of Aβ42 while at the same time show no cross reactivity with further forms of Aβ and other amyloidogenic peptides have yet to be generated.

1.4 Objectives of this study

The aim of this work is to generate conformational specific Aβ42 antibodies that can discriminate between different forms of Aβ42 such as monomers, oligomers and mature fibrils. The further characterization of these binders will cover the aspects of specificity, affinity and their potency to inhibit fibrillogenesis.

Initially, two amyloid-β specific phage display antibody gene libraries are being established and subsequently screened, together with two previously generated naive libraries (Hust et al., 2011), using the phage display technology. After obtaining a panel of different scFvs these antibodies will additionally be converted into the scFv-Fc format to further examine possible effects attributed to the bivalent format on the fibrillogenesis of and the specificity towards Aβ42. All antibody formats will be produced in HEK293-6E cells and purified. Further investigation of the antibodies include their tendency to bind to other amyloidogenic peptides and their exact specificity towards different forms of aggregated and amyloid-β oligomers as well as monomers and mature fibrils. Additional characterizations include epitope mapping and affinity measurements.

After establishing the ground parameters with biochemical and biophysical methods, *in vitro* studies on the inhibition of fibrillization and the disruption of preformed amyloid-β fibrils are to follow. The results obtained in these experiments are going to be verified subsequently in SH-SY5Y cells regarding the impact on Aβ42 induced cytotoxicity thus providing an insight on the efficacy of the antibodies.

2. Material

2.1 Devices and technical equipment

During the course of this work the following devices and technical equipment were used (table 2.1).

table 2.1: devices and technical equipment with model name and manufacturer

Device	Model	Manufacturer
Balances	Laboratory LC 6200 D E 1200 S A 120 S	Sartorius, Göttingen
Blotting device	Trans Blot SD	BioRad, München
Centrifuges	5414 D 5810 R Heraeus Multifuge 3 S-R Sorvall RC5B Plus Sorvall RC6 Plus Sprout	Eppendorf, Hamburg Eppendorf, Hamburg ThermoFisherScientific, Offenbach ThermoFisherScientific, Offenbach ThermoFisherScientific, Offenbach Heathrow Scientific, Illinois (USA)
Chromatography system	Äkta-Prime	GE Healthcare, München
Dry bath incubator	Thermomixer *comfort* Thermomixer *compact*	Eppendorf, Hamburg
Electrophoresis device	40-0708 Mini Protean III	PeQLab, Erlangen BioRad, München
ELISA reader	Tecan SUNRISE Tecan Ultra	Tecan, Crailsheim
ELISA washer	Columbus Plus	Tecan, Crailsheim
FACS	Accuri C6	BD Bioscience, Allschwil (Switzerland)
Filtration unit	Columbus Plus	Tecan, Crailsheim
Fluorescence microplate reader	Analyst AD	Molecular Devices (Switzerland)

Device	Model	Manufacturer
Freezer	Herafreeze	Thermo Fisher Scientific, Offenbach
Gel documentation device	Gel Jet Imager	Intas, Göttingen
Incubators	Typ BE400	Memmert, Schwabach
MTP shaker	Titramax 101	Heidolph Instruments, Schwabach
MTP shaking incubators	Thermo Shaker PST-60H-4	Lab4you, Berlin
pH-meter	CG810	Schott, Mainz
Pipettes	Research Multipette Plus *e*1200	Eppendorf, Hamburg Eppendorf, Hamburg BIOHIT, Helsinki (Finnland)
Pipettor	Accu-jet	Brand, Wertheim
Power supplies	EPS 301 und 601	GE Healthcare, München
Protein purification	Profinia Purification	BioRad, München
Rotors	SS34 (Sorvall) F9S-4×1000y F12S-6×500y F21-8×50	ThermoFisherScientific, Offenbach FIBERLite, Santa Clara (USA) FIBERLite, Santa Clara (USA) FIBERLite, Santa Clara (USA)
Shaking incubators	Certomat BS-1 Minitron Multitron	Braun, Melsungen Infors HT, Bottmingen (Schweiz) Infors HT, Bottmingen (Schweiz)
Spectrophotometer	ND1000 Libra S11 Cary 100 UV-Vis	PeqLab, Erlangen Biochrome, Cambridge (England) Agilant Technologies, Basel (Switzerland)
SPR analyzer	BIAcore2000™	GE Healthcare, München
Suction pump	ISM 832	Ismatec, Glattbrugg (Schweiz)
TEM	Tecnai G2 Spirit	FEI, Oregon (USA)
Thermocycler	PTC-200	MJ Research, Waltham (USA)
Ultrapure water filtration	Arium 611	Sartorius, Göttingen
Vacuum pump	Laboport	KNF Neuberger, Freiburg
Vortex mixer	Vortex Genie 2	Scientific Industries, NewYork (USA)
Water bath	Wasserbad GFL	Laborbedarf, Braunschweig
Work bench	MSC-Advantage HERAsafe	ThermoFisherScientific, Offenbach ThermoFisherScientific, Offenbach

2.2 Consumables

Consumables used in this work are listed in table 2.2.

table 2.2: consumables with type and manufacturer

Material	Type	Manufacturer
BIAcore chips	CM5 CMD50m	GE Healthcare, München Xantec Bioanalytics, Düsseldorf
Combitips plus	1.0 mL	Eppendorf, Hamburg
Filter	0.2 µm; 0.45 µm, 0.8 µm	Sartorius, Göttingen
Filter paper	3 mm	BioRad, München
Micro titer plates	96well, Costar, 9018 96well, Maxisorp 96well	Corning, New York (USA) Nunc, Wiesbaden Greiner Bio-one, Frickenhausen
Microtiter plate covers	AeraSeal, SealPlate	Excel Scientific, Wrightwood USA
Nitrocellulose membrane		Carl Roth, Karlsruhe
PCR reaction tubes		Sarstedt, Nümbrecht
Petri dish	7 cm	Greiner Bio-one, Frickenhausen
Pipette tips		Sarstedt, Nümbrecht
PVDF membrane	T830.1	Carl Roth, Karlsruhe
Reaction tubes	1.5 mL, 2 mL 15 mL, 50 mL	Sarstedt, Nümbrecht Corning, New York (USA)
Screw cap tube	2 mL	Sarstedt, Nümbrecht
Serological pipettes	2.5 mL, 5 mL, 10 mL; 25 mL	Corning, New York (USA)
Shaking flasks	125 mL (Polycarbonate)	Corning, New York (USA)
Spatulas	L-shape	VWR, Darmstadt
TEM grids	FCF200-Cu	EMS, Hatfield (USA)
Tissue culture flask	75 cm^2, 150 cm^2	TPP, Trasadingen (Switzerland)
Tissue culture plates	BD Falcon, 24well	Corning, New York (USA)

2.3 Chemicals and reagents

The chemicals and reagents used in this work are summarized in table 2.3. If not listed, these items met the necessary levels of purity and were obtained from the following companies: AppliChem (Darmstadt), BD (Sparks, USA), Carl Roth (Karlsruhe), GE Healthcare (München), MBI Fermentas (St. Leon-Rot), Merck (Darmstadt), Riedel-de Häen (Sarstedt), Roche (Mannheim), Fluka/Sigma-Aldrich (Neu-Ulm) and Serva (Heidelberg).

table 2.3: chemicals and kits with manufacturer mentioned

Product	Manufacturer
25 mM $MgCl_2$	MBI Fermentas, St. Leon-Rot
Affinity chromatography	BioRad, München
SUPrA™ Bio-Scale™ Mini Desalting Cartridge	
SUPrA™ Bio-Scale™ Mini UNOsphere	
BIAcore amine coupling Kit	GE Healthcare, München
CM5 chip	
Ethylene dichloride (EDC)	
N-Hydroxysuccinimide (NHS)	
HBS-EP-Puffer (10×)	
DNA loading buffer (6×)	MBI-Fermentas, St. Leon-Rot
DNA marker	MBI-Fermentas, St. Leon-Rot
GeneRuler™ 1kb DNA Ladder Plus	
DNA purification kits	
Nucleo Spin Extract II (PCR)	Macherey-Nagel, Düren
Nucleo Spin Plasmid (Miniprep)	Macherey-Nagel,Düren
Nucleobond® Xtra (Midi/Maxi)	Macherey-Nagel, Düren
peqGOLD Plasmid Miniprep Kit I	PeqLab, Erlangen
dNTPs	MBI-Fermentas, St. Leon-Rot
Desalting column	BioRad, München
Enzyme buffer	
GoTaq® buffer (5×)	Promega, Mannheim
Phusion buffer (5×)	NEB, Frankfurt a. M.
Buffer 1–4 for endonucleases	NEB, Frankfurt a. M.
T4-DNA ligase buffer	Promega, Mannheim
Protein marker	
Precision Plus Protein™ Unstained Standard	BioRad, München
Precision Plus Protein™ DualColor Prestained Std.	BioRad, München
PageRuler Prestained Protein Ladder	ThermoFisherScientific, Offenbach

Product	Manufacturer
SEC columns	
TSKgel G4000PWxl	Tosoh Bioscience, Stuttgart
Superose 6 HR 10/30	GE Healthcare, München
Superdex75 10/300 GL	GE Healthcare, München

2.4 Buffers and other solutions

All buffers and solutions were produced using dH_2O from the ultra pure water filtration system (Sartorius, Göttingen) and, if necessary, autoclaved. The buffers and solutions used in this work are summarized in table 2.4.

table 2.4: composition of buffers and solutions

Buffers and other solutions	amount	substance
Common		
1xPBS (pH 7.4)	137 mM	NaCl
	2.70 mM	KCl
	8.10 mM	$Na_2HPO_4 \times 2H_2O$
	1.76 mM	KH_2PO_4
1xPBS-T	0.10 % (v/v)	Tween20 in 1xPBS
1xPBS-T for ELISA washer	0.05 % (v/v)	Tween20 in 1xPBS
DNA elution buffer (pH 8.5)	2.50 mM	Tris
Glycerol	80 % (v/v)	Glycerol
M-PBS-T	02.0 % (w/v)	Milk powder in 1xPBS
Agarose gel electrophoresis		
1xTAE buffer (pH 8.0)	40 mM	Tris-HCl
	20 mM	Acetic acid
	2 mM	EDTA
5xTBE buffer (pH 8.0)	445 mM	Tris-HCl
	445 mM	Borate
	10 mM	EDTA
Agarose gel	1.0 % (w/v)	Agarose in 1×TAE
Ethidium bromide solution	10 g/L	Ethidium bromide

Buffers and other solutions	amount	substance
Coomassie staining solutions		
destaining solution	10 % (v/v)	Acetic acid
staining solution	10 % (v/v) 0,05 % (w/v)	Acetic acid Coomassie Brilliant Blue R250
ELISA		
Stop solution ELISA	500 mM	H_2SO_4
TMB substrate buffer	10 parts 0.5 parts	TMB-A TMB-B
TMB-A solution	30 mM 1 % (w/v)	Potassium citrate Citric acid; pH 4.1
TMB-B solution	10 mM 10 % (v/v) 90 % (v/v) 80 mM	3,3',5,5'-Tetramethylbenzidine Acetone Ethanol H_2O_2 (30%)
Phage precipitation		
PEG/NaCl solution	20 % (w/v) 2.5 M	PEG 6000 NaCl
Phage Dilution Buffer (pH 7.5)	10 mM 20 mM 2 mM	Tris-HCl NaCl EDTA
Competent cells		
TFB1 (pH 5.8)	10 mM 30 mM 100 mM 50 mM 15 % (v/v)	$CaCl_2$ Potassium acetate RbCl $MnCl_2$ Glycerol
TFB2 (pH 8.0)	10 mM 10 mM 75 mM 15 % (v/v)	MOP RbCl $CaCl_2$ Glycerol
Panning		
100 mM Na-Borate (pH 8.6)	6.2 g/L	Boric acid
Citric buffer	100 mM 200 mM	Citric acid Na_2HPO_4
Ethanolamine	50 mM	in 1×PBS
Glycine buffer	100 mM 100 mM	Glycine NaOH

Buffers and other solutions	amount	substance
Na-Acetate buffer (pH 5.0)	10 mM	Sodium acetate
Panningblock	1 % (w/v) 1 % (w/v)	Milk powder BSA in 1xPBS-T
Trypsin solution	10 mg/L	Trypsin in 1xPBS
Protein purification		
5x Profinia™ IMAC binding buffer (pH 7.4)	2500.0 mM 50.0 mM 100.0 mM 100.0 mM	NaCl Imidazole Na_2HPO_4 NaH_2PO4
5x Profinia™ IMAC elution buffer (pH 7.4)	685.0 mM 13.5 mM 21.5 mM 40.5 mM	NaCl KCl Na_2HPO_4 KH_2PO_4
5x Profinia™ protein A binding and desalting buffer (pH 7.4)	685.0 mM 13.5 mM 21.5 mM 40.5 mM	NaCl KCl Na_2HPO_4 KH_2PO_4
5x Profinia™ protein-A elution buffer (pH 3.0)	500 mM	Sodium citrate
SDS-PAGE		
Acrylamide mix	30 % (w/v) 0.8 % (w/v)	Acrylamide Bis-acrylamide
5x Laemmli loading buffer	10 % (w/v) 50 % (v/v) 0.02 % (w/v) 15 % (v/v)	SDS Glycerol Bromphenole blue β-Mercaptoethanol
Buffer for stacking gel (pH 6.8)	1.0 M	Tris-HCl; pH 8.8
SDS stock solution	10 % (w/v)	SDS
SDS-PAGE running buffer (pH 8.3)	25 mM 192 mM 0.1 % (w/v)	Tris-HCl Glycerol SDS stock solution
Buffer for separation gel (pH 8.8)	1.5 M	Tris-HCl
WB and Immunostaining		
5-Brom-4-chlor-3-indoxylphosphat (BCIP)	15 g/L	in 70 % (v/v) DMF
AP substrate buffer	100 mM 0.5 mM	Tris-HCl (pH 9.5) $MgCl_2$

Buffers and other solutions	amount		substance
DAB staining solution	10	mL	DAB substrate buffer
	200	µL	DAB (3,3‘-Diaminobenzidine)
	1	µL	30 % (v/v) H_2O_2
DAB substrate buffer	8.0	g	NaCl
	200	mg	KCl
	1.44	g	$Na_2HPO_4 \times 2H_2O$
	240	mg	KH_2PO_4
	0.02	% (w/v)	$CoCl_2$ in 1xPBS
Nitro blue tetrazolium chloride (NBT)	30	g/L	in 70 % (v/v) DMF
WB running buffer (pH 8.3)	25	mM	Tris-HCl
	192	mM	Glycine
Cell culture			
Polyethylenimine	1.0	mg/mL	Polyethylenimine
MTT stock solution	5	mg/mL	MTT
Stop solution	100	%	DMSO
ThT assay			
Glycine NaOH (pH 8.5)	500	mM	Glycine
Thioflavin T stock solution	1	mM	Thioflavin T
TEM			
Uranyl acetate	2	% (w/v)	Uranyl acetate
SPR analysis			
EDC	0.5	M	EDC
NHS	0.1	M	NHS
SEC			
100 mM Na-Borate (pH 8.6)	6.2	g/L	Boric acid
Storage buffer	20	% (v/v)	Ethanol

2.5 Cultivation media and supplements

2.5.1 Prokaryotic cultivation

If not stated otherwise, bacteria were cultivated in double yeast tryptone medium (2xYT medium). For cultivation plates 15 g/L of agar-agar was added to the media. All media and supplements were produced using H_2O.

table 2.5: media for prokaryotic cultivation

Medium	Composition	
2×YT medium (pH 7.0)	1.6 % (w/v)	Tryptone
	1.0 % (w/v)	Yeast extract
	0.5 % (w/v)	NaCl
SOC-Medium (pH 7,0)	2.00 % (w/v)	Tryptone
	0.50 % (w/v)	Yeast extract
	0.05 % (w/v)	NaCl
	1 M	$MgCl_2$
	1 M	$MgSO_4$
	20 mM	Glucose

Supplements were composed as stock solutions, autoclaved or sterile filtered and added to the media in a sterile environment after its temperature dropped below 50 °C.

table 2.6: supplements for prokaryotic cultivation

Supplements	Stock solution	Final concentration
Glucose	2.0 M	100 mM
10×GA solution		
Glucose	1.0 M	100 mM
Ampicillin	2.0 mg/mL	100 µg/mL
IPTG	1.0 M	50 µM
Sucrose	2.5 M	50 mM
Ampicillin	100.0 mg/mL	100 µg/mL
Kanamycin	50.0 mg/mL	500 µg/mL
Tetracycline	10.0 mg/mL	500 µg/mL
Penicillin	10,000 U/mL	100 U/mL
Streptomycin	10,000 µg/mL	100 µg/mL

2.5.2 Eukaryotic cultivation

All media for eukaryotic cultivation were obtained from PAA (Pasching, Austria) or Gibco (Invitrogen, Switzerland, table 2.7).

table 2.7: media for eukaryotic cultivation

Medium	Supplements			Manufacturer
F17 medium	4,0	mM	L-Glutamin	PAA, Pasching (Austria)
	0,1	% (v/v)	Pluronic F-68	AppliChem, Darmstadt
	25,0	µg/mL	G418	AppliChem, Darmstadt
F17 feeding medium	4,0	mM	L-Glutamin	PAA, Pasching (Austria)
	0,1	% (v/v)	Pluronic F-68	AppliChem, Darmstadt
	0,1	% (w/v)	Trypton N1	PAA, Pasching (Austria)
DMEM + Glutamax medium	4.5	g/L	D-Glucose	Gibco, Invitrogen
	110.0	mg/L	Pyruvate	(Switzerland)
12 Nut Mix (Ham) medium	146	mg/L	L-Glutamine	Gibco, Invitrogen (Switzerland)
Transfection medium	F17 medium without G418			PAA, Pasching (Austria)

2.6 Cell lines, bacteriophage and microorganisms

Cell lines, bacteriophage and microorganisms that were used in this work are listed below.

table 2.8: cell lines, bacteriophage and microorganisms with description and origin

Name	Description / genotype	Reference / origin
E. coli XL1-Blue MRF'	Δ(*mcr*A)183 Δ(*mcr*CB-*hsd*SMR-*mrr*)173 *end*A1 *sup*E44 thi-1 *rec*A1 *gyr*A96 *rel*A1 *lac* [F' proAB *lacI*qZΔM15 Tn10 (Tetr)]	Stratagene, (La Jolla, USA)
Hyperphage	Helper phage for a polyvalent display of scFvs	(Rondot et al., 2001)R
M13K07	Helper phage for a monovalent display of scFvs	(Vieira and Messing, 1987)
SH-SY5Y	Human neuroblastoma cell line	(Biedler et al., 1978)
HEK293-6E	Human embryonic kidney cell line	(Durocher et al., 2002)

2.7 Antibody phage display libraries

Antibody phage display libraries that were used in this work are listed below.

table 2.9: antibody phage display libraries with description and origin

Name	Description / genotype	Reference / origin
HAL7/8	Naive human pHAL14 based antibody phage display library	(Hust et al., 2011)
PaD153.1/.2	Immune macaque pHAL35 based antibody phage display library	This work

2.8 Plasmids

Plasmids that were used in this work are listed below.

table 2.10: plasmids with specification and origin

Plasmid	Specification	Origin
pCSE2.5-hIgG1-Fc-XP	Vector for mammalian cell production, scFv-Fc antibodies	workgroup Dübel
pCSE2.5-His-XP	Vector for mammalian cell production, scFv antibodies	workgroup Dübel
pHAL35	Phagemid, for phage display library construction	workgroup Dübel

2.9 Oligonucleotides

Oligonucleotides that were used in this work are listed below.

table 2.11 oligonucleotides with sequence and description
Stated is the name of the primer and its sequence (5' to 3'). The abbreviation "f*" (forward) or "r" (reverse) indicates the orientation of the primer for the PCR amplification

Name	Sequence (5‘ – 3‘)	Description
MHgIII_r	CTAAAGTTTTGTCGTCTTTCC	Amplification of scFv genes from pHAL vectors
MHLacZ-pro_f	GGCTCGTATGTTGTGTGG	Amplification of scFv genes from pHAL vectors
Tor-pCMV-mIgG01-Fc-f	CACTTTGCCTTTCTCTCC	Amplification of scFv(-Fc) genes from pCSE2.5 vectors
Tor-pCMV-mIgG01-Fc-r	CAGATGGCTGGCAACTAG	Amplification of scFv(-Fc) genes from pCSE2.5 vectors
TM-Fc-seq-r	GGGAGATCATGAG	Amplification of scFv-Fc genes from pCSE2.5 vectors
PaD213-A5_BssHII	CTGGCGCGCACTCCATGGCCC AGGTGCAGCTG	Addition of a *BssH*II restriction site for cloning of PaD213-A5 in pCSE2.5
MHMacVK-MluI_f1	ACCGCCTCCACGCGTAGAHAT CGAGCTCACNCAGTCTCC	Amplification of V_{kappa}, *Mlu*I restriction site addition
MHMacVK-MluI_f6	ACCGCCTCCACGCGTAGAGCT CCWGATGACMCAGTCTCC	Amplification of V_{kappa}, *Mlu*I restriction site addition
MHMacVL-MluI_f1	ACCGCCTCCACGCGTACAGTCT GTGCTGACTCAGCCRCC	Amplification of V_{kappa}, *Mlu*I restriction site addition
MHMacVL-MluI_f2	ACCGCCTCCACGCGTACAGTCT GCCCTGACTCAGCCT	Amplification of V_{kappa}, *Mlu*I restriction site addition
MHMacVL-MluI_f3	ACCGCCTCCACGCGTATCCTAT GAGCTGACWCAGCCACC	Amplification of V_{kappa}, *Mlu*I restriction site addition
MHMacVL-MluI_f4	ACCGCCTCCACGCGTATCTTCT GAGCTGACTCAGGACCC	Amplification of V_{kappa}, *Mlu*I restriction site addition
MHMacVL-MluI_f5	ACCGCCTCCACGCGTACWGCC TGTGCTGACTCAGCC	Amplification of V_{kappa}, *Mlu*I restriction site addition
MHMacVL-MluI_f6	ACCGCCTCCACGCGTACAGCC GGCCTCCCTCTCAGCATCT	Amplification of V_{kappa}, *Mlu*I restriction site addition
MHMacVL-MluI_f7	ACCGCCTCCACGCGTACAGRC TGTGGTGACYCAGGAGCC	Amplification of V_{kappa}, *Mlu*I restriction site addition

Name	Sequence (5‘ – 3‘)	Description
MHMacVL-MluI_f8	ACCGCCTCCACGCGTACAGCC TGTGCTGACTCAGCCA	Amplification of V_{kappa}, *Mlu*I restriction site addition
MHMacKappaCL-NotI_r	ACCGCCTCCGCGGCCGCGACA GATGGTGSAGCCAC	Amplification of V_{lambda}, *Not*I restriction site addition
MHMacLambdaCL-NotI_r	ACCGCCTCCGCGGCCGCAGAG GAGGGCGGRAAWAGAGTGAC	Amplification of V_{lambda}, *Not*I restriction site addition
MHIgGCH1scFv-HindIII_r	GTCCTCGCAAAGCTTGACCGAT GGGCCCTTGGTGGA	Amplification of V_H, *Hind*III restriction site addition
MHMacVH-SfiI_f1	CGCGTGGCCCAGCCGGCCATG GCCSAGGTGCAGCTGGTGSAG TCTGGG	Amplification of V_H, *Sfi*I restriction site addition
MHMacVH-SfiI_f2	CGCGTGGCCCAGCCGGCCATG GCCCAGGTGCAGCTRCTCGAG TCKGG	Amplification of V_H, *Sfi*I restriction site addition
MHMacVH-SfiI_f3	CGCGTGGCCCAGCCGGCCATG GCCSAGGTGCAGCTGCTCGAG TCKGG	Amplification of V_H, *Sfi*I restriction site addition
MHMacVH-SfiI_f4	CGCGTGGCCCAGCCGGCCATG GCCCAGGTACAGCTCGAGCAG TCAGG	Amplification of V_H, *Sfi*I restriction site addition
MHMacVH-SfiI_f5	CGCGTGGCCCAGCCGGCCATG GCCGAGGTGCAGCTGCTCGAG TCTGG	Amplification of V_H, *Sfi*I restriction site addition
MHMacVH-SfiI_f6	CGCGTGGCCCAGCCGGCCATG GCCCAGGTGCAGCTRCTCGAG TSGGG	Amplification of V_H, *Sfi*I restriction site addition

2.10 Enzymes

Enzymes that were used in this work are listed below.

table 2.12: enzymes and manufacturer

Enzyme	Manufacturer
CIP (calf-intestinal alkaline phosphatase)	New England Biolabs, Frankfurt a. M.
GoTaq® DNA polymerase	Promega, Mannheim
Phusion DNA polymerase	ThermoFisherScientific, Offenbach

Enzyme	Manufacturer
Endonucleases for restriction	New England Biolabs, Frankfurt a. M.
T4 DNA ligase	Promega, Mannheim
Trypsin	Carl Roth, Karlsruhe

2.11 Antigen and antibodies

The antigen and a summary of antibodies that were used in this work are listed in table 2.13 and table 2.14 respectively.

table 2.13: antigen with description and manufacturer

Antigen	Description	Manufacturer
Aβ42 peptide (also Aβ42-CR)	42 amino acid long cleavage product of the APP transmembrane protein after processing with β- and γ-secretases	Synthesized and purified as TFA salts by Dr. James I. Elliott, W. M. Keck Facility, Yale University, New Haven (USA)

table 2.14: antibodies, dilutions and the manufacturers

Antibody	Dilution	Manufacturer
Mouse α c-myc-tag IgG 9E10-21 (monoclonal)	1:1,000	workgroup Dübel
Mouse α His-tag IgG (monoclonal)	1:5,000	Qiagen, Hilden
Mouse α pIII IgG PSKAN3 (monoclonal)	1:1,000	MoBiTec, Göttingen
Goat α human-Fc IgG-AP 109-055-098 (polyclonal)	1:4,000	Dianova, Hamburg
Goat α human-Fc IgG-HRP A0170 (polyclonal)	1:70,000	Sigma-Aldrich, München
Goat α mouse-Fc IgG-AP A2429 (polyclonal)	1:10,000	Sigma-Aldrich, München
Goat α mouse-Fc IgG-HRP A0168 (polyclonal)	1:50,000	Sigma-Aldrich, München

2.12 Software

The software used in this work is listed below.

table 2.15: software, provider and the targeted application

Name	Provider	Application
BIAevaluation 4.1	GE Healthcare Life Science	Affinity determination
Intas Geldocumentation	Intas	Display of agarose gels
MultAlin	http://multalin.toulouse.inra.fr/multalin	Comparison and analysis of DNA sequences
NanoDrop ND-1000	Coleman Technologies	Determination of nucleic acid and protein concentration
NCBI	http://www.ncbi.uhm.nih.gov	Literature research
FlowJo V	Treestar	FACS analysis
Office 2007	Microsoft	Presentations, graphs calculations and texts
Unicorn 5.1	GE Healthcare Life Science	Analysis of SEC data
VBASE2	http://www.vabse2.org	Sequence analysis of antibodies
Zotero 4.0.20	http://zotero.org	Reference management software
BD Accuri C6 Software.	BD Bioscience	FACS analysis

3. Methods

3.1 Microbiological methods

3.1.1 Sterilization

Culture media (liquid/solid), additives, buffer and solutions were autoclaved at 121 °C and 1 bar overpressure for at least 20 min. substances sensitive to heat (e.g. antibiotics) were sterile filtered (0.2 µm) and added to the solutions or media in a sterile environment. For solid growth media, agar-agar (Bacto) was added to the culture media before autoclaving.

3.1.2 Cultivation of *Escherichia coli (E. coli)*

3.1.2.1 Cultivation on plates

For obtaining single bacteria colonies, bacteria from a glycerol stock was spread on a 2xYT cultivation plate containing appropriate antibiotics using an inoculation loop. Incubation was carried out at 37 °C for up to 20 h. For longer storage (up to 4 weeks) plates were sealed with parafilm and stored at 4 °C.

3.1.2.2 Liquid cultivation

Liquid cultivation of *E. coli* was carried out in 2xYT medium with the appropriate antibiotics in shaking flasks. Single colony were picked from cultivation plates by a inoculation loop, or bacteria from glycerol stocks were used. Incubation was carried out at 37 °C for 14 - 18 h.

3.1.3 Storage of *E. coli* cells

For prolonged storage of *E. coli* cells, a glycerol was added to a bacterial culture to a final concentration of 20 % (v/v) and samples were stored at -80 °C.

3.1.4 Determination of cell density

The determination of cell density was assessed photometrical (Biochrome, Cambridge) by measuring the optical density (OD) at 600 nm wave length (λ = 600 nm). Inoculated culture medium was used as a reference.
An OD_{600} of 0.5 of *E. coli* bacteria corresponds to about $5*10^8$ cells/mL.

3.1.5 Production of chemo-competent *E. coli* cells

According to Sambrook (Sambrook and Russell, 2001).
100 mL 2xYT liquid culture medium with the appropriate antibiotics was inoculated with 1 mL from an overnight culture. Incubation was carried out at 37 °C and 250 rpm until OD_{600} reached 0.5. The cells were sedimented (3,220 xg, 4 °C, 10 min) and the supernatant was discarded. Cells were taken up in 15 mL ice-cold TTFB1 buffer and incubated for 90 min on ice. The cells were pelleted (3,220 xg, 4 °C, 5 min), supernatant was discarded and the cell pellet was carefully taken up in 4 mL of ice-cold TBF2 buffer. The cells were then aliquoted and stored at -80 °C.

3.1.6 Transformation by heat shock

50 µL of chemo-competent *E. coli* cells were thawed on ice. 10 µL of the ligation mixture was added and incubated for 20 min on ice. The heat shock was carried out at 42 °C for exactly 1 min. After further incubation on ice for 2 min 100 µL of SOC medium was added and the solution was spread on 2xYT-GA cultivation plates. Incubation was carried out at 37 °C over night.

3.1.7 Transformation by electroporation

Electro-competent *E. coli* XL1blue MRF' cells were obtained from Stratagene (Stratagene, La Jolla). Ligation mixtures were precipitated before electroporation, taken up in 30 µL of dH_2O and mixed with 50 µL of electro-competent cells. Incubation was carried out on ice for 10 min. Cuvettes for the electroporation (1 mm distance between electrodes) were incubated on ice as well. After the incubation on ice, the bacteria solution was added to the cuvette and a pulse of 1.7 kV was applied for about 5 ms. 1 mL of SOC medium was added immediately after the pulse and the bacteria were incubated at 37 °C and 600 rpm for 1 h before being spread on 2xYT-GA cultivation plates.

3.1.8 Production of M13 antibody phage

30 mL 2xYT-GA medium was inoculated from an overnight culture with bacteria bearing the appropriate phagemids. Washed off bacteria from cultivation plates were also used as inoculum. Incubation was carried out at 37 °C and 250 rpm until OD_{600} of 0.5 was reached. For the panning process 5 mL (25 mL for antibody phage display library construction) were infected with 250 µL (1,250 µL) M13K07 helperphage. The solution was stored at 37 °C for 30 min without agitation and then incubated at 37 °C and 250 rpm for 30 min. Cells were pelleted (3,220 xg, 20 °C, 10 min) and taken up in 30 mL (200 mL) 2xYT-AK culture medium. Production of scFv-phage was carried out at 30 °C and 250 rpm for 20 h. The cells were sedimented (3,220 xg, 20 °C, 10 min), the supernatant contains the phage. During the panning rounds, 2 mL of phage solution was sterile filtered (0.45 µm) and kept at 4 °C in a screw cap tube.

For library construction, the supernatant was mixed with 1/5 volume of PEG/NaCl solution and the phage were precipitated on ice for 1 h on a rocker. Phage were subsequently pelleted (10,000 xg, 4 °C, 60 min), the supernatant was discarded and the phage pellet was taken up in ice-cold phage dilution buffer (PDB). Remaining debris was discarded by transferring the supernatant after a second centrifugation (16,000 xg, 4 °C, 30 min) and antibody phage were again precipitated by mixing with 1/5 volume of PEG/NaCl solution and incubation on ice for 20 min on a rocker. Another centrifugation step (16,000 xg, 4 °C, 30 min) was carried out and the pellet was taken

up in 1 mL ice-cold PDB. A last centrifugation step (16,000 xg, 20 °C, 1 min) assured a pure antibody phage supernatant without cell debris that was transferred into a screw cap tube and stored at 4 °C.

3.1.9 Antibody selection with scFv phage display libraries

For the selection of scFv fragments that specifically detected Aβ42 two naive human antibody phage display libraries HAL7 and HAL8 (Hust et al., 2011), based on the pHAL14 vector, were used as well as the macaque derived immune libraries PaD153.1 and PaD153.2, based on the pHAL35 vector, that were constructed in this work.

On the surface of a cavity of a microtiter plate (MTP, Nunc MAXIsorp or Corning Costar) 1 µg of the target antigen in 150 µL 100 mM Na-Borate, pH 8.6 was absorbed at 4 °C over night. All following steps were carried out at room temperature (RT) on a rocker. After discarding the antigen solution the cavity was blocked with 2 % M-PBS-T for 2 h. In parallel one additional well was blocked with 150 µL panningblock (1 % BSA and 1 % M-PBS-T). After 1 h the panningblock was discarded and replaced with a total volume of 150 µL (200 µL) of panningblock including 3-5 µg per competitor antigen and the libraries with $1*10^{11}$ phage particles each (100 µL of amplified phage). Incubation was carried out for 1 h.

After the incubation, the phage containing solution was collected in a 1.5 mL reaction cap and the MTP was washed with 1xPBS-T. Afterwards the phage solution was added to the cavity with the target antigen and incubated for 2 h. Unspecific or weakly bound phage were washed off with 1xPBS-T depending on the panning round. All cavities were washed 10 times during the first panning round, 20 times during the second round and so on. Specific binding phage were eluted with 50 µL of trypsin (10 µg/mL) for 30 min at 37 °C without agitation. The eluted phage were used for infecting 130 µL of *E. coli* XL1blue MRF' during their exponential growth phase at an OD_{600} = 0.5. Incubation for 30 min at 37 °C without agitation. After addition of 20 µL of 10xGA the infected bacteria were incubated at 30 °C and 800 rpm for 20 h.

3.1.10 Amplification of antibody presenting phage

180 µL of 2xYT-GA was mixed with 5 µL or 10 µL of the overnight culture (3.1.9) and incubated at 37 °C, 800 rpm for 1.5 h in a Polystyrene MTP. Measurement of the OD at 620 nm was conducted in an ELISA reader until OD_{620} was between 0.3 - 0.4. Addition of $2x10^9$ M13K07 phage per well and incubation at 37 °C for 30 min without agitation, then 37 °C for 30 min at 800 rpm. Afterwards the cells were pelleted (3,220 xg, 20 °C, 10 min), supernatant was discarded and replaced with 180 µL of 2xYT-AK. Incubation at 30 °C and 800 rpm for 20 h. The cells were pelleted (3,220 xg, 20 °C, 10 min) and the supernatant containing the phage was stored at 4 °C.

3.1.11 Titer determination of antibody phage

50 mL of 2xYT-T medium was inoculated with 500 µL from an overnight culture of *E. coli* XL1blue MRF'. Incubation was carried out at 37 °C and 250 rpm until OD_{600} = 0.5. The eluted phage (3.1.9) were diluted in 1xPBS (10^{-2} - 10^{-4}). 10 µL of diluted phage were incubated with 50 µL of *E. coli* for 30 min at 37 °C without agitation. The solutions were plated on 2xYT-GA cultivation plates and incubated at 37 °C for 20 h. Titer were determined by colony counting.

3.1.12 Production of soluble scFvs in MTPs

For the initial characterization soluble scFvs were produced in a MTP (96well) scale. Single colonies of the titer plates were used to inoculate 180 µL of 2xYT-GA medium per well. The MTP was sealed with a breathable membrane and incubated at 37 °C and 800 rpm for 16 h. A new MTP was provided with 180 µL of 2xYT-GA medium per well and inoculated with 10 µL of the overnight cultures. The plate was incubated at 37 °C and 800 rpm for 2 h. The cells were pelleted (3,220 xg, 20 °C, 10 min), supernatant was discarded and 200 µL of production medium (2xYT-A with 50 µM IPTG) was added per well. Incubation at 37 °C and 800 rpm for 16 h. The cells were pelleted (3,220 xg, 4 °C, 10 min) and the antibody containing supernatant was transferred to a new MTP.

3.2 Molecular biology methods

3.2.1 Preparation of plasmid-DNA from *E. coli*

For the preparation of plasmid-DNA from *E. coli*, 2 mL [50 mL] of an overnight culture was processed with *peqGOLD™ Plasmid Miniprep Kit I* (PeqLab, Erlangen) [*Plasmid DNA Purification Kit NucleoBond™ Xtra Midi* (Machery und Nagel, Düren)] according to manufacturers' instructions. The obtained DNA was stored at 4 °C.

3.2.2 DNA amplification

DNA amplification was achieved by polymerase chain reaction (PCR) (Mullis et al., 1992).

3.2.2.1 Standard PCR

DNA amplification for cloning was carried with phusion DNA polymerase (Finnzymes) in a 50 µL scale.

table 3.1: composition and temperature profile of a standard PCR

component	volume
template DNA	1.0 µL
5x phusion buffer	10.0 µL
40 mM dNTPs (á 10 mM)	1.0 µL
forward primer (10 pmol/µL)	2.5 µL
reverse primer (10 pmol/µL)	2.5 µL
phusion polymerase	0.5 µL
H_2O	32.5 µL

temperature	time	
98 °C	**120 s**	
94 °C	**60 s**	
56 °C	**60 s**	30x ↺
72 °C	**45 s**	
72 °C	**600 s**	
16 °C	∞	

3.2.2.2 Colony PCR (cPCR)

For cPCRs, colonies were picked with a sterile pipette tip from the cultivation plates and resuspended in GoTaq PCR mixture in a 10 µL scale.

table 3.2: composition and temperature profile of a colony PCR

component	volume
bacteria pellet	0.0 µL
5x GoTaq Flexi buffer	2.0 µL
40 mM dNTPs (á 10 mM)	0.2 µL
forward primer (10 pmol/µL)	0.5 µL
reverse primer (10 pmol/µL)	0.5 µL
$MgCl_2$ (50 mM)	0.4 µL
GoTaq polymerase	0.05 µL
H_2O	6.35 µL

temperature	time	
95 °C	**120 s**	
94 °C	**20 s**	
56 °C	**15 s**	30x ↺
72 °C	**90 s**	
72 °C	**600 s**	
16 °C	∞	

3.2.3 Purification of DNA fragments

Purification of PCR products or DNA from preparative agarose gel electrophoresis was carried out with *NucleoSpin Extract Kit II* (Machery Nagel, Düren) according to manufacturers' instructions. The purity of the obtained DNA was determined photometrically.

3.2.4 Photometric determination of DNA concentration

The DNA concentration was determined using a *Nanodrop™ ND-1000 Spektrometer* (Peqlab, Erlangen) at a wavelength of $\lambda = 260$ nm. An absorption of $A_{260} = 1$ corresponds to a concentration of 50 µg/mL of pure double stranded DNA.

3.2.5 Enzymatic restriction of DNA

In order to obtain DNA fragments of defined sizes, DNA was digested using type-II restriction endonucleases. Enzymes, buffer and supplements were added according to manufacturers' instructions. After restriction the solution was heat inactivated for 20 min at 65 - 80 °C. DNA was purified and if necessary dephosphorylated.

table 3.3: composition of a restriction digest

component	volume
DNA	< 25.0 µL
enzyme buffer	5.0 µL
endonuclease 1 (20 U/µL)	0.5 µL
endonuclease 2 (20 U/µL)	0.5 µL
H_2O	ad 50.0 µL

3.2.6 DNA dephosphorylation

Religation of DNA ends was prevented by dephosphorylation. After the purification step, 0.5 U of calf intestine phosphatase (CIP) was added twice for 30 min at 37 °C to the restriction mixture.

3.2.7 Agarose gel electrophoresis

Separation of DNA was carried out on 0.8 - 1.5 % agarose gels, stained with 25 µg/mL Ethidium bromide (EtBr) at a voltage of 130 V and an amperage of 400 mA for 20 - 40 min. The running buffer was 1xTBE and all samples were mixed with 6x DNA loading dye prior to the run. *Gene Ruler 1 kb DNA Ladder* (Fermentas, St.Leon-Rot) was used for size determination. DNA detection was carried out with UV light at a wavelength of λ = 312 nm an a video camera system (Intas, Göttingen).

3.2.8 DNA ligation

Ligation of DNA was carried out with T4-DNA ligase (Promega, Mannheim) with a molar ratio of insert : vector of 2:1 - 8:1. After incubation for 1 - 3 h at 20 - 32 °C or for 12 - 18 h at 16 °C the ligase in the mixture was heat inactivated for 20 min at 65 °C.

table 3.4: **composition of a restriction digest**
indicated is the composition of a restriction digest for normal cloning (left) as well as for the construction of phage display libraries (right)

	normal cloning		library construction	
component	**volume**	**amount**	**volume**	**amount**
10x T4-DNA ligase buffer	1.0 µL	1x	10.0 µL	1x
vector DNA	1.0 - 2.0 µL	≈ 50 ng	10.0 - 30.0 µL	≈ 1000 ng
insert DNA	2.0 - 7.0 µL	≈ 150 ng	20.0 - 70.0 µL	≈ 300 ng
T4-DNA ligase	0.2 µL	1 U	1. µL	3 U
H_2O	ad 10.0 µL		ad 100.0 µL	

3.2.9 DNA sequencing

DNA sequencing was carried out at GATC-Biotech AG (Konstanz) according to manufacturers' instructions.

3.3 Biochemical methods

3.3.1 Protein A purification of scFv-Fc antibody fragments by Profinia™

For the purification of transiently produced scFv-Fc antibody fusion proteins from culture supernatant of HEK293-6E cells the Profinia™ Protein Purification System (BioRad, München) was used according to manufacturers' instructions. In short: culture supernatant containing the produced antibody fragments was mixed with 10x Protein A binding buffer (end concentration: 1x), degassed (0.45 µm filter) and added to a 1 mL Protein A column with a flow rate of 1 mL/min. After washing the column with 12 column volumes (CV) of Protein A binding buffer, antibody fragments were eluted using 4 CV citric acid buffer before subsequent dialysis with 4 mL of 1xPBS on a 10 mL desalting cartridge. Antibodies were stored at -20 °C.

3.3.2 IMAC purification of scFv antibody fragments by Profinia™

For the purification of transiently produced scFv antibodies from culture supernatant of HEK293-6E cells the Profinia™ Protein Purification System (BioRad, München) was used according to manufacturers' instructions. In short: culture supernatant containing the produced antibody fragments was mixed with 10x binding buffer (end concentration: 1x), degassed (0.45 µm filter) and added to a 1 mL HisTrap column with a flow rate of 2 mL/min. After washing the column twice with 4 CV of binding buffer, antibody fragments were eluted using 4 CV imidazole containing elution buffer before subsequent dialysis with 4 mL 1xPBS on a 10 mL desalting cartridge. Antibodies were stored at -20 °C.

3.3.3 Photometric determination of protein concentration

Antibody concentration was determined by the Profinia™ system and in rare cases additionally by using a *Nanodrop™ ND-1000 Spektrometer* (Peqlab, Erlangen) at a wavelength of λ = 280 nm (3.2.4).

After antigen purification (3.5.2) protein concentration was determined with a spectrophotometer. 10 minutes prior to the measurement the instrument was switched on to preheat the lamp. The baseline was set with 100 µL running buffer in a 10 mm path length UV cell. 100 µL of the obtained Aβ42 fractions were measured at wavelength of λ = 280 nm. The concentration was calculated from the absorbance according to the Beer-Lambert-law:

$$c = A / \varepsilon * d$$

A = absorbance at λ = 280 nm

ε = molar extinction co-efficient of Aβ42 monomers = 1490 $M^{-1}cm^{-1}$

d = UV cell path length (10 mm = 1 cm)

3.3.4 SDS-PAGE

According to Laemmli (Laemmli, 1970).

The electrophoretic separation of proteins was carried out by discontinuous SDS-PAGE with a 4 % stacking gel and a 12 % separation gel in tris-glycine buffer. Additionally, precast 4 % - 12 % gradient Bis-tris gels and MES SDS running buffer (Invitrogen, Carlsbad) were used for separation of amyloid-β peptides.

table 3.5: composition of PAA gels for a discontinuous SDS-PAGE

component	stacking gel [4 %]	separation gel [12 %]
30 % (w/v) Acrylamid-Mix	260.0 µL	1600.0 µL
1.0 M Tris-HCl, pH 6,8 [µL]	200.0 µL	-
1.5 M Tris-HCl, pH 8,8 [µL]	-	1000.0 µL
10 % SDS [µL]	15.0 µL	40.0 µL
10 % APS [µL]	15.0 µL	40.0 µL
TEMED [µL]	2.0 µL	2.0 µL
H_2O [µL]	1000.0 µL	1300.0 µL

For reducing conditions all samples were mixed 1:5 with 5x Laemmli protein buffer with β-ME and incubated at 95 °C for 10 min. After application on the gel separation was carried out at an amperage of 30 mA and voltage of 300 V per PAA gel. The run was finished when the Bromphenol blue reached the end of the gel (ca. 35 - 45 min). The relative molecular mass was estimated using a protein standard (BioRad, Hercules). Gels were stained with Coomassie or via silver staining subsequent to the run or the total protein load was transferred to a PVDF membrane by Western Blot and used for immunostaining.

3.3.5 Coomassie staining of PAA gels

After electrophoresis the separation gel was transferred into a glass bowl and covered with Coomassie staining solution. After heating in the microwave just below boiling point, the gel was incubated for 10 min at 20 °C on a rocker. The staining solution was discarded and destaining solution was added.. Agai9n, after heating in the microwave

just below boiling point, the gel was incubated at 20 °C on a rocker until the protein free gel matrix was completely destained.

3.3.6 Silver staining of PAA gels

Silver staining was carried out using SilverXpress Silver staining Kit (Invitrogen, Carlsbad) according to manufacturers' instructions.

3.3.7 Western Blot

Subsequent to separation by gel electrophoresis proteins were transferred to a PVDF membrane by semi-dry western blotting (WB). All membranes and paper were presoaked in SDS-PAGE running buffer without SDS with the PVDF membrane additionally being incubated in 100 % EtOH. The composition of the WB from the anode to the katode of the transfer system was: 3x Whatman paper, PVDF membrane, PAA gel, 3x Whatman paper. Protein transfer was carried out for 30 min at 20 V and 330 mA per gel.

3.3.8 Immunostaining

After transfer of the proteins onto a PVDF membrane, this membrane was incubated in 2 % M-PBS for 1 h at 20 °C or over night at 4 °C to block unspecific binding sites. All other incubation steps were carried out at 20 °C on a rocker. After incubation for 1 h with the primary antibody, diluted in 2 % M-PBS, the membrane was rinsed 3 times with 1xPBS for 5 min each. After incubation for 1 h with the secondary antibody, diluted in 2 % M-PBS, the membrane was rinsed 3 times with 1xPBS for 5 min each before subsequent equilibration for 10 min in alkaline phosphatase (AP) substrate buffer. Specific detection of the proteins was carried out with AP substrate (NBT/BCIP á 100 µL in 10 mL of AP substrate buffer) until bands were visible (ca. 2 - 10 min). The reaction was stopped by rinsing the membrane with H_2O and drying it between two sheets of paper.

3.3.9 Enzyme linked immunosorbent assay (ELISA)

The ELISA was used in this work to select antibodies after the panning process and to compare scFvs or scFv-Fcs specificities.

100 ng antigen in 100 µL of buffer was added per cavity of a Corning Costar MTP and incubated over night at 4 °C without agitation. The following incubation steps were carried out at 20 °C on a rocker. Discard the antigen and block the remaining unspecific binding sites of the MTP by addition of 350 µL 2 % M-PBS for 1 h. The blocking solution was discarded and all cavities were washed three times with 1xPBS-T using an ELISA washer (Columbus plus, Tecan). 100 µL/cavity of antibody containing supernatant from MTP productions or purified scFvs or scFv-Fcs, each mixed with 2 % M-PBS were added and incubated for 1.5 h before being washed three times with 1xPBS-T using an ELISA washer. 100 µL/cavity of primary antibody solution in 2 % M-PBS was incubated for 1 h before an additional washing step with the ELISA washer. Either the primary antibody was HRP-conjugated (horse radish peroxidase) or a secondary antibody was necessary. Again, the incubation of 100 µL/cavity of enzyme conjugated secondary antibody mixed with 2 % M-PBS was followed by three washing steps with the ELISA washer. For detection, the enzymatic reaction was started by addition of 100 µL/cavity of substrate (TMB A + TMB B, ratio 20:1). After 3 - 15 min of incubation the reaction was stopped using 100 µL/cavity of 1 N H_2SO_4 followed by a subsequent read out of the absorption at a wavelength λ = 450 nm subtracted by the reference wavelength λ = 620 nm in an ELISA reader (Sunrise, Tecan).

3.3.10 Thioflavin T measurement

To assess the state of fibrillogenesis by Thioflavin T (ThT) measurement, 20 µL of the desired sample was mixed with 10 µL of a 100 µM ThT solution and 70 µL of 500 mM glycine NaOH, pH 8.5 in one well of a black 384-well Nunc plate (Sigma-Aldrich, München) by pipetting. The sample was measured with on an Analyst™ AD fluorometer (Molecular Devices Cooperation) at an excitation wavelength of λ = 450 nm and emission wavelength of λ = 485 nm.

3.4 Cell-biological methods

3.4.1 Cultivation of HEK293-6E cells

HEK293-6E cells were cultivated in 100 mL polycarbonate shaking flasks (Corning, New York) at 37 °C, 5 % CO_2 and 110 rpm in 50 mL of Gibco FreeStyle F17 Expression Medium (Invitrogen, Carlsbad) supplemented with 7.5 mM L-glutamine, 0.1 % PF68 and 1 % Penicillin/Streptomycine.

3.4.2 Cultivation of SH-SY5Y cells

SH-SY5Y cells were cultivated in 75 cm^2 tissue culture flasks (TPP, Trasadingen) at 37 °C and 5 % CO_2 in 20 mL of 50 % of DMEM GlutaMAX medium and 50 % of Ham's F12 Nutrient Mix medium (Invitrogen, Carlsbad) supplemented with 10 % FBS and 1 % Penicillin/Streptomycine.

3.4.3 Transfection of HEK293-6E cells

For the transient expression of scFvs and scFv-Fcs in mammalian cells, human HEK293-6E were transfected with the transfection reagent polyetylenimine (PEI). 1.5 - 2*10^6 cells per mL were transfected with a mixture of DNA and PEI. This mixture consisted of 25 µg of DNA plus 62.5 µL of PEI (1 mg/mL), each component was added separately to 1.25 mL of serum free medium. The PEI solution was added to the DNA solution, mixed cautiously and incubated for 20 min at 20 °C without agitation. Subsequently, all was added to 25 mL of cell suspension in a shaking flask and incubated at 37 °C, 5 % CO_2 and 110 rpm for 48 h. 25 mL of cell free medium was fed to the cell suspension and further incubated under the same conditions for 72 h additional hours. Antibodies were harvested by pelleting the cells in a 50 mL reaction tube and using the supernatant for purification (3.3.1 and 3.3.2).

3.4.4 Fluorescence activated cell sorting (FACS)

Cytotoxicity in SH-SY5Y cells was assessed via propidium iodide (PI) staining and subsequent readout in a FACS. For this, 35,000 SH-SY5Y cells per well were plated in a 96 well plate in 100 µL of 50 % of DMEM GlutaMAX medium and 50 % of Ham's F12 Nutrient Mix medium (Invitrogen, Carlsbad) supplemented with 10 % FBS and 1 % Penicillin/Streptomycine and incubated at 37 °C with 5 % CO_2 for 24 h. The medium was aspirated and replaced with the desired concentrations of Aβ42-CR and antibodies provided in 100 µL of 50 % of DMEM GlutaMAX medium and 50 % of Ham's F12 Nutrient Mix medium (Invitrogen, Carlsbad) supplemented with 1 % Penicillin/Streptomycine without 10 % FBS. Incubation at 37 °C with 5 % CO_2 for 24 h. The medium was apirated and 30 µL of 0.25 % Trypsin/EDTA (Gibco, Invitrogen) was added. Incubation was carried out at 37 °C with 5 % CO_2 for 20 min. During incubation, DMEM medium (-FBS) was preheated to 37 °C in a water bath and 1 mg/mL PI stock solution (Sigma-Aldrich, München) was diluted 1:40 in 1xPBS (final concentration 12.5 µg/mL). After the cells were incubated for 20 min, 120 µL of DMEM medium and 150 µL of PI dilution was added per well. The cell layer was disrupted by carefully pipetting the cells up and down 40x followed by FACS measurement at an excitation wavelength of λ = 488 nm and emission wavelength of λ = 640 nm.

3.4.5 MTT reduction assay

35,000 SH-SY5Y cells per well were plated in a 96 well plate in 100 µL of 50 % of DMEM GlutaMAX medium and 50 % of Ham's F12 Nutrient Mix medium (Invitrogen, Carlsbad) supplemented with 10 % FBS and 1 % Penicillin/Streptomycine and incubated at 37 °C with 5 % CO_2 for 24 h. The medium was aspirated and replaced with the desired concentrations of Aβ42-CR and antibodies provided in 100 µL of 50 % of DMEM GlutaMAX medium and 50 % of Ham's F12 Nutrient Mix medium (Invitrogen, Carlsbad) supplemented with 1 % Penicillin/Streptomycine without 10 % FBS. Incubation at 37 °C with 5 % CO_2 for 24 h. 5 µl/well of the MTT stock solution (5 mg/mL) was added directly onto the cells. Incubation at 37 °C with 5 % CO_2 for 3.5 h. The medium was carefully aspirated and 100 µL DMSO were added. Incubation at 20 °C for 5 min on a rocker. Cells were fully lysed by pipetting up and down 30x

followed by a subsequent read out of the absorption at a wavelength λ = 570 nm subtracted by the reference wavelength λ = 690 nm in an ELISA reader (Sunrise, Tecan).

3.5 Biophysical Methods

3.5.1 Affinity measurement of antibodies

The dissociation constant (K_D) of scFv antibodies was determined by SPR (surface plasmon resonance) using a BIAcore2000™. A dextrane coupled chip (BIAcore Sensor Chip CM5 or Xantec CMD50m) was coupled covalently with Aβ42 monomers, protofibrils or fibrils via amine coupling. Activation of the chips was carried out with NHS/EDC according to manufacturers' instructions before coupling of the antigen (c = 2.5 - 4 µg/mL in 10 mM Na-Ac, pH4.5) until the desired R.U. was achieved. Subsequently, the chips were blocked with 1 M ethanol amine. HBS-EP+ was used as running buffer. Antibody binding was carried out with different scFv concentrations (100 nM - 10,000 nM, additionally with 15,000 nM for PaD97-D6 and 15,000 nM + 20,000 nM for PaD213-A5) at a flow rate of 25 µL/min with an association time of 200 s and dissociation for 600 s. 85 mM, 87.5 mM, and 125 mM NaOH was used for sensor chip regeneration. Data fitting was carried out with the program BIAevaluation™ with the mathematical algorithm "1:1 binding with drifting baseline".

3.5.2 Size exclusion chromatography for Aβ42 antigen preparation

Antigen fractionation was achieved with size exclusion chromatography (SEC) in an ÄKTA™ purifier system by three different ways according of the desired preparations. The system and buffer solutions were kept at 4 - 8 °C the whole time. 0.22 µm filtered 10 mM Tris-HCl, pH 7.4 or 100 mM Na-Borate, pH 8.6 were used as running buffers and absorption was measured at 280 nm with additional 215 nm measurement if possible.

3.5.2.1 Obtaining sole Aβ42 monomers

1.0 - 1.5 mg of lyophilized Aβ42 peptide was dissolved in 1 mL of 6 M Guanidine-HCl (Gn-HCl) and mixed until a clear solution is achieved. Larger aggregates are pelleted by centrifugation (13,000 xg, 4 °C, 3 min). The solution is taken up in a syringe and injected into the SEC. Fractionation is carried out on a Superdex75 10/300 GL column (GE Healthcare, München) that was previously equilibrated with 10 mM Tris-HCl, pH 7.4 running buffer. The flow rate was set to 0.5 mL/min with a fraction size of 1 mL. Aβ42 monomers elude after 0.45 - 0.6 column volumes (CV, 11 - 14 mL) and were used immediately or stored at -20 °C if necessary.

3.5.2.2 Obtaining Aβ42 monomers and protofibrils

1.5 - 2.0 mg of lyophilized Aβ42 peptide was dissolved by addition of 50 µL DMSO, 800 µL dH_2O and 10 µL 2 M Tris-HCl, pH 7.6 and immediately mixed until a clear solution is achieved. Larger aggregates are pelleted by centrifugation (13,000 xg, 4 °C, 3 min). The solution is taken up in a syringe and injected into the SEC. Fractionation is carried out on a Superdex75 10/300 GL column that was previously equilibrated with 10 mM Tris-HCl, pH 7.4 or 100 mM Na-Borate, pH 8.6 running buffer. The flow rate was set to 0.3 - 0.4 mL/min with a fraction size of 1 mL. Aβ42 protofibrils elude after 0.3 - 0.4 CV (7 - 9 mL) while Aβ42 monomers elude after 0.45 - 0.55 CV (11 - 13 mL). The antigen was used immediately or stored at -20 °C if necessary.

3.5.2.3 Obtaining Aβ42 oligomers of different sizes

To distribute the protofibrils fractions further in order to get fractions of more distinct sizes of oligomers it is necessary to purify the Aβ42 peptide by two columns connected in series. The first column is a TSKgel 4000PWXL (TOSOH Bioscience) that is connected by a short tube to the second column, a Superose 6 10/300 GL (GE Healthcare, München).

2.0 - 2.5 mg of lyophilized Aβ42 peptide was dissolved by addition of 60 µL DMSO, 800 µL dH_2O and 13 µL 2 M Tris-HCl, pH 7.6 and immediately mixed until a clear solution is achieved. Larger aggregates are pelleted by centrifugation (13,000 xg, 4 °C, 3 min). The solution is taken up in a syringe and injected into the SEC. Fractionation is carried out on the columns mentioned above, previously equilibrated with 100 mM Na-Borate, pH 8.6 running buffer. The flow rate was set to 0.3 mL/min with a fraction size

of 1 mL. Aβ42 oligomers elude over 9 - 10 fractions. The antigen was used immediately or stored at -20 °C if necessary.

3.5.3 Preparation of TEM grids

On a formvar coated 200 mesh TEM grid (EM Science, Hatfield) 5 - 10 µL of the fraction sample (3.5.2) was applied and incubated for 1 minute. Excess fluids were wicked away with a piece of filter paper. The grid was washed twice by applying 10 µL of dH_2O before staining the sample twice with 10 µL of 2 % uranyl acetate. The grid was dried with a vacuum pump, incubated for 5 min and 20 °C to completely dry off and then stored in the designed container until further use.

4. Results

4.1 Purification of Aβ42

Aβ42 peptides were purified in different forms depending on the desired purity of the fractions. For solely obtaining pure Aβ42 monomers (4.2 kDa) the lyophilized Aβ42 peptide was dissolved in 6 M Guanidine-HCl (Gn-HCl) and purified with a Superdex75 10/300 GL column resulting in one distinct peak over 2 - 3 fractions after 0.45 - 0.6 column volumes (CV) (11 - 14 mL) (figure 4.1, A).

To obtain monomers and different sized oligomers, lyophilized Aβ42 peptide was initially dissolved in DMSO with dH_2O and 2 M Tris-HCl, pH 7.6 added directly afterwards in that order. Fractionation of this solution, termed Aβ42 crude (Aβ42-CR), was achieved by size exclusion chromatography (SEC). Depending on the later purpose of the antigen two different techniques were applied.

Purification with a Superdex75 10/300 GL column results in two peaks (figure 4.1, B). The first peak consists of two fractions after 0.3 - 0.4 CV (7 - 9 mL) and represents a mixture of oligomers of various sizes, namely protofibrils. These protofibrils range between 15 kDa and 500 kDa and display various forms and morphologies, with diameters of 8 - 10 nm and a length of up to 200 nm. The second peak after 0.45 - 0.55 CV (11 - 13 mL) is distributed as well over two fractions and represents Aβ42 monomers.

In order to obtain fractions of more discrete size oligomers, a two step purification was carried out using two different columns connected in series (figure 4.1, C). After an initial separation by a TSKgel4000 PWXL column the flow-through was further separated by a Superose6 10/300 GL column resulting in the sub fractionation of the Aβ42 protofibrils and the distribution over multiple fractions.

Earlier fractions include filaments significantly larger than 200 nm (LO = large oligomers) while later fractions consist predominantly of short fibrils (MO = medium

oligomers) of up to 100 nm and small, circular aggregates (SO = small oligomers) that can be smaller than 10 nm.

Formation of mature Aβ42 fibrils was achieved by either incubating a pure monomer fraction at 37 °C for 24 h with gentle agitation (300 rpm) or for 96 h without agitation. The resulting fibrils show a helical twisted structure, are longer than 1 µM and have a relative molecular mass of greater than 1 MDa.

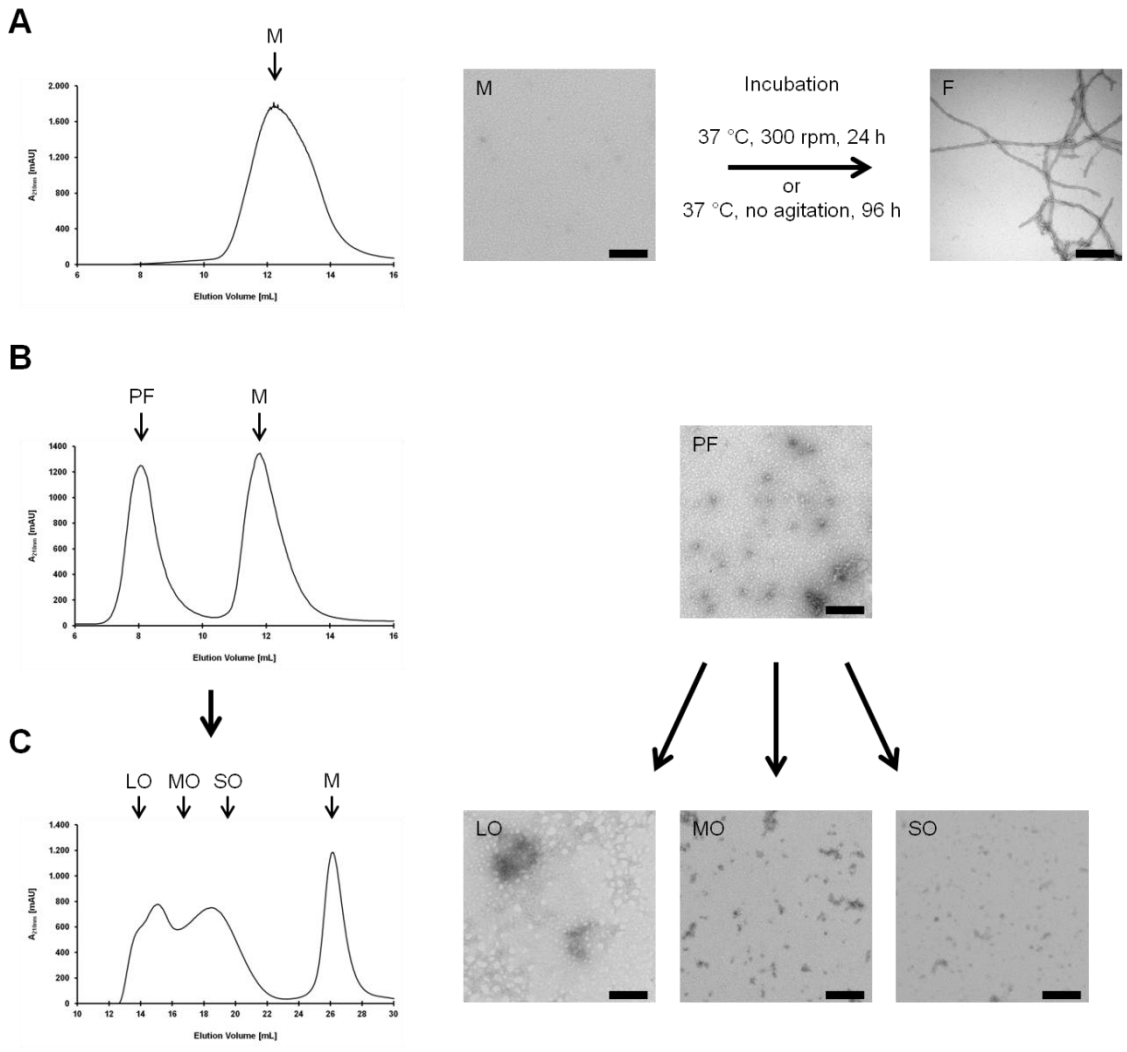

figure 4.1: **purification of Aβ42 peptide**
(A) purification of monomers (M) by the Gn-HCl method, fibrils (F) are derived from monomers by incubation at 37 °C, **(B+C)** purification by the DMSO method via one column **(B)** to obtain protofibrils (PF) or by two columns connected in series **(C)** to obtain large (LO), medium (MO) or small oligomers (SO), representative TEM images, scale bar corresponds to 200 nm

4.2 Construction of two immune phage display libraries PaD153.1 and PaD153.2

To elevate the prospects of obtaining conformation specific antibodies two immune phage display library were constructed. Immunization with small Aβ42 oligomers (SO) was carried out in P. Thulliers lab (*Centre de Recherche du Service de Santé des Armées* in La Tronche Cedex, France) as described (Avril et al., 2014).

Subsequently the variable heavy chain (V_H) and the variable light chain (V_L) genes were amplified via PCR with specific primers allowing the addition of restriction sites. *Mlu*I and *Not*I were added to V_L and *Sfi*I and *Hind*III were added to V_H for the integration into pHAL35.

First, V_L was subcloned into the phagemid vector pHAL35. To maximize the diversity of the V_L chains two forward primers and one reverse primer were used for the amplification of V_{Kappa} and three forward primers and one reverse primer for V_{Lambda} respectively. A total of six different forward primers and one reverse primer were used for the amplification of V_H. The insert rates were again determined by colony-PCR of 15 individual clones for the Kappa-library (PaD153.2) (60 %) and 10 clones for the Lambda-library (PaD153.1) (80 %) (figure 4.2).

Some clones displayed an aberrant size in the agarose gel after colony-PCR running at a height between full length insert and negative control. This is due to additional restriction sites in the V_L or V_H genes.

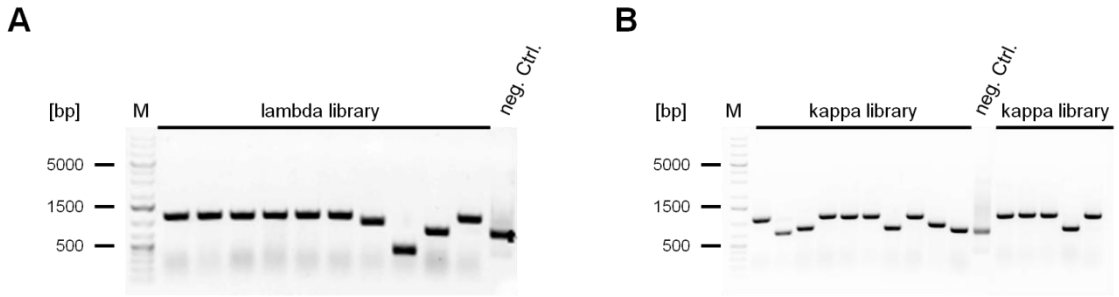

figure 4.2: **determination of full size insert rate for the lambda and kappa library**
insert rates for the **(A)** lambda library (PaD153.1) and **(B)** kappa library (PaD153.2) were determined by colony-PCR, samples were separated on a 1 % agarose gel, negative control (neg. Ctrl.) is pHAL35 including only VH

The maximal theoretical diversity is restricted by the efficiency of transformation and was determined to be $1*10^7$ individual binders for the Lambda and $1.9*10^7$ for the Kappa sublibrary.

4.2.1 Packaging of PaD153.1 and PaD153.2

For the subsequent panning process both sublibraries were produced in *E. coli* XL1blue MRF' using the helperphage M13K07 and Hyperphage. M13K07 allows for monovalent scFv presentation on the phage surface, circumventing avidity effects that occur when using the polyvalent scFv presenting helperphage Hyperphage.

Titer determination was conducted by a dilution series on agar plates. The titer for PaD153.1 (lambda) was $9.7*10^{13}$ pfu/mL with M13K07 and $1.1*10^{11}$ pfu/mL with Hyperphage. PaD153.2 (kappa) was equally well produced with titers of $5*10^{13}$ pfu/mL in M13K07 and $1.6*10^{12}$ pfu/mL in Hyperphage.

Both titers with Hyperphage were significantly lower than with M13K07 due to the fusion protein (antibody:pIII) expression that doesn't allow production of solely pIII protein.

Detection of the minor coat protein pIII by Immunoblot revealed a remote antibody presentation on the phage for both sublibraries with M13K07 while presentation on Hyperphage was close to 50 % as estimated from the Western Blots (figure 4.3).

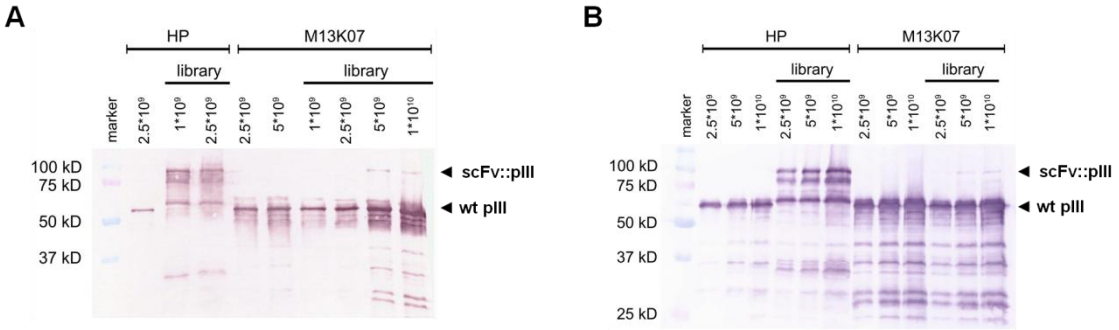

figure 4.3: **detection of the pIII protein in PaD153.1 and PaD153.2**
(A) PaD153.1 (lamba) and **(B)** PaD153.2 (kappa) were packaged with Hyperphage (HP) or M13K07 phage, after separation on a 12 % PAA gel and transfer to a PVDF membrane the pIII protein was detected as wildtype (wt) protein and antibody fusion protein (scFv::pIII) by immunostaining

4.3 Generation of Aβ42 specific scFvs from naive and immune phage display libraries

To obtain specific antibodies directed against β-amyloid monomers, different size oligomers and fibrils an antibody selection process (panning) was conducted. Together, four libraries were used, two IgM derived naive human phage display libraries (HAL7/8) and two IgG derived immune phage display libraries specific for Aβ42 that were constructed in this dissertation. Pannings were carried out on monomers, oligomers of different sizes, and fibrils with or without preabsorption with unwanted forms of Aβ42 (table 4.1).

table 4.1: overview over pannings and antigens used for competition
different panning strategies were applied to obtain specific scFvs, the target antigen is mentioned in the first column, black squares indicate the antigens used for competition, panning strategies with HAL7/8 colored grey, panning strategies with PaD153.1/.2 colored white

		competitors					
antigen	total number of pannings	none	monomers	small oligomers	medium oligomers	large oligomers	fibrils
monomers	14x	■					
		■					
						■	
							■
				■			■
					■		■
						■	■
				■	■		■
				■	■	■	■
small oligomers	20x	■					
			■				
							■
			■				■
		■					
							■
			■		■	■	■
medium oligomers	5x	■					
		■					
			■				
							■
			■	■		■	■
large oligomers	8x	■					
		■					
			■				
							■
			■				■
			■		■		■
fibrils	7x	■					
		■					
				■			
			■			■	

4.3.1 Panning with naive phage display libraries HAL7/8

The pannings were carried out with the naive human scFv phage display libraries HAL7/8 in Nunc PolySorp ELISA plates with decreasing concentration of antigen in the three panning rounds with or without addition of competitor antigens in solution

After the third round up to 184 clones were produced in microtiter plates and analyzed by ELISA for each panning to verify specific antigen binding.

One antibody (PaD97-D6) from the HAL7 library showed a signal to noise ratio of greater than 5 and was further analyzed (figure 4.4).

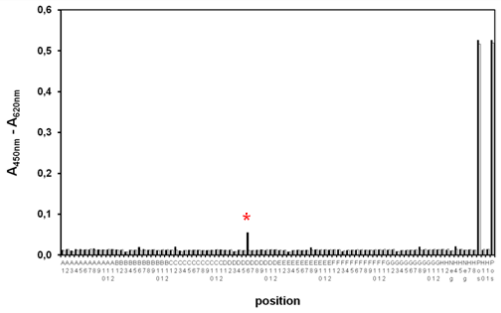

figure 4.4: **identification of monoclonal antibodies form HAL7/8**
screening ELISA with supernatant of MTP production, PaD97-D6 is indicated by a red asterisk

4.3.2 Panning with immune phage display libraries PaD153.1 and PaD153.2

In order to expand the chances to obtain conformation specific antibodies that distinguish between Aβ42 monomers, oligomers of different sizes, and fibrils a total of 26 pannings with the Aβ42 specific macaque derived immune scFv phage display libraries were conducted. In most of the pannings the focus lied on the competition with unwanted Aβ42 forms during the process.

The pannings were carried out on ELISA plates. 1 µg of Aβ42 antigen was coated in all three panning rounds with or without addition of a 3 - 5-fold surplus of competitor antigens in solution.

After the third round 92 clones were produced in microtiter plates and analyzed by ELISA for each panning to verify specific antigen binding.

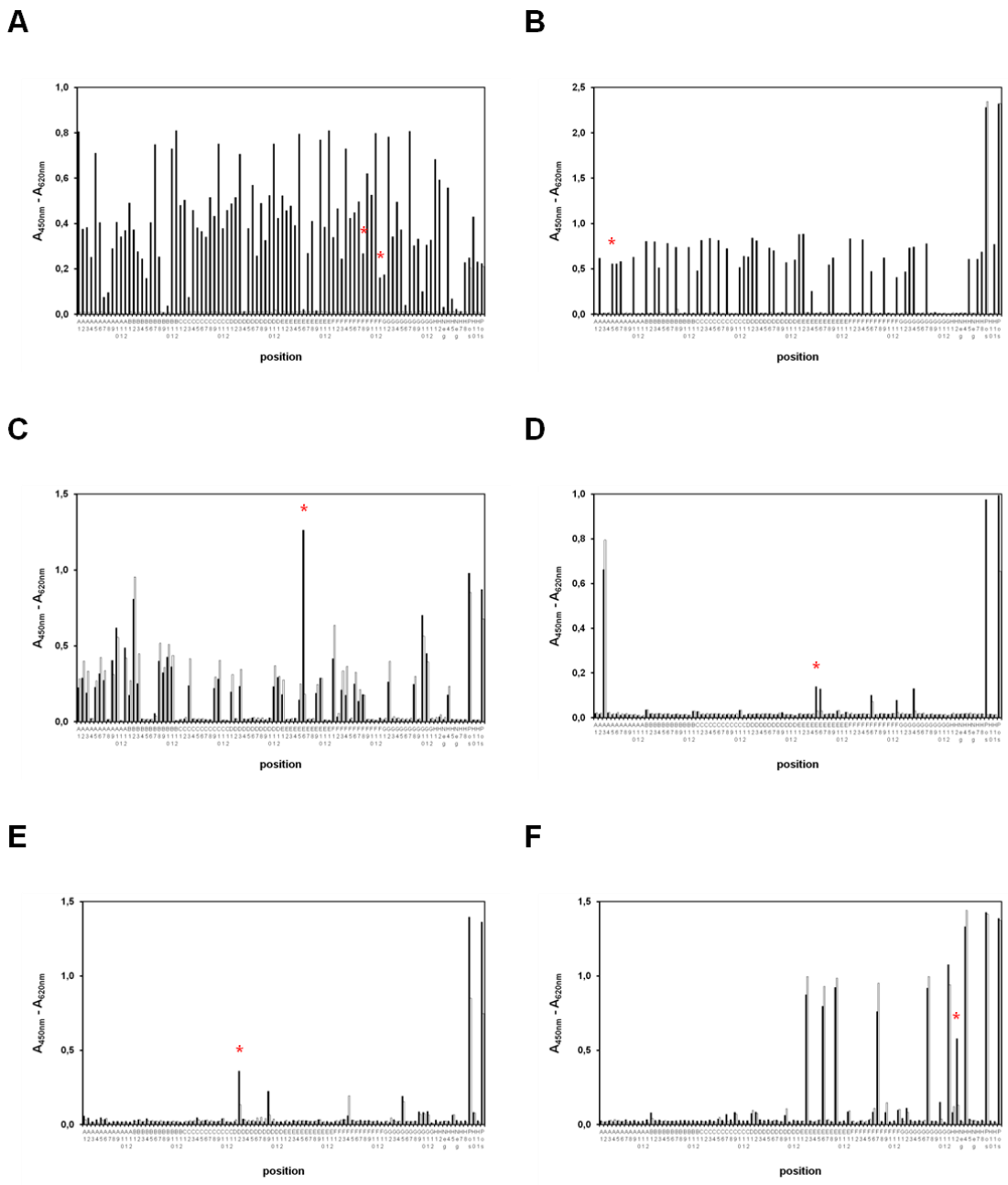

figure 4.5: **identification of monoclonal antibodies form PaD153.1 and PaD153.2**
screening ELISAs with supernatant of MTP productions, red asterisks mark the antibodies that were chosen for further investigation, **(A)** PaD172-F8 and PaD172-F12, **(B)** PaD213-A5, **(C)** PaD218-E6, **(D)** PaD233-E5, **(E)** PaD235-D2, **(F)** PaD236-H2

In this process 7 individual binders were obtained (figure 4.5). 2 from pannings on monomers (PaD218-E6, PaD233-E5), 2 from pannings on small oligomers (PaD172-F8, PaD172-F12), 2 from pannings on large oligomers (PaD235-D2, PaD236-H2) and 1 from a panning on fibrils (PaD213-A5).
These antibodies were either chosen for their unique specificity (PaD213-A5), their above average absorption or because of their high signal to noise ratio in the screening ELISAs.
Sequence analysis substantiated that all 8 binders obtained from the HAL7 and PaD153.1/153.2 libraries were unique antibodies.

table 4.2: **summary of antibodies obtained from panning**
total number of clones investigated from all 4 libraries, specific hits and unique binders isolated

	libraries		
	HAL7/8	**PaD153.1/.2**	**total**
clones investigated	3236	2852	6088
hits	2	610	612
unique binders	1	7	8

4.4 Conversion into the scFv-Fc format and production in a 50 mL scale

For large scale productions the antibodies were subcloned in mammalian expression vectors. The phage display vector pHAL14 (human naive library) HAL7/8 or pHAL35 (immune library) was digested with *Nco*I and *Not*I to obtain the scFv coding regions spanning V_H and V_L and as well as the linker. Target vectors for mammalian cell production were the vectors pCSE2.5-HIS-XP for monovalent scFv expression and pCSE2.5-hIgG1-Fc-XP for the bivalent scFv-Fc format.
For antibody production eukaryotic HEK293-6E cells were transfected via PEI and cultivated in suspension in a 50 mL scale over a period of 5 days. The antibodies were

purified from the supernatant by affinity chromatography via Ni-NTA (scFvs) or Protein A (scFv-Fcs) in the Profinia™ system and protein concentration was photometrically determined at A_{280nm} (table 4.3).

The volumetric yields of the scFv-Fc productions ranged from 14 mg/L for PaD218-E6-Fc to about 60 mg/L for PaD97-D6-Fc whereas scFvs were produced significantly better with yields from about 14 mg/L for PaD218-E6 to 400 mg/L for PaD97-D6.

Remarkably, the order of yields per clone from highest to lowest is the same for both formats with PaD97-D6 being produced best and PaD218-E6 obtaining the lowest concentration.

PaD172-F8, PaD218-E6 and PaD235-D2 were not produced properly and disregarded for the following experiments.

table 4.3: **yields of antibody production in different formats**
yields of scFvs and the corresponding scFv-Fcs after production in 50 mL scale in HEK293-6E cells

	yield [mg/L]	
antibody	**scFv**	**scFv-Fc**
PaD97-D6	392.0	57.6
PaD172-F8	2.4	0.0
PaD172-F12	40.0	37.6
PaD213-A5	296.0	44.8
PaD218-E6	13.6	14.4
PaD233-E5	32.8	17.6
PaD235-D2	4.0	0.0
PaD236-H2	32.0	56.8

4.5 Specificity determination on Aβ42 aggregates

Antigen specificity was determined with antibodies in the scFv-Fc format via titration ELISA on different forms of Aβ42: monomers, small, medium and large size oligomers and fibrils. Bovine Serum Albumin (BSA) was used as negative control (figure 4.6).

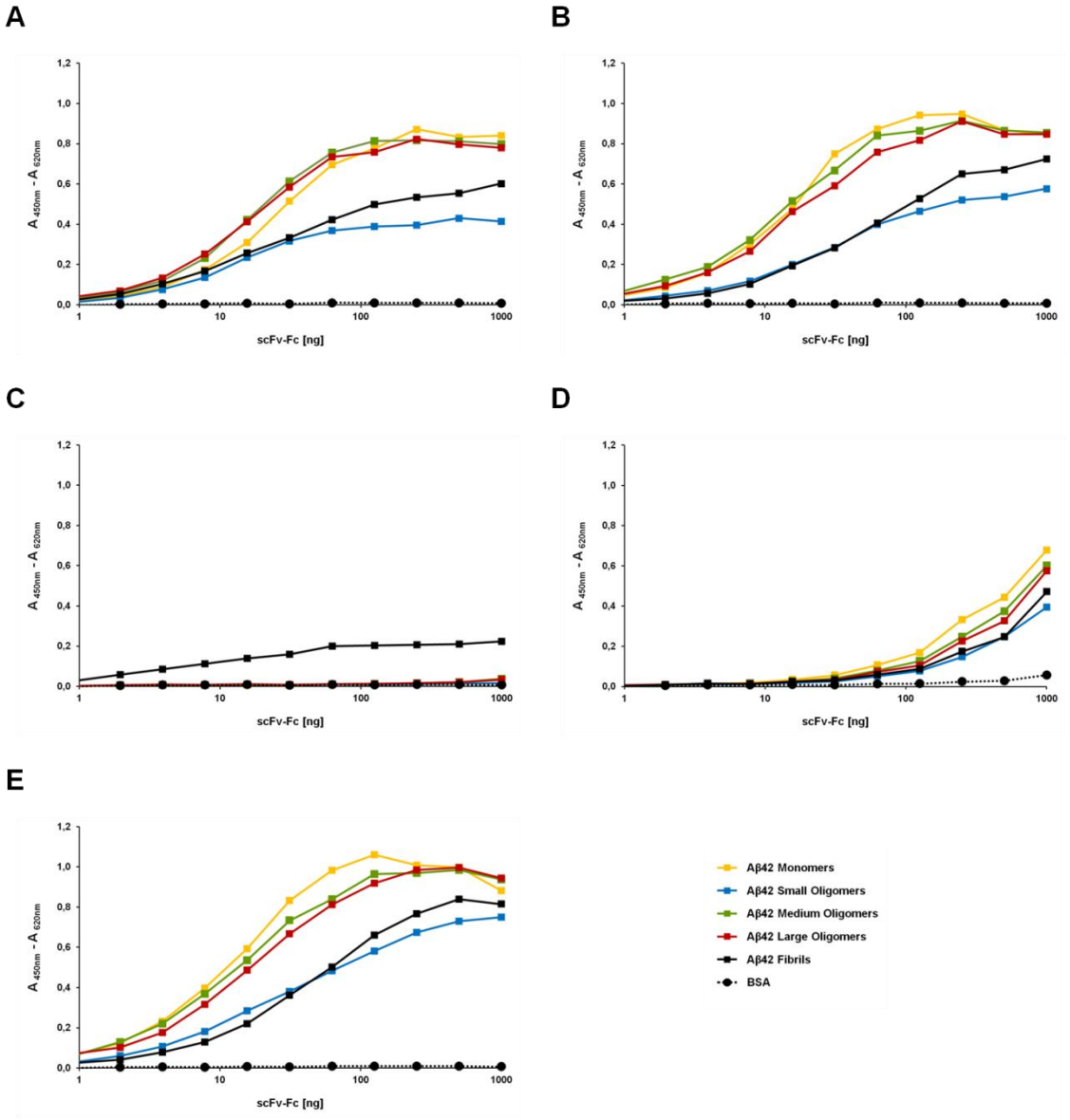

figure 4.6: **specificity determination of antibodies on various forms of Aβ42**
titration ELISA of **(A)** PaD97-D6-Fc, **(B)** PaD172-F12-Fc, **(C)** PaD213-A5-Fc, **(D)** PaD233-E5-Fc and **(E)** PaD236-H2-Fc on Aβ42 monomers (yellow), small oligomers (blue), medium oligomers (green), large oligomers (red), fibrils (black) and BSA (dotted black)

None of the antibodies bound to the negative control peptides but only PaD213-A5 distinguished between different forms of Aβ42 as it specifically detected Aβ42 fibrils. Strikingly the EC_{50} among four of the five tested antibodies in the scFv-Fc format is around 15 ng with the exception of PaD233-E5-Fc. This antibody didn't reach saturation but by estimation of the curve progression the EC_{50} is roughly 500 ng.

4.5.1 Specificity determination on other amyloidogenic peptides

The specificities of the antibodies were further evaluated by ELISA on various amyloidogenic peptides in their fibril forms to check for unspecific binding to the preserved beta-sheet structures (figure 4.7).

The fibrils were derived from the peptides Aβ40, α-Synuclein, Huntington peptides aa 105 - 138 (Htt105-138) and three Tau variants namely wildtype (Tau-wt), the region spanning the four microtubuli binding repeats K18 of Tau (Tau-K18) and the PHF6 motif in the K18 region (Tau-PHF6). Aβ42 protofibrils and fibrils served as positive controls.

All Aβ42 specific antibodies also exhibited binding to Aβ40. Aβ40 differs from Aβ42 only by a C-terminal truncation of two amino acids. The signals on Aβ40 and Aβ42 indicated that none of the scFv-Fcs detect the C-terminal region of the peptides.

PaD97-D6-Fc showed elevated binding to Tau WT.

PaD172-F12-Fc, PaD233-E5-Fc and PaD236-H2-Fc were all specific for Aβ40 and Aβ42 and didn't show elevated affinity towards any of the other fibrils.

Surprisingly, PaD213-A5-Fc did not exhibit binding to any of the antigens including the positive controls Aβ42 protofibrils and fibrils.

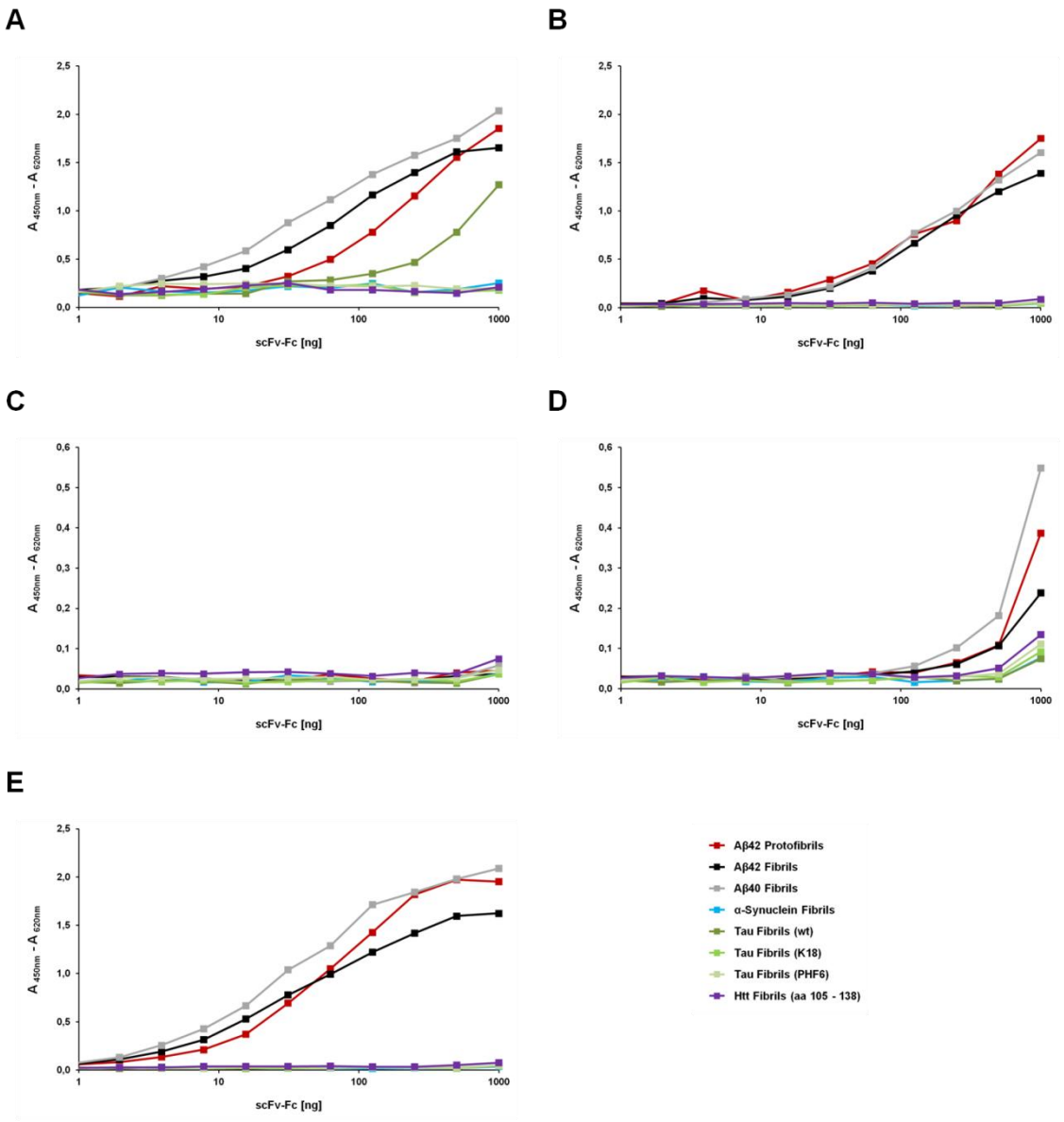

figure 4.7: **specificity determination of antibodies on various amyloidogenic peptides** titration ELISA of **(A)** PaD97-D6-Fc, **(B)** PaD172-F12-Fc, **(C)** PaD213-A5-Fc, **(D)** PaD233-E5-Fc and **(E)** PaD236-H2-Fc on Aβ42 protofibrils (red), Aβ42 fibrils (black), Aβ40 fibrils (grey), α-synuclein (blue), various Tau fibrils (green) and Htt (aa 105 - 138) fibrils (pink)

4.5.2 Specificity of PaD213-A5 towards different types of Aβ42 fibrils

The discrepancy in the Aβ42 fibrils between the two specificity ELISAs was the purification of the peptides in varying buffers. To further investigate the selective binding of PaD213-A5 Aβ42 monomers were purified in Tris-HCl, pH 7.4 and in 100 mM Na-Borate, pH 8.6. Afterwards, fibrils were obtained by incubation at 37 °C and 300 rpm in a 1.5 mL reaction tube for 24 h.

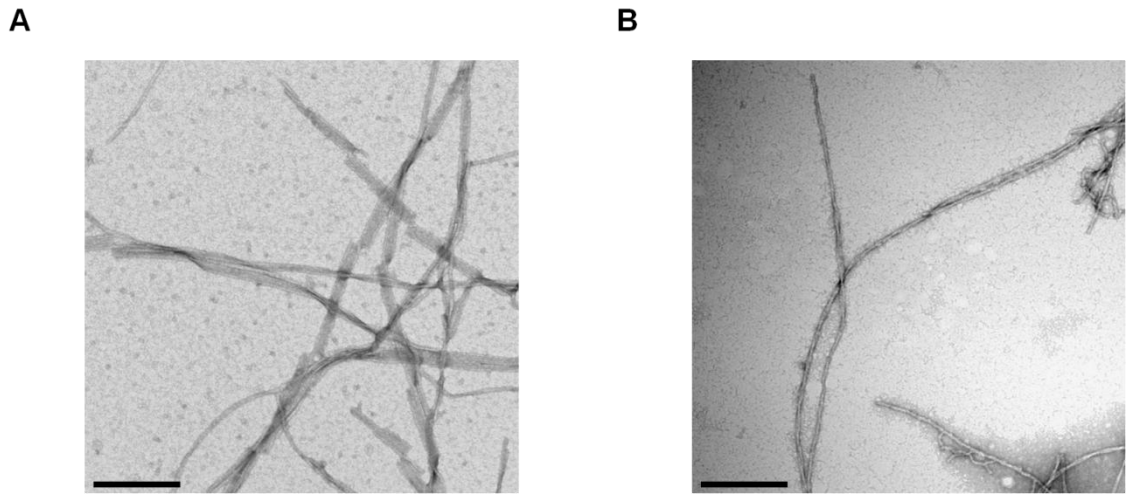

figure 4.8: difference in Aβ42 fibrils structures depending on pH
representative TEM images of Aβ42 fibrils obtained from monomers purified in (A) 100 mM Na-Borate, pH 8.6 or (B) 10 mM Tris-HCl, pH 7.4, the scale bar corresponds to 200 nm

Surprisingly, PaD213-A5 only bound to the fibrils that were produced in 100 mM Na-Borate, pH 8.6 (figure 4.9). Comparison of both types of fibrils via TEM exhibited a major difference in their quaternary structures (figure 4.8). While fibrils from Tris buffer consisted of one discrete Fibril, twisted helically around its axis about every 50 nm, Na-Borate derived fibrils showed a compact bundle of 4 to 8 individual fibrils with a helical twist every 130 - 150 nm.

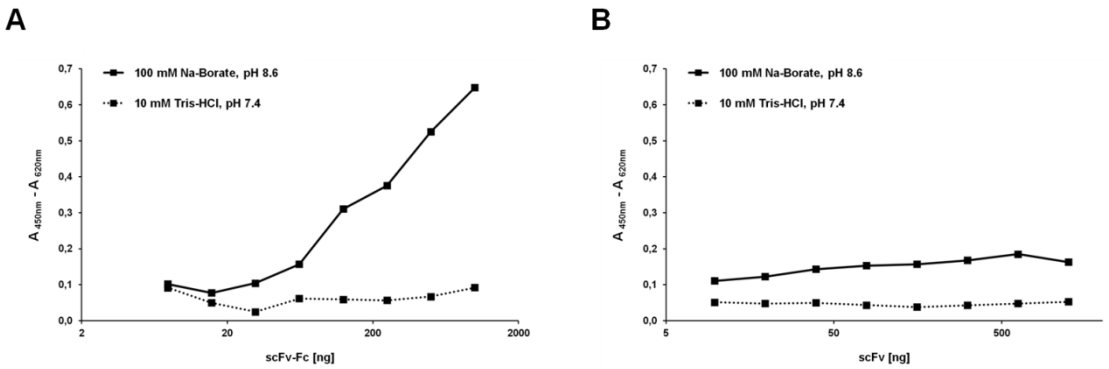

figure 4.9: **specificity of PaD213-A5 towards different Aβ42 fibrils**
titration ELISA of PaD213-A5 as **(A)** scFv-Fc and **(B)** scFv on Aβ42 fibrils obtained from monomers purified in 100 mM Na-Borate, pH 8.6 or 10 mM Tris-HCl, pH 7.4

4.6 Immunoblot analysis

To render more precisely if the antibodies could discriminate between different aggregates a Western Blot with subsequent Immunostaining was carried out. Total protein load was further assessed by Coomassie- and Silverstaining showing major bands below 10 kDa and at approximately 15 kDa (figure 4.10).

PaD97-D6-Fc, PaD172-F12-Fc and PaD236-H2-Fc did not discriminate between specific states of aggregation of Aβ42 and detected Aβ42 aggregates from monomers, running at an aberrant height of 8 kDa, to complex aggregates with a size considerably larger than 170 kDa.

PaD233-E5-Fc showed unspecific staining of the PVDF membrane.

PaD213-A5-Fc as a Aβ42 fibrils specific antibody did not detect any forms of Aβ42.

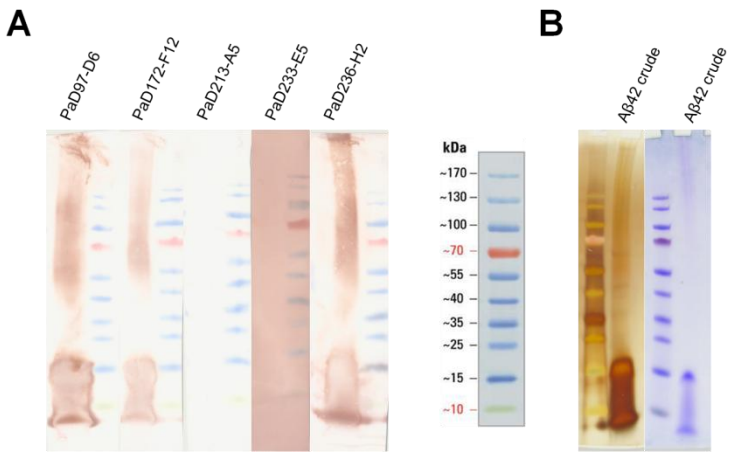

figure 4.10: **staining of crude Aβ42 mixture after SDS-PAGE**
crude Aβ42 was separated on a 4 - 12 % Novex BisTris gradient gel, **(A)** immunostaining with scFv-Fc antibodies after protein transfer to a PVDF membrane, **(B)** verification of protein load by silver- and Coomassie staining

To circumvent the problem of separation of larger aggregates with SDS-PAGE and the difference in signals due to diverse concentrations a Dot-blot was performed on Aβ42 monomers, protofibrils and fibrils (figure 4.11) on a nitrocellulose membrane to circumvent unspecific staining as occurred with the PVDF membrane (figure 4.10).
Again, PaD97-D6-Fc, PaD172-F12-Fc, PaD233-E5-Fc and PaD236-H2-Fc stained all three forms of aggregates while PaD213-A5-Fc only detected Aβ42 fibrils.
Contrary to the other three antibodies, PaD213-A5-Fc and PaD233-E5-Fc exhibited poor staining.

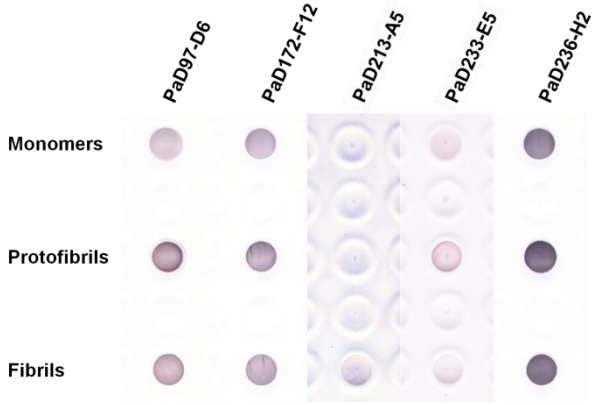

figure 4.11: **dot blot on Aβ42 monomers, protofibrils and fibrils**
2.5 µg per antigen was spotted on nitrocellulose membrane followed by immunostaining with scFv-Fc antibodies

Cellulose peptide spot membranes were used for the determination of the exact epitopes of the antibodies (figure 4.12). Each spot on the membrane consisted of 15 AA of the Aβ42 peptide with an offset of 1 AA to specifically define the epitope.
PaD97-D6, PaD172-F12 and PaD236-H2 all detected N-terminal epitopes spanning the AA from position 1 to 13 "DAEFRHDSGYEVH" (PaD97-D6), 4 to 13 "FRHDSGYEVH" (PaD172-F12) and 5 to 13 "RHDSGYEVH" (PaD236-H2). PaD233-E5-Fc targets the central region of Aβ42 spanning the AA 17 to 22 "LVFFAE". Again, as with the Dot blot, PaD233-E5 showed no cross reactivity with the cellulose membrane.
PaD213-A5-Fc is Aβ42 Fibril specific and showed no staining (data not shown).

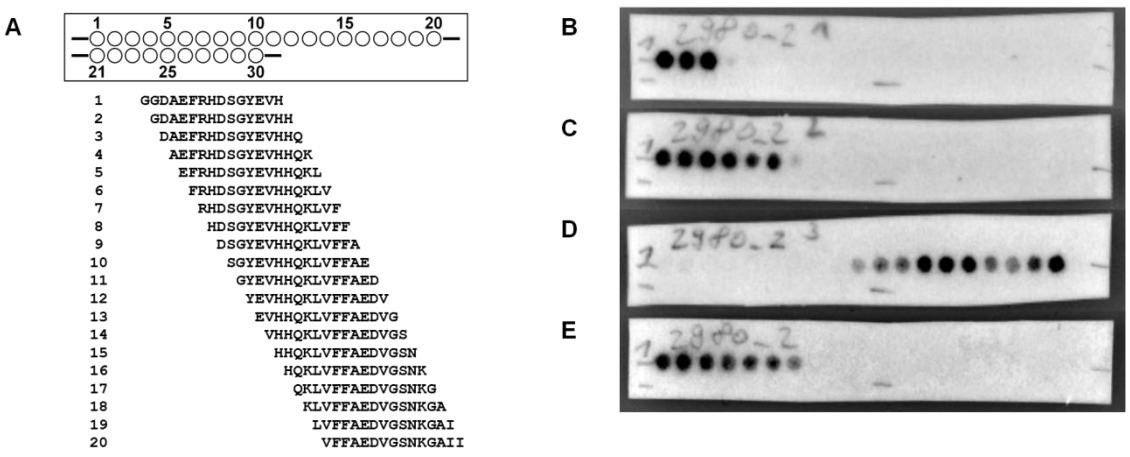

figure 4.12: epitope mapping
(A) distribution of peptide spots on the membrane and the amino acid sequence per spot, immunostaining of the epitope membranes for **(B)** PaD97-D6, **(C)** PaD172-F12, **(D)** PaD233-E5 and **(E)** PaD236-H2

The N-terminal epitopes are in the same region on the Aβ42 peptide although they differ in the first amino acid indicating variable attachments of the antibodies to the peptide. PaD97-D6, PaD172-F12 and PaD236-H2 bind to an unstructured part (random coil) of the β-amyloid peptide whereas PaD233-E5 detects the α-helical core of Aβ42 (figure 4.13).

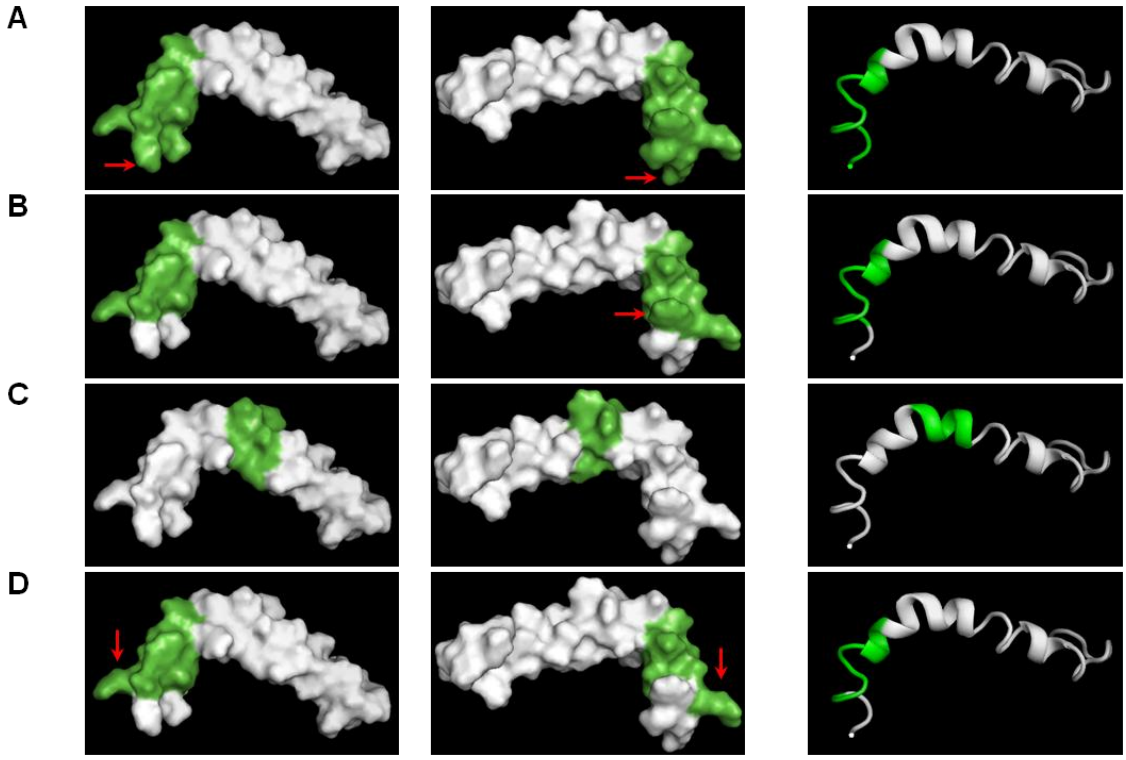

figure 4.13: **visualization of the epitopes on a Aβ42 molecule**
area of the potential epitopes are colored green for **(A)** PaD97-D6, **(B)** PaD172-F12, **(C)** PaD233-E5 and **(D)** PaD236-H2, red arrow in (A), (B) and (D) to visualize the protrusion of the first amino acid

4.7 SPR analysis for affinity measurement of antibodies

To investigate the exact affinities towards different aggregated forms of Aβ42 SPR measurements were carried out (figure 4.14 and table 4.4). The three Aβ42 antigens comprised monomers, protofibrils and fibrils.

PaD97-D6 exhibited a dominant affinity towards Aβ42 fibrils, a twofold and fourfold increase respectively in comparison to Aβ42 monomers and protofibrils.

PaD172-F12 and PaD236-H2 showed nearly equal affinity to the three different forms of aggregates of beta-amyloid with a K_D of around $1*10^{-6}$ M for PaD172-F12 and a K_D between 3.5 and $6.2*10^{-6}$ M for PaD236-H2.

PaD233-E5 demonstrated a clear preference to Aβ42 monomers with a more than 100fold increased affinity over Aβ42 protofibrils and fibrils.

PaD213-A5 exhibited binding only on Aβ42 fibrils with a K_D of $3.7*10^{-6}$ M.

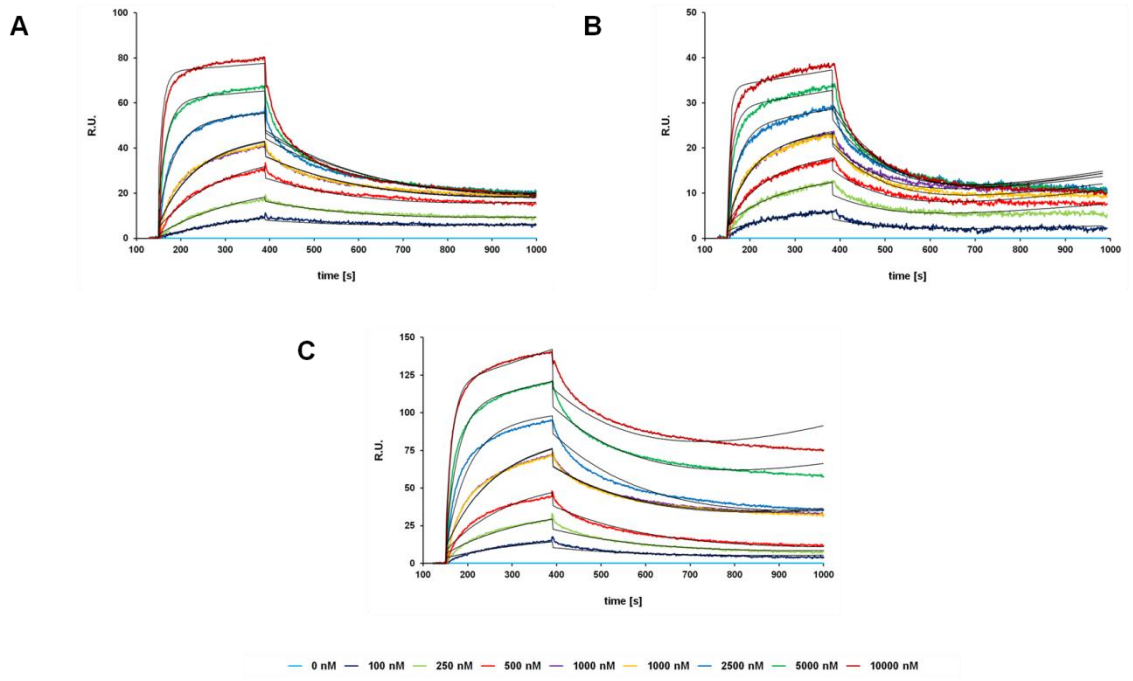

figure 4.14: **analysis of affinity by SPR measurement**
example of SPR measurements for different concentrations of PaD236-H2 on **(A)** Aβ42 monomers, **(B)** Aβ42 protofibrils and **(C)** Aβ42 fibrils

table 4.4: **affinity measurements on Aβ42 monomers, protofibrils and mature fibrils**
k_a: association rate, k_d: dissociation rate, Chi^2: error, K_D: binding constant

Antibody	Antigen [Aβ42]	k_a [1/Ms]	k_d [1/s]	Chi^2	K_D [M]
PaD97-D6	monomers	$2.7*10^3$	$6.2*10^{-3}$	4.9%	**$2.3*10^{-6}$**
	protofibrils	$1.7*10^3$	$7.3*10^{-3}$	2.4%	**$4.2*10^{-6}$**
	fibrils	$3.7*10^3$	$3.3*10^{-3}$	2.3%	**$9.1*10^{-7}$**
PaD172-F12	monomers	$5.5*10^3$	$5.1*10^{-3}$	2.4%	**$9.4*10^{-7}$**
	protofibrils	$7.9*10^3$	$1.1*10^{-2}$	1.7%	**$1.5*10^{-6}$**
	fibrils	$6.0*10^3$	$5.5*10^{-3}$	2.4%	**$9.2*10^{-7}$**
PaD213-A5	monomers				
	protofibrils			no binding	
	fibrils	$6.3*10^2$	$2.4*10^{-3}$	1.1%	**$3.7*10^{-6}$**
PaD233-E5	monomers	$1.4*10^3$	$1.5*10^{-5}$	6.6%	**$1.0*10^{-8}$**
	protofibrils	$2.2*10^3$	$8.1*10^{-3}$	1.4%	**$3.6*10^{-6}$**
	fibrils	$4.0*10^3$	$4.8*10^{-3}$	1.4%	**$1.2*10^{-6}$**
PaD236-H2	monomers	$9.5*10^3$	$3.3*10^{-3}$	2.5%	**$3.5*10^{-7}$**
	protofibrils	$1.2*10^4$	$7.2*10^{-3}$	1.9%	**$5.8*10^{-7}$**
	fibrils	$6.0*10^3$	$3.7*10^{-3}$	5.7%	**$6.2*10^{-7}$**

4.8 Inhibition of Aβ42 fibrillization by antibody addition

4.8.1 Inhibition of fibrillization by addition of scFv-Fcs

To investigate the effect of the antibodies on the inhibition of Aβ42 fibrillogenesis 5 µM of Aβ42 monomers were incubated with various concentrations of scFv-Fcs (molar ratio 1:10, 2:10 and 4:10 antibody:Aβ42 monomers) over the time course of 96 h. Fibrillogenesis was assessed via ThT fluorescence and visualized by TEM. No significant changes in the ThT fluorescence were observed after 48 h of incubation (figure 4.15). TEM pictures were taken after 48 h incubation of the 2 µM antibody sample (figure 4.16).PaD172-F12-Fc and PaD213-A5-Fc as well as the negative control (TM43-E10-Fc) showed no inhibiting properties while PaD97-D6-Fc, PaD233-E5-Fc and PaD236-H2-Fc displayed inhibition in a concentration dependent manner.

Incubation with 0.5 µM, 1 µM or 2 µM of Pad172-F12-Fc, PaD213-A5-Fc or the negative control showed no statistic deviations in the ThT fluorescence compared to the negative control. Antibody addition resulted in mature paired Aβ42 fibrils, no considerable aggregates were visible.

Addition of 2 µM PaD97-D6-Fc reduced ThT fluorescence by 30 %.

PaD236-H2-Fc displayed a decrease of 20 % ThT fluorescence for 0.5 µM and 1 µM and 50 % for 2 µM compared to the negative control. Incubation with PaD97-D6-Fc and PaD236-H2-Fc resulted in shortened single fibrils with a length of 100 - 400 nm as well as small circular aggregates with a diameter of about 15 - 20 nm.

PaD233-E5-Fc displayed the strongest impact on the fibrillization process. ThT fluorescence was decreased to 60 % (0.5 µM, 1 µM) and 50 % (2 µM) respectively. After 48 h incubation small unstructured Aβ42 aggregates were visible ranging from 15 nm - 100 nm in length.

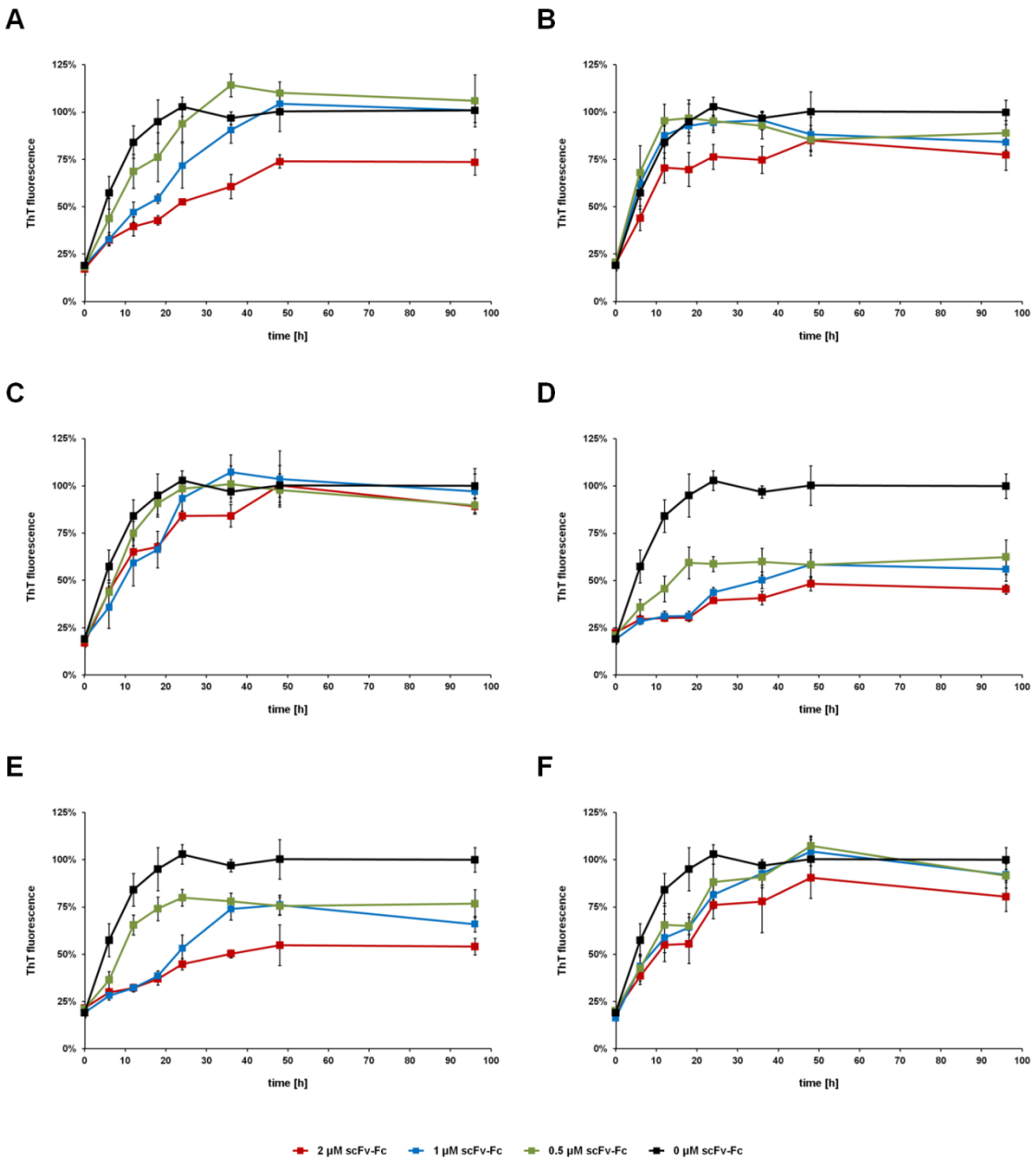

figure 4.15: **influence of scFv-Fc antibody addition on Aβ42 fibrillogenesis**
ThT measurement of **(A)** PaD97-D6-Fc, **(B)** PaD172-F12-Fc, **(C)** PaD213-A5-Fc, **(D)** PaD233-E5-Fc, **(E)** PaD236-H2 or **(F)** a negative control scFv-Fc, antibodies were added to 5 µM of Aβ42 monomers with a concentration of 2 µM (red), 1 µM (blue), 0.5 µM (green) or 0 µM (black) to monitor the impact on Aβ42 fibrillogenesis

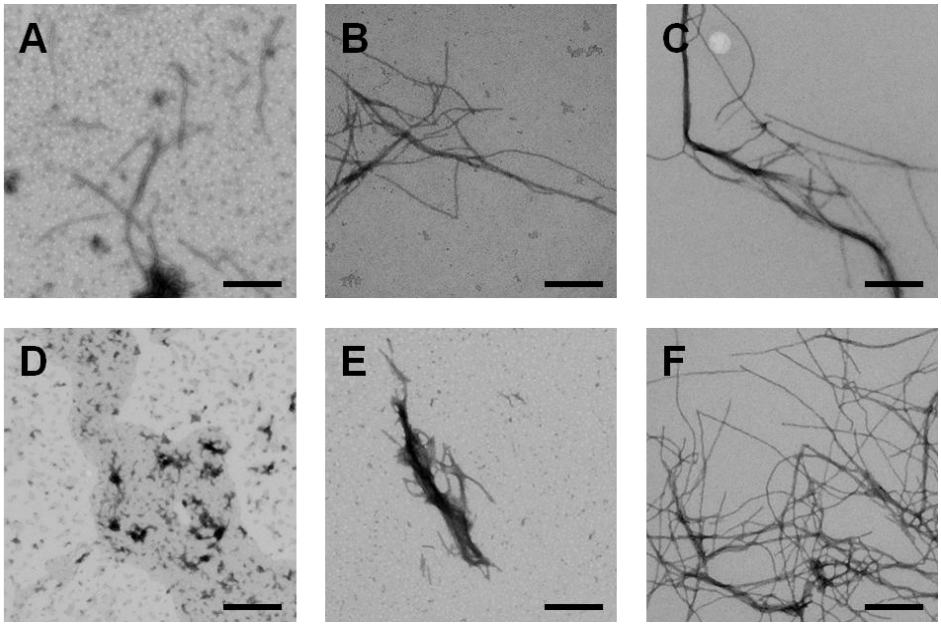

figure 4.16: Aβ42 fibrils after incubation with scFv-Fc antibodies for 96 h
representative TEM images of Aβ42 fibrils 96 h after addition of 2 µM of **(A)** PaD97-D6-Fc, **(B)** PaD172-F12-Fc, **(C)** PaD213-A5-Fc, **(D)** PaD233-E5-Fc, **(E)** PaD236-H2-Fc and **(F)** negative control antibody, scale bar corresponds to 400 nm

4.8.2 Inhibition of fibrillization by addition of scFvs

To examine the effect of the antibodies on the inhibition of Aβ42 fibrillogenesis 5 µM of monomers were incubated with various concentrations of scFvs (molar ratio 2:10, 4:10 and 8:10 antibody:Aβ42 monomers) over the time course of 96 h. The elevated ratio was due to the monovalent properties of the scFv in comparison to the bivalent scFv-Fc format.

Fibrillogenesis was assessed via ThT fluorescence and visualized by TEM. No significant changes in the ThT fluorescence were observed after 48 h of incubation (figure 4.17). TEM pictures were taken after 36 h incubation of the 4 µM antibody sample (figure 4.18).PaD97-D6 is the sole antibody that did not exhibit a decline in ThT fluorescence over the 48 h time course. All other scFvs showed a concentration dependent retardation in Aβ fibrillogenesis of over 50 % for the highest antibody concentration, most explicitly PaD233-E5 and the negative control (JoZ42-C4) with up to 70 % reduction in ThT fluorescence.

When comparing these signals to the TEM pictures it became apparent that fibrillogenesis was in fact not reduced or stopped for any scFv with the exception of PaD233-E5 and to a low extent PaD213-A5.

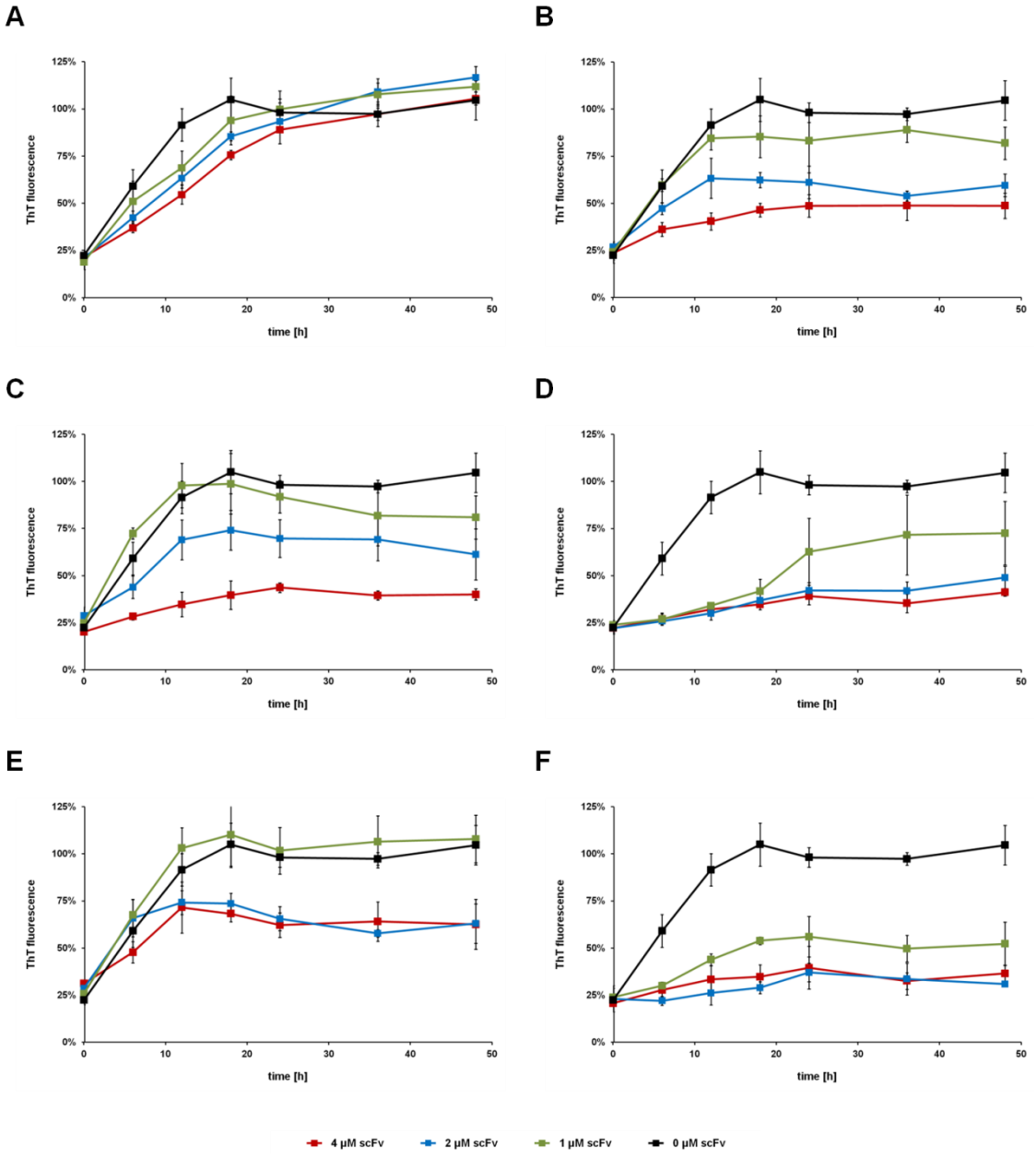

figure 4.17: **influence of scFv antibody addition on Aβ42 fibrillogenesis**
ThT measurement of **(A)** PaD97-D6, **(B)** PaD172-F12, **(C)** PaD213-A5, **(D)** PaD233-E5, **(E)** PaD236 or **(F)** a negative control scFv, antibodies were added to 5 µM of Aβ42 monomers with a concentration of 4 µM (red), 2 µM (blue), 1 µM (green) or 0 µM (black) to monitor the impact on Aβ42 fibrillogenesis

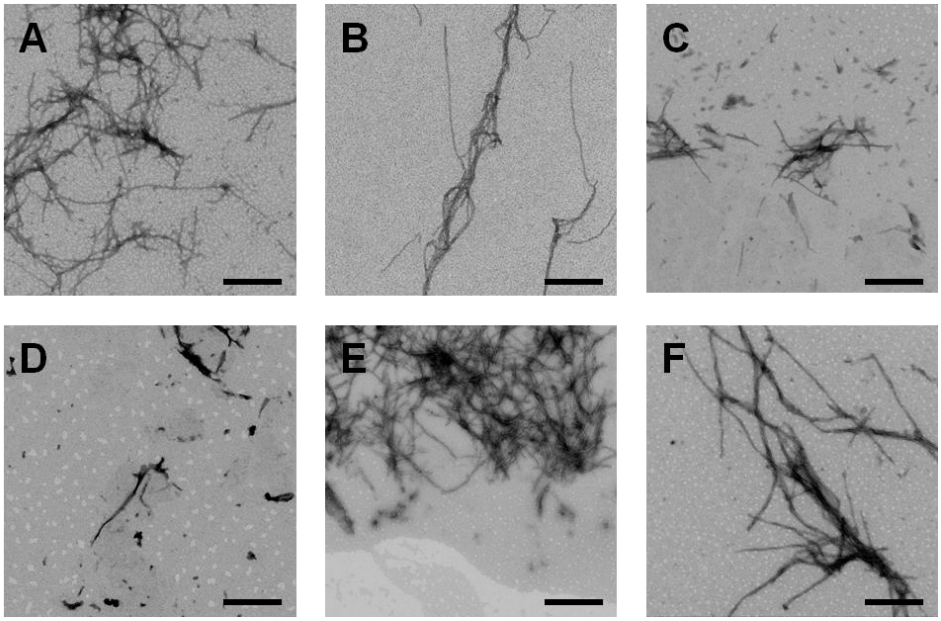

figure 4.18: Aβ42 fibrils after incubation with scFv antibodies for 96 h
representative TEM images of Aβ42 fibrils 96 h after addition of 4 µM of **(A)** PaD97-D6, **(B)** PaD172-F12, **(C)** PaD213-A5, **(D)** PaD233-E5, **(E)** PaD236-H2 and **(F)** negative control antibody, scale bar corresponds to 400 nm

4.8.3 Elution buffer influence on the inhibition of fibrillization

Due to the discrepancy between the TEM pictures and the ThT fluorescence measurements of the inhibition via scFvs the buffer solutions of both antibody formats (scFv and scFv-Fc) were examined in reference to their ability to interfere with ThT measurements. Surprisingly, while the Protein-A elution buffer exhibited no effect on the measurement the Ni-NTA elution buffer decreased ThT fluorescence by 50 % (figure 4.19). This influence interfered solely with the fluorescence measurement and not with fibrillogenesis as indicated by the negative control scFv sample (JoZ42-C4).

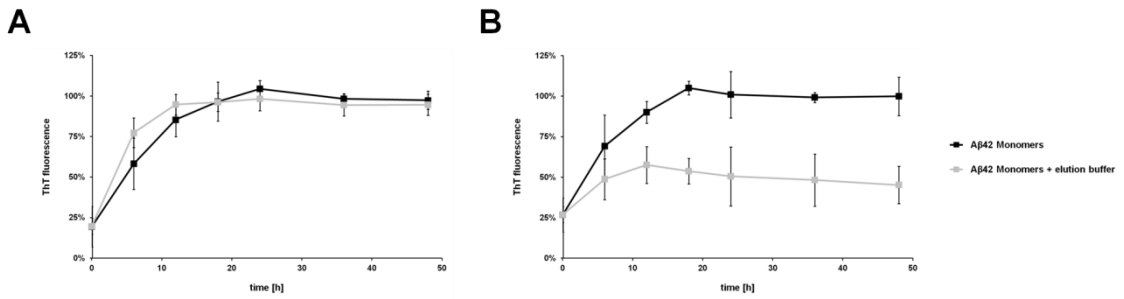

figure 4.19: influence of the elution buffer on the absorbance of Thioflavin T
influence of the **(A)** Protein-A elution buffer for scFv-Fc antibodies and **(B)** the His-Tag elution buffer for scFv antibodies on the absorbance measurement of ThT

4.9 Disaggregation of preexisting Aβ42 fibrils by addition of scFv-Fcs

The disaggregation of preexisting fibrils is a tool to observe the potential of plaque clearance of β-amyloid specific antibodies *in vitro*. To test the effect of the antibodies on the disaggregation of preexisting Aβ42 fibrils 5 µM of fibrils were incubated with various concentrations of scFv-Fcs (molar ratio 1:10, 2:10 and 4:10 antibody:Aβ42 monomers) over the time course of 96 h. The presence of Aβ42 fibrils was assessed by ThT fluorescence.

Because of the inhibitory effects of the Ni-NTA elution buffer on the fibrillogenesis of Aβ42 monomers no scFv antibodies were tested.

None of the antibodies showed a significant impact on the stability of mature Aβ42 fibrils as indicated by the consistent ThT fluorescence over the time period of 48 h (figure 4.20). Hence no antibody decomposed the ordered fibrilar structure into small aggregates or even monomers.

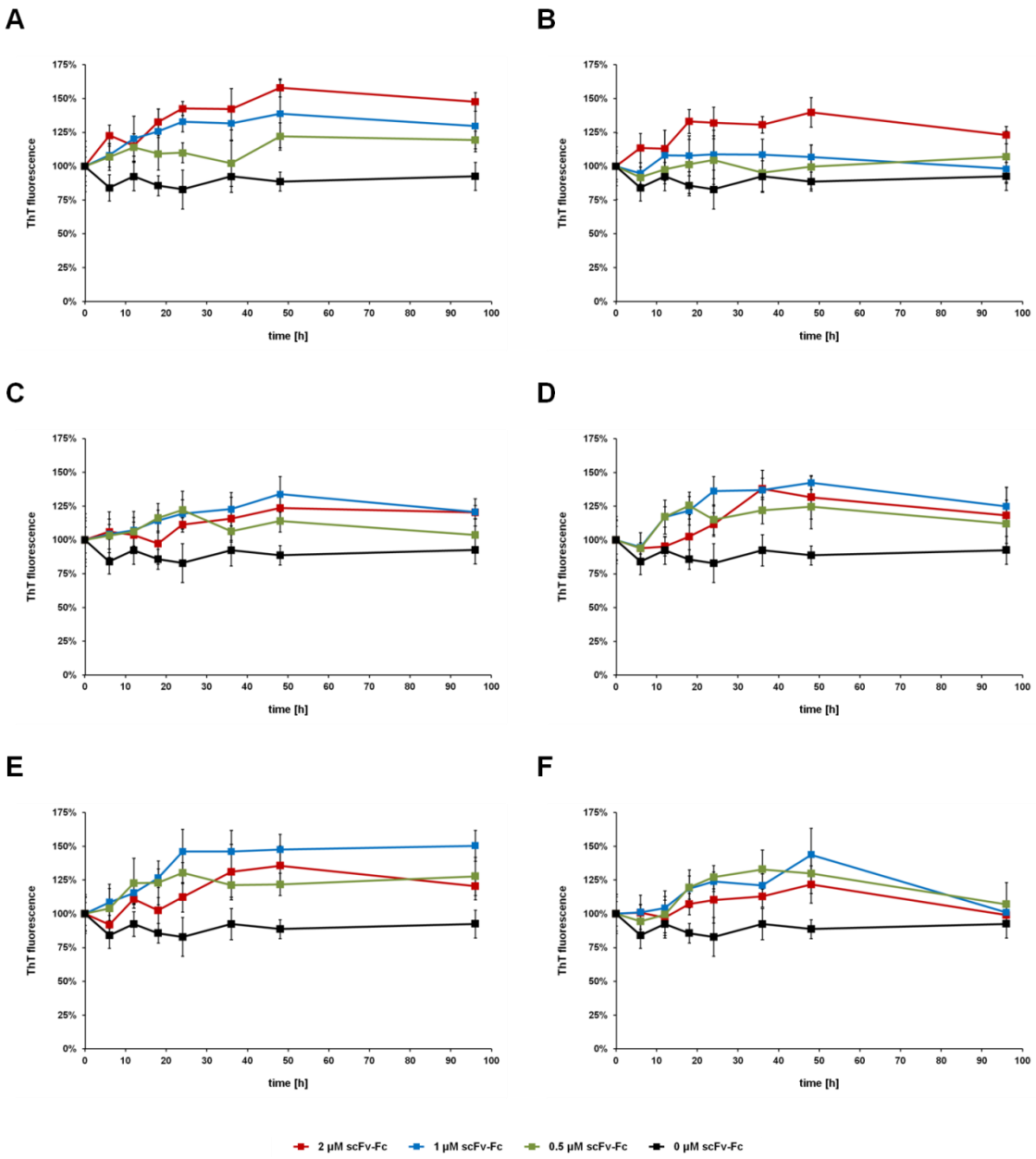

figure 4.20: **influence of scFv-Fcs on the disaggregation of preformed Aβ42 fibrils**
ThT measurement of **(A)** PaD97-D6-Fc, **(B)** PaD172-F12-Fc, **(C)** PaD213-A5-Fc, **(D)** PaD233-E5-Fc, **(E)** PaD236-H2 or **(F)** a negative control scFv-Fc, antibodies were added to 5 µM of Aβ42 fibrils with a concentration of 2 µM (red), 1 µM (blue), 0.5 µM (green) or 0 µM (black) to monitor the impact on preformed Aβ42 fibrils

4.10 Aβ42 induced cytotoxicity in human SH-SY5Y cells

The crude Aβ42 peptide (Aβ42-CR) consists of a mixture of monomers and protofibrils and has a substantial effect on the cells, even causing cell death if applied in high dosage. To test if this effect can be obviated by antibodies binding to the amyloid-β peptide, human SH-SY5Y cells were subjected to increasing concentrations of Aβ42-CR and a constant amount of antibodies. Toxicity and metabolism impairment was assessed by FACS (PI staining) and MTT reduction assay.

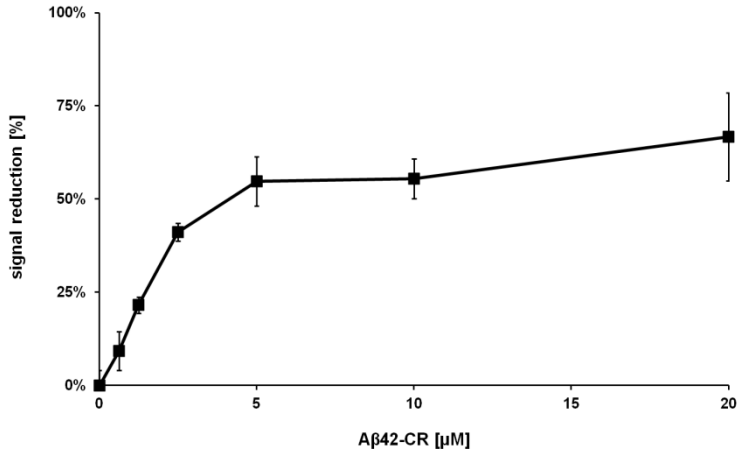

figure 4.21: influence of Aβ42 peptide on the SH-SY5Y cells metabolism
40,000 SH-SY5Y cells were incubated for 24 h with different concentrations of Aβ42-CR, the impact of the peptide was determined by MTT reduction assay

Aβ42-CR has an inhibitory effect on the metabolism of SH-SY5Y cells in a concentration dependent manner (figure 4.21). Addition of 1.25 µM Aβ42-CR to 40,000 cells resulted in a MTT signal reduction of almost 25 % and addition of 5 - 20µM resulted in a MTT signal reduction of 50 % and more compared to the untreated sample after 24 h of incubation. This effect is not attributed to cell death as verified by PI staining (figure 4.22). Only the 20 µM Aβ42 crude sample showed a distinct decrease in total cell count and viable cells with nearly 70 % of the remaining cells being PI positive, thus verifying cell death.

The impact of 10 µM Aβ42 crude was clearly more pronounced after a total of 48 h of incubation, indicating a time dependent toxicity of Aβ42 crude (data not shown).

4. Results

For the toxicity assay 1 µM - 4 µM of Aβ42-CR was incubated on 35,000 cells. The concentrations were chosen from the prior MTT reduction assay for its pronounced decrease in absorption. PI staining indicated that the antibodies had no toxic effect on the SH-SY5Y cells over the 24 h time course of the experiment (figure 4.23).

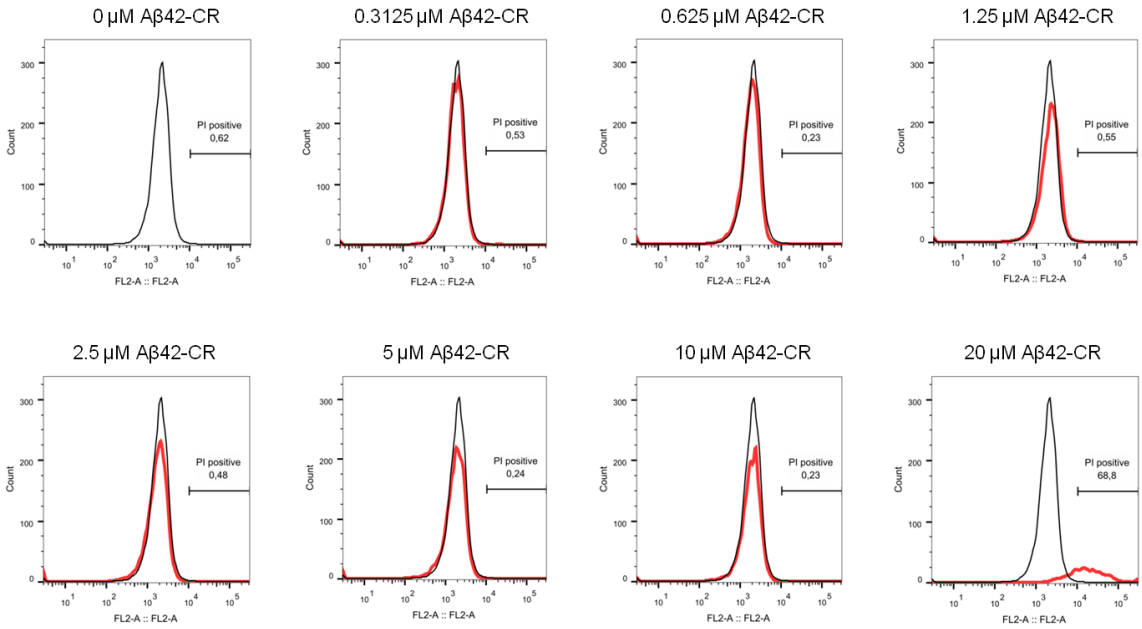

figure 4.22: **FACS analysis of Aβ42-CR toxicity**
40,000 SH-SY5Y cells were incubated for 24 h with different concentrations of Aβ42-CR, toxicity was assessed by FACS via PI staining by correlation the Aβ42-CR treated population (red curve) to untreated cells (black curve)

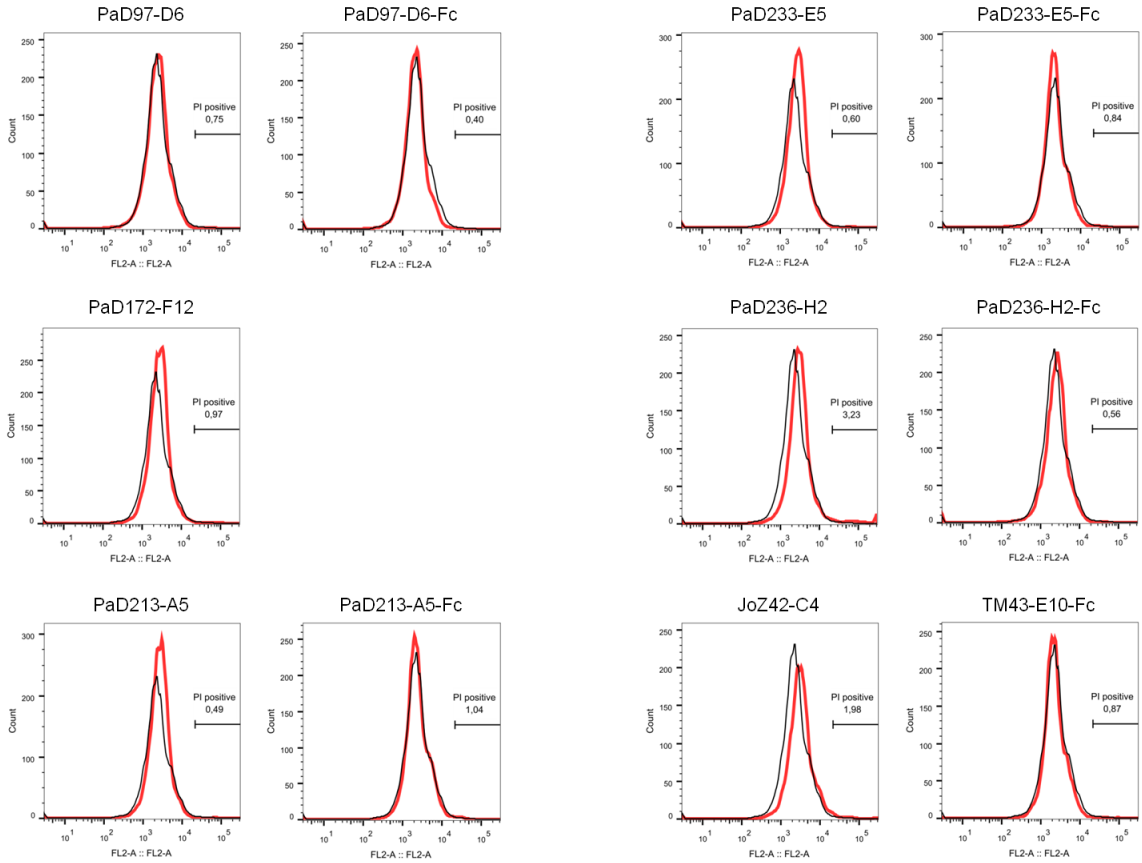

figure 4.23: **FACS analysis of antibody toxicity**
40,000 SH-SY5Y cells were incubated for 24 h with 1 µM of scFv or 0.4 µM of scFv-Fc antibody, toxicity was assessed by FACS via PI staining by correlation the antibody treated population (red curve) to untreated cells (black curve)

4.10.1 Inhibition of Aβ42 induced cytotoxicity by scFv administration

To investigate an antibody induced rescue of the Aβ42-CR effect, cells were treated with 1 µM scFv in addition to the 1 µM, 2 µM or 4 µM of toxic antigen (molar ratio of 1:1, 1:2 and 1:5) (figure 4.24).

At a molar ratio of 1:1 all scFv antibodies exhibited a beneficial influence on the cells metabolism with a rescue of 30 % for PaD172-F12 and up to roughly 40 % for PaD213-A5.

A positive effect is still present with 2 µM Aβ-CR but solely for PaD97-D6 with a rescue of close to 40 % and more surprisingly for PaD213-A5 with a very high significantly increased rescue of 50 %.

At a concentration of 4 µM Aβ42-CR PaD213-A5 is the only scFv that exhibits an effect with a very high significant rescue of 20 %.

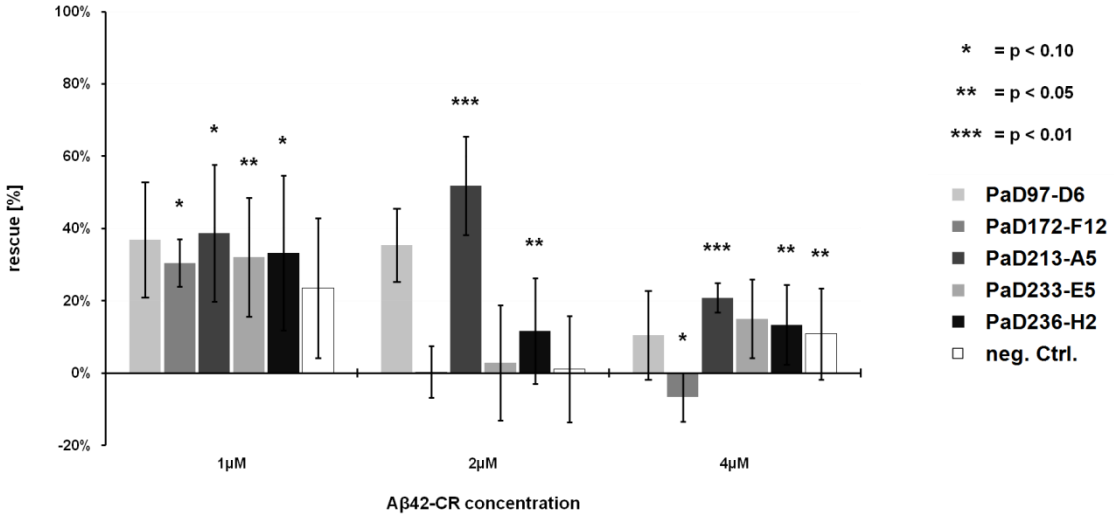

figure 4.24: **inhibition of Aβ42-CR induced cytotoxicity by scFv administration**
35,000 SH-SY5Y cells were co incubated for 24 h with 1 µM of scFv antibody and increasing concentrations of Aβ42-CR, rescue was determined by MTT absorbance measurement, untreated cells were set to 100 %, cells with Aβ42 were set to 0 %

4.10.2 Inhibition of Aβ42 induced cytotoxicity by scFv-Fcs administration

To investigate an antibody induced rescue of the Aβ42 crude effect by addition of scFv-Fc antibodies, cells were treated with 0.4 µM scFv-Fc in addition to the 1 µM, 2 µM or 4 µM of toxic antigen (molar ratio of 1:2.5, 1:5 and 1:10).

The results for the scFv-Fc antibody treatment differ profoundly from the ones retrieved for scFv antibodies (figure 4.25).

At a molar ratio of 1:2.5 only PaD97-D6-Fc and PaD213-A5-Fc exhibited a highly significant rescue of the cells metabolism with 35 % for PaD97-D6-Fc and close to 50 % for PaD213-A5.

PaD97-D6-Fc is the sole scFv-Fc antibody that shows an effect at a molar ratio of 1:5 with 35 % and a very high significance.

No scFv-Fc antibody has any impact on the cells metabolism at a molar ratio of 1:10.

The effect of PaD172-F12-Fc could not be investigated.

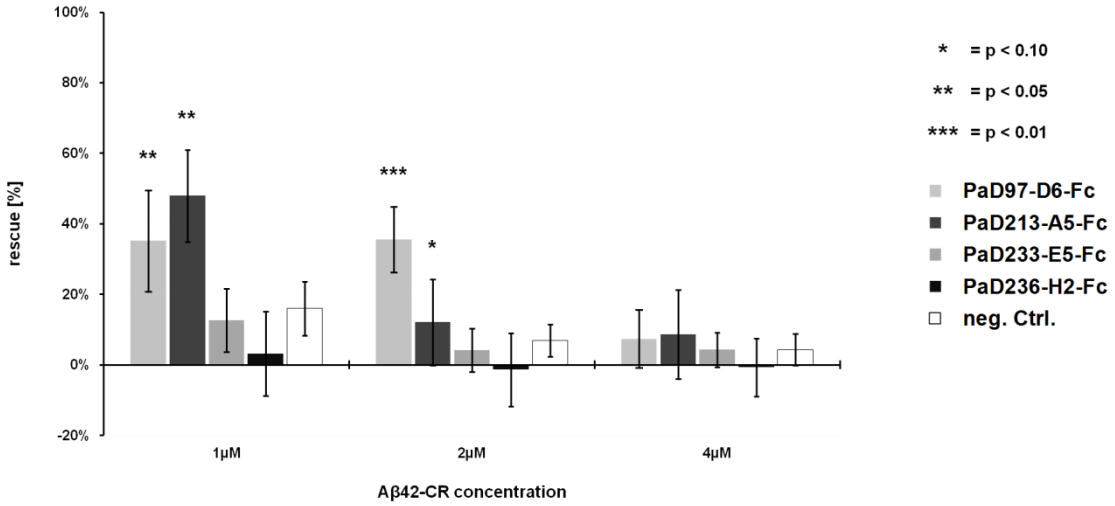

figure 4.25: inhibition of Aβ42-CR induced cytotoxicity by scFv-Fc administration
35,000 SH-SY5Y cells were co incubated for 24 h with 0.4 µM of scFv-Fc antibody and increasing concentrations of Aβ42-CR, rescue was determined by MTT absorbance measurement, untreated cells were set to 100 %, cells with Aβ42 were set to 0 %

5. Discussion

Alzheimer's Disease (AD) is a neurodegenerative disorder and the most common form of dementia in the elderly today. As of 2012, 35.6 Million people worldwide and 1.4 Million in Germany alone are affected by dementia with 60 - 80% of these cases being attributed to AD. These numbers will most likely more than triple by the year 2050 resulting in costs exceeding 1 trillion dollars annually (www.who.int, www.deutsche-alzheimer.de, world alzheimer report 2013). To suppress the progress of the disease most efficiently it is essential to start potential therapies early, making the need for a diagnostic tool that detects AD at a presymptomatic stage highly desirable.

One of the key proteins that play a role in the progression of AD is the amyloid-β peptide. It is released from the amyloid precursor protein (APP), a type 1 transmembrane protein, via subsequent cleavage by β- and γ-secretase resulting predominantly in peptides of 40 or 42 amino acid length, hence the terms Aβ40/42. These peptides have the tendency to aggregate forming the extracellular amyloid plaques that are, together with the intracellular neurofibrillary tangles (NFTs) comprised of hyperphosphorylated Tau protein, the characteristic histological hallmarks for AD. Previous studies have shown that not the insoluble fibrillar form of β-amyloid but rather the soluble oligomers are the neurotoxic species making it one of the main goals to monitor the incidence and distribution of specific Aβ oligomers in the brain and correlate their abundance to disease progression. Here, highly selective antibodies that can discriminate between different forms of amyloid-β appear to be promising tools to investigate the structure-function correlation of Aβ42 aggregates of diverse morphologies.

In this dissertation, antibodies were isolated that can discriminate between distinct forms of Aβ42. Small oligomers were used for immunization to establish an immune phage display library. After a selection process and a broad screening approach from this library and the well established naive human libraries HAL7/8 (Hust et al., 2011),

several antibodies were discovered which were further evaluated with diverse biophysical and biochemical methods.

5.1 Antigen preparation

The main focus in obtaining highly specific antibodies is the homogeneity of the antigen. In this dissertation the purification was carried out by FPLC in different buffers depending on the later purpose of the β-amyloid fractions as described by Jan et al. (Jan et al., 2010b).

Pure Aβ42 monomers were obtained by the dissolution of the peptide in 6M Guanidin-HCl (Gn-HCl) and subsequent size exclusion chromatography (SEC). The corresponding transmission electron microscopy (TEM) pictures verified the purity of these fractions that showed no contamination with larger aggregates. However, the possibility of very small oligomeric aggregates appearing must not be excluded by analysis of the SEC and TEM data alone since Aβ42 monomers are very unstable and aggregate rapidly at concentrations above a critical threshold. These impurities can have a strong effect on the outcome of subsequent panning and screening procedures. The purification after dissolution of the peptide in DMSO via one column resulted in two peaks, one monomer and one protofibrils peak. Aβ42 protofibrils are a heterogeneous mixture of larger aggregates and high molecular weight oligomers of diverse morphologies and sizes, with diameters of 8 - 10 nm and a length of up to 200 nm (Jan et al., 2010b; Lashuel et al., 2003; Walsh et al., 1999). To obtain distinct forms of β-amyloid oligomers of more narrowly confined sizes a wider separation is achieved by connecting two columns in series (Jan et al., 2010a).

5.2 Generation of immune libraries and obtaining specific antibodies

Antibody phage display is a technology to obtain highly specific antibodies *in vitro* by a process called "panning" - similar to affinity chromatography. Generating antibodies

that are highly selective for a certain form of Aβ42 aggregates is not only depending on the purity of the antigen utilized in the panning process, it also involves a library with a great variety of binders against the desired target. To increase the possibilities of obtaining antibodies that are highly selective for one form of Aβ42 but show low affinity towards any other forms a β-amyloid specific immune phage display library was constructed. For this, a male non human primate (*Macaca fascicularis*) was immunized with small oligomers of Aβ42 as previously described (Rülker et al., 2012). This antigen was specifically chosen for immunization since it is regarded as the most toxic form of β-amyloid (Haass and Selkoe, 2007) and antibodies detecting Aβ oligomers might give a deeper insight into the link between β-amyloid distribution in the brain and the progression of AD. The generated immune libraries PaD153.1 and PaD153.2 present a combined theoretical diversity of $2.9*10^7$ clones and the also applied naive human phage display libraries HAL7/8 contained $5.2*10^9$ scFvs (Hust et al., 2011). The advantage of an immune phage display library is the enrichment with highly selective and affine binders against the desired target due to the immunization process thus providing a large source of potentially specific antibodies.

Library packaging into phage particles was carried out with two different types of helperphage, Hyperphage (Rondot et al., 2001) and M13K07. In contrast to the remote scFv presentation on the M13K07 phage, Hyperphage exhibited a nearly 1:1 ratio of wt pIII and scFv::pIII fusion protein. Because of the mutated gene for pIII which makes the fusion protein of scFv and pIII the sole source for the minor coat protein, Hyperphage allows for an oligovalent display of scFvs on its surface (Rondot et al., 2001). A presentation of more than one antibody and the accompanied avidity effects might be advantageous when obtaining binders from naive libraries such as HAL7/8 that, contrary to immune phage display libraries, have a smaller percentage of specific binders in their repertoires. In the case of immune libraries with a supposed vast majority of antibodies directed against the target antigen a monovalent display, as provided by M13KO7 phage, is favored because of the increased possibility of selecting more affine binders.

To select for scFvs, HAL7/8 and PaD153.1/153.2 were incubated on five different antigen preparations with or without competition of other Aβ42 preparations. Together, 8 unique antibodies were obtained from these libraries with PaD97-D6 emerging from

HAL7 and PaD172-F8, PaD172-F12, PaD213-A5, PaD218-E6, PaD233-E5, PaD235-D2 and PaD236-H2 from the immune libraries PaD153.1/153.2.

5.3 Assessment of antibody properties with biochemical and biophysical methods

For further studies all scFvs were additionally converted into the scFv-Fc format. The scFv-Fc format is a dimer consisting of two scFvs connected to a human IgG1 Fc part giving the antibody similarities with a natural occurring Immunoglobulin G (Moutel et al., 2009). For example, the dimerization results in a stabilization of the antibody making it more applicable for long term incubation studies (Fennell et al., 2013). Production in mammalian cell culture and purification by affinity chromatography of scFvs and scFv-Fcs resulted in large quantities with close to zero impurities. Three antibodies (PaD172-F8, PaD218-E6 and PaD235-D2) were repeatedly produced in such low yields that further studies could not be conducted.

Specificity of the five remaining antibodies was initially investigated by ELISA on various forms of Aβ42 oligomers, monomers and fibrils. PaD97-D6, PaD172-F12, PaD233-E5 and PaD236-H2 exhibited nearly equal affinity to all forms of Aβ42 while PaD213-A5 showed selective binding to fibrillar aggregates alone.

The unique conformational arrangement that all amyloid fibrils share is a cross β-sheet (Fändrich, 2007). To exclude the possibility that the investigated antibodies interacting unspecifically with these structures the binding to other amyloidogenic peptides was analyzed. Again, PaD97-D6, PaD172-F12, PaD233-E5 and PaD236-H2 bound equally strong to Aβ42 protofibrils and fibrils as well as Aβ40 fibrils, indicating the detection of a conserved epitope among the investigated forms that does not include the C-terminus of the peptide since Aβ40 is missing two amino acids at the carboxy-terminal end compared to Aβ42. Furthermore, PaD97-D6 exhibited an elevated affinity towards Tau (wt) fibrils that is not due to sequence homologies of Aβ42 and any Tau isoform. A plausible explanation would be a structural homology between Tau (wt) and Aβ42 that was not further investigated in this dissertation.

The absence of specific antibodies isolated by the panning process and the resulting lack of differentiation between the various aggregates of Aβ42 is influenced by three main factors. First, the integrity of the antigen can be compromised due to the binding to the plastic surface of the ELISA cavities during the panning process which can result in the unfolding of the protein and subsequentially the loss of conformational epitopes. This risk can be circumvented by capturing the antigen with another antibody thus keeping its conformation intact. While this set up is thought to retain the β-aymloid in its native form it increases the risk of an undesired masking of the epitope with the capture antibody. Albeit multiple approaches being carried out no binders were identified in this work. The second factor that might play a role are the possible interactions between the β-aymloid peptide and a hydrophobic part of the M13 major coat protein pVIII. The pVIII, abundantly expressed with nearly 2700 copies on the phage surface, has a hydrophobic middle part (Haigh and Webster, 1998) that might be able to interact with the hydrophobic sections on the surface of Aβ42 (Chen and Glabe, 2006). The third, and most significant factor for the lack of differentiation is the transient nature of the β-amyloid antigen. The additional amino acids Isoleucine and Alanine at the C-terminus of Aβ42, compared to Aβ40, contribute greatly to the hydrophobicity of the peptide and elevate the interaction with itself. The outcome of this interaction of monomers and oligomers are metastable entities that exhibit diverse morphologies accompanied by a multitude of exposed epitopes during the panning process making Aβ42 monomers and oligomers rather challenging targets for antibody generation.

In contrast to the other binders, PaD213-A5 showed a highly selective behavior towards Aβ42 fibrils and did not detect any other β-amyloid form, including Aβ40 fibrils. Compared to monomers and oligomers, fibrils are thermodynamically more stable making them an easier to handle antigen when generating antibodies against Aβ42. Interestingly, the exact preparation of β-amyloid fibrils plays a vital role for the binding of PaD213-A5. In this work Aβ42 monomers were purified in two different buffers, namely 10 mM Tris-HCl with a pH of 7.4 and 100 mM Na-Borate with a pH of 8.6. Fibrils are derived from these monomers by prolonged incubation at a physiological temperature of 37 °C. Depending on the chosen buffer, the fibrils show major differences in their morphologies regarding the number of individual fibers packed together and the resulting width as well as the crossover distance giving the fibrils their typical twisted structure (Chamberlain et al., 2000). These distinctions are most likely

being induced by the difference in the buffer pH. It can be assumed that PaD213-A5 distinguishes between both types of fibrils through the detection of a conformational epitope spanned by the interspace between the two single strands that make up the mature β-amyloid Fibril (Meinhardt et al., 2009). This Fibril specificity was not detectable with the other antibodies.

The problem with evaluating the specificity of the antibodies via ELISA lays within the purity of the antigen fractions. By separation via SEC with two columns connected in series it is possible to obtain Aβ42 oligomers of various sizes, yet it is impossible to obtain only a single sort of macromolecule (e.g. only decamers). Hence, an exact separation in order of size is highly desirable. For this challenge crude Aβ42 peptide containing divers forms ranging from monomers to large protofibrils, was solubilized and separated by gradient PAA-gels. While multiple bands or a more prominent smear at higher molecular weights would be expect to be seen on the stained gel, SDS disaggregates Aβ42 protofibrils resulting in predominant bands at low molecular weights, i.e. monomers, di- and trimers (Walsh et al., 1997). Another explanation for these predominant bands is that protofibrils exist in a rapid equilibrium with low molecular weight oligomers (Bitan et al., 2005) and disintegrate during SDS-PAGE. PaD97-D6, PaD172-F12 and PaD236-H2 stained all forms of β-amyloid ranging from monomers to large aggregates that remained in the gel pockets and could not penetrate the gel due to their size. Taken together with the results from the dotblot carried out on distinct forms of Aβ42 aggregates, it is confirmed that these antibodies do not detect a certain conformational variant of Aβ42. PaD213-A5 reprised the already described specificity by exhibiting no binding to any form other than mature fibrils. The unspecific binding of PaD233-E5 to the PVDF membrane is most likely due to hydrophobic interactions between the membrane and the scFv. ScFvs are not natural but engineered antibody fragments consisting of the two variable parts of a Fab fragment connected by a linker. The removal of the constant domains C_L and C_H can result in an exposition of hydrophobic patches at the former interface between variable and constant domain (Nieba et al., 1997). These patches can play a role in the hydrophobic effect and ultimately might explain the interaction of PaD233-E5 and the PVDF membrane. This hypothesis is supported by the lack of unspecific staining of the nitrocellulose membrane.

Three of the four non specific antibodies detected epitopes at the amino terminal end of

Aβ42. PaD97-D6 spanned $Aβ_{1-13}$ (DAEFRHDSGYEVH) while PaD172-F12 and PaD236-H2 bound further downstream with $Aβ_{4-13}$ (FRHDSGYEVH) for PaD172-F12 and $Aβ_{5-13}$ (RHDSGYEVH) for PaD236-H2. The sequences start with the first amino acid that is essential for antibody binding but the precise epitope cannot be detected with this set-up since the peptide spots comprised 15 amino acids each. Even though the majority of B-cell epitopes vary between 5 - 20 amino acids in size (EL-Manzalawy et al., 2008; Singh et al., 2013) shorter peptide spots would have been needed to locate also the last amino acid accurately. There are various antibodies that detect epitopes of the same sequences. Most notably, the murine antibody 3D6, better known as Bapineuzumab (the name of its humanized form), binding to $Aβ_{1-5}$ (DAEFR) (Johnson-Wood et al., 1997) similar to PaD97-D6. Like PaD172-F12 and PaD236-H2, various antibodies have been described that are also directed against the N-terminus of β-amyloid without including the first amino acids. Examples are the Hybridoma clones 10D5 recognizing $Aβ_{3-6}$ (EFRH) (Bacskai et al., 2002), 12A11 binding to $Aβ_{3-7}$ (EFRHD) (Bard et al., 2003) or W0-2 detecting $Aβ_{5-8}$ (RHDS) (Ida et al., 1996). These results contribute to the previous findings that the amino-terminal region of Aβ42 (1-16) is immunodominant in non human primate (Lemere et al., 2004) and human forms of β-amyloid (Lee et al., 2005). For PaD233-E5, the epitope was traced in more detail as $Aβ_{17-22}$ (LVFFAE), a part of the hydrophobic core element (LVFF) that plays an essential role in β-sheet formation during the process of fibrillization (Hilbich et al., 1992). Important representatives of antibodies detecting the central region of Aβ42 are the murine antibody m266, better known as Solanezumab (the name of its humanized form), binding to $Aβ_{16-24}$ (KLFFAEDV) (Moreth et al., 2013) and 4G8 binding to $Aβ_{17-24}$ (LVFFAEDV) (Kang et al., 2013). PaD213-A5 did not stain any spot on the membrane since the antibody is conformation specific for Aβ42 fibrils. The lack of staining is either due to the alteration of the tertiary structure of the Aβ42 monomer due to fibrillization or an epitope that is spanned by more than one Fibril, i.e. the detection of a specific Fibril arrangement. A similar antibody is WO1, described by O'Nuallain et al. But while PaD213-A5 binds to Aβ42 fibrils alone WO1 additionally binds other amyloid fibrils suggesting the detection of the cross β-sheet structure retained by all (O'Nuallain and Wetzel, 2002).

To merge the results from the titration ELISAs and Immunoblot analysis to a value of specific affinity, SPR measurements on divers Aβ42 preparations were carried out.

5. Discussion

Consistent with the results obtained so far, the antibodies directed against the N-terminal part of Aβ42, PaD97-D6, PaD172-F12 and PaD236-H2, did not show any preference to either monomers, protofibrils or mature fibrils but bound all forms with roughly the same affinity. While PaD233-E5 also detected all forms of Aβ42 here investigated, it exhibited a significantly increased affinity towards Aβ42 monomers. A previously described scFv directed against the same epitope as PaD233-E5 showed identical affinities to monomers as for oligomers of various sizes (Nisbet et al., 2013) while for m266 and its humanized version Solanezumab specificity towards soluble Aβ42 (monomers and oligomers) was also described and binding to amyloid plaques, i.e. fibrils, could not be detected (Dodart et al., 2002).The elevated affinity of PaD233-E5 towards Aβ42 monomers most likely lays within the easier accessibility of the epitope in that specific conformational state. Consistent with the previous results PaD213-A5 only exhibited binding to Aβ42 fibrils. All antibodies showed remote binding ranging from low micromolar (10^{-6} M) to high nanomolar (10^{-7} M) affinities towards the antigens while other scFvs directed against Aβ42 from naive human scFv libraries (Liu et al., 2004; Wang et al., 2009) or derived from Hybridoma clones (Cattepoel et al., 2011; Robert et al., 2009) show 10- to 100fold higher affinities in the medium to low nanomolar range (10^{-8} - 10^{-9} M).

The aim throughout all pannings was to obtain highly selective binders that would distinguish between different aggregates of β-amyloid, hence the competition with a multitude of competitor antigens. This technique can theoretically improve affinity because of the selection pressure applied to phage with a fast off-rate. But the effect might be averted and the low affinities could be attributed to the before mentioned hydrophobic interaction between β-amyloid and the major phage coat protein pVIII resulting in an elevated apparent affinity during the panning process that is lost when the obtained antibody fragments are solubly expressed. With the set up utilized in this work and taking the results of the antibody production and ELISA assays into account it is more probable that an enrichment of scFvs with improved production yields in *E. coli* was achieved.

5.4 Antibodies impact the fibrillization of Aβ42 but lack effects on fibril disaggregation

After the biochemical and biophysical characterizations the impact of these Aβ42 specific antibodies on β-amyloid was examined in terms of the efficacy to retard fibrillogenesis and disaggregate preformed fibrils as well as the potential inhibition of toxicity towards mammalian cells.

The fibrillogenesis of Aβ42 is a nucleation-dependent polymerization process that can be sub-divided into three stages (Harper and Lansbury, 1997). The first stage, the lag phase, is where monomers interact but the formation of stable entities is not thermodynamically favored. However, above a certain concentration threshold small aggregates termed "nuclei" accrue and polymerization starts. During the second stage, the growth phase, these nuclei are elongated by addition of monomers forming larger aggregates. In the third and last stage, the steady state phase, monomers and fibrils have reached an equilibrium and the concentration of free monomers in solution is below the critical concentration threshold.

Addition of antibodies to a monomer solution during the lag phase can intervene in the initial aggregation by preventing interactions of β-amyloid peptides thus retarding or even inhibiting the polymerization process (Solomon et al., 1996). To investigate this potential, β-amyloid monomers were co-incubated with different but in all cases substoichiometric concentrations of scFv and scFv-Fc antibodies.

The differentiation between scFvs and scFv-Fcs allows for discriminating the results in regards of a higher stability of the scFv-Fcs or to verify if the bivalent form contributes in another way to the impact of the antibody on Aβ42 such as crosslinking or by avidity effects. Various antibodies that target the amino-terminal end of amyloid-β exhibited an inhibitory effect on the fibrillogenesis (Frenkel et al., 2000; Legleiter et al., 2004). Legleiter et al. could show a reduction for the number of fibrils as well as a decrease in length for the 3D6 antibody. As previously described, this initial murine form of Bapineuzumab binds $A\beta_{1\text{-}5}$ suggesting that PaD97-D6 behaves in a familiar way. Actually, PaD97-D6 does show a concentration dependent retardation in fibril formation. This effect is slightly more pronounced visible for PaD236-H2 which binds four amino acids downstream of the amino terminus of Aβ42. A similar mode of action as for PaD236-H2 was described for W0-2 or polyclonal mouse sera specifically

detecting $A\beta_{4-10}$ (McLaurin et al., 2002; Robert et al., 2009). While PaD97-D6 and PaD236-H2 slow down the formation of β-amyloid fibrils they do not prevent fibrillogenesis in total when using substoichiometric concentrations of antibodies. This indicates a possible steric hindrance provoked by the attachment of scFv-Fcs at least partially masking the amyloid-β sequence elements necessary for accumulation of β-amyloid and mature fibril formation. Why PaD172-F12, also directed against the amino terminal end of Aβ42, does not possess any inhibiting potential remains unclear although a plausible explanation might be indicated by the epitope sequence. PaD172-F12 specifically recognizes an epitope starting with the Arginine at position $A\beta_5$. This amino acid is directed away from the core element of LFVV ($A\beta_{17-20}$) which is as previously mentioned essential for fibril formation, suggesting that the antibody binding does not interfere with the accumulation of amyloid-β monomers. PaD233-E5 specifically detects $A\beta_{17-22}$, spanning this core element and consequentially exhibiting the strongest effect on fibril formation similar to m266, the murine form of Solanezumab (Legleiter et al., 2004). The underlying mechanism with this antibody is similar to PaD97-D6 or PaD236-H2 but three modes of action are plausible. Either the steric hindrance is much more potent due to the binding of the antibody to the center of Aβ42 thus completely preventing accumulation of other amyloid-β monomers at this site. Or, smaller filamentous Aggregates do appear but elongation is prevented by binding of the antibody to the ends of the fibrillar entity. The third mode of action is the occupation of Aβ42 monomers and smaller oligomers by PaD233-E5 shifts the concentration threshold of soluble β-amyloid beneath the critical limit and preventing aggregation. PaD213-A5, as anticipated from previous results, has no effect on the formation of fibrils due to its high selectivity solely for Aβ42 fibrils obtained at a basic pH of 8.6.

When comparing the data of the scFv-Fcs to the results obtained from the antibodies in the monovalent scFv format major discrepancies can be witnessed. Every scFv antibody, except PaD97-D6, shows a concentration depended inhibitory effect on fibril growth when measuring the ThT signal. These observations are somewhat unexpected in particular for the negative control since no binding to any form of β-amyloid was detected for this antibody before. Deeper investigation by monitoring the β-amyloid morphologies via electron microscopy revealed mature fibrils for most of the antibodies with the exception for PaD213-A5 and PaD233-E5 which led to the assumption that a compound in the antibody buffer interferes with ThT measurement. Eligible substances

are either trace amounts of Imidazole, resulting from insufficient automated dialysis, or Ni^{2+}, from Nickel leakage of the column. Previous studies have shown that Imidazole does not interfere with ThT fluorescence (Noormägi et al., 2012; Zovo et al., 2010) leaving Nickel as the main culprit for the observed effects. While an inhibitory effect on fibril formation has been described for Nickel (Yu et al., 2010) it does not appear in these experiments leaving the exact cause for the diminished ThT fluorescence in the dark.

The next step in the evaluation process was to determine if the scFv-Fc antibodies have an effect on preformed amyloid-β fibrils *in vitro*. The disaggregation of preexisting fibrils gives an indication of the antibodies' potential of plaque clearance in the brain. The end product of the fibrillization process are mature Aβ42 fibrils that exist in an equilibrium with monomers, meaning rather than to retain a fixed form amyloid-β monomers emerge constantly from the fibrillar backbone and are being replace by other monomers. Jan et al. could demonstrate this constant recycling by addition of Aβ40 monomers to Aβ42 aggregates (Jan et al., 2008). Taking into account this mechanism and the previous results regarding the inhibition of fibril formation obtained from the scFv-Fc antibodies, an interaction of these antibodies with mature fibrils would be something to be expected. Contrary to various other antibodies described in the literature (Mamikonyan et al., 2007; Solomon et al., 1997; Yamada et al., 2009) none of the investigated scFv-Fcs exhibited an impact on the concentration of mature β-amyloid fibrils that was detectable by considerable disaggregation. Plausible are two diverging explanations that are accountable for this effect. At first, the low affinities of the antibodies might play a central role. While 4 out of 5 scFv-Fcs can bind to Aβ42 monomers emerging from the Fibril, the low affinities observed during BIAcore measurement prevent the antibodies from effectively occupying the soluble amyloid-β entities in the pool of available Aβ42 monomers. As a result, there is no disruptive effect on the equilibrium between filamentous and non filamentous amyloid-β and the steady state is maintained. The second effect is a stabilizing force from the scFv-Fcs on the β-amyloid fibrils. The sequestering of Aβ42 monomers is suppressed through the binding of the bivalent antibodies to the Fibril ends. Since the dynamic recycling of monomers only takes place at the ends of the mature Fibril (Jan et al., 2008), the high concentrations of scFv-Fcs in this assay circumvent the lack of affinity of the antibodies.

5.5 Administration of antibodies inhibits Aβ42 induced toxicity

Although none of the antibodies was able to disrupt preexisting fibrils most of them bind all forms of Aβ42 and are, as demonstrated, capable of a concentration dependent prevention of aggregation. This severe influence on β-amyloid fibrillogenesis might play a vital role in preventing cytotoxicity. The manner in which Aβ42 contributes to cell death is still under strong investigation. So far numerous studies have been conducted to elucidate the precise mechanism, identifying multiple ways by, among others, either activating apoptosis (Loo et al., 1993), impairing cellular respiration (Rhein et al., 2009), interfering with cell signaling pathways (Ling et al., 2002; Tran et al., 2002), influence the permeability of the membrane by pore integration (Lashuel, 2005), alter the membrane fluidity (Mason et al., 1999) and polymerization (Jan et al., 2010a) and fibril formation (Okada et al., 2008).

As an initial efficacy investigation and to verify if the obtained antibodies have the potential to prevent Aβ42 induced cytotoxicity the impact of scFvs or scFv-Fcs combined with various amounts of β-amyloid on cells was evaluated by MTT reduction assays and propidiumiodide (PI) staining. MTT can penetrate intact cell membranes and accumulates in metabolic active cells while PI only stains cells if their cell walls are perforated, i.e. dead cells. Hence, when a substance has a cytotoxic effect the MTT absorbance decreases while the PI signal rises. The obtained results show that while Aβ42-CR has a deteriorating effect on the cells metabolism it does not contribute to cell death at concentrations of up to 10 µM Aβ42-CR within the first 24 h.

All scFvs showed a beneficial influence on the cells metabolism at a 1:1 ratio of antibody to Aβ42-CR. While this effect was also detectable for the negative control it's being annihilated by the large range of the standard deviation. PaD97-D6 and PaD213-A5 were the only scFvs that exhibited cytoprotective properties with higher surplus of Aβ42. This tendency was also visible in a similar fashion for the scFv-Fc antibody variants with PaD97-D6-Fc and PaD213-A5-Fc being the only cytoprotective antibodies. Surprisingly, PaD233-E5 did not show any beneficial effect although having a strong impact on retarding fibrillogenesis. Additionally, another antibody binding to the same epitope exhibited a strong influence on amyloid-β induced cytotoxicity (Liu et al., 2004).

The outcome of the toxicity assay diverges from the previous results where PaD97-D6, 233-E5 and PaD236-H2 were potent inhibitors to fibrillogenesis and all antibodies, except the fibril specific PaD213-A5, showed binding to Aβ42 monomers and protofibrils, suggesting to exhibit a stronger effect when inhibiting cytotoxicity. These results show that there is no exact nature in which amyloid-β influences the cells' metabolism and delivers toxic effects but rather a combination of parameters that can be modified by antibody administration.

6. Outlook

The field of antibody research in Alzheimer's Disease has produced a broad range of antibodies that detect different epitopes in β-amyloid but as of now, truly conformational specific antibodies are rare. To monitor the distribution of amyloid-β aggregates in the brain and to determine if the levels correlate to disease progression it is essential to have tools at hand that can discriminate between various Aβ42 morphologies. As demonstrated in this work, the phage display technology is capable of generating specific antibodies against β-amyloid from non-human primate immune libraries and human derived naive libraries that might lay the foundation for a potent differentiation. Establishing an immune phage display library was the first step in elevating the prospects to generate highly selective antibody fragments. The obtained scFvs can be produced in very high yields of close to 400 mg/L and in most cases exhibited no cross reactivity with other amyloidogenic peptides like α-synuclein or various Tau derivates. While three of the five antibodies investigated possessed a general specificity towards β-amyloid it is PaD213-A5 and PaD233-E5 that presented a tendency to certain forms of Aβ42. PaD213-A5 is highly specific for mature Aβ42 fibrils and was able to distinguish between various fibrillar structures depending on the acidity of the surrounding milieu during fibrillogenesis while PaD233-E5, albeit binding also oligomers and fibrils, showed a 100fold increased affinity towards monomers. It is also one of the three antibodies exhibiting an inhibitory effect on the fibrillization of Aβ42 monomers, verified by TEM analysis and reduced ThT absorption. In the subsequent cell culture assay in human SH-SY5Y neuroblastoma cells the antibodies presented a protective effect on the β-amyloid induced influence on the cells metabolism.

All scFvs have been solidly characterized in their biochemical and biophysical properties and their impact on Fibril formation as well as disaggregation. To reveal the full potential of these antibodies it is essential to further examine their effects in a set up that is closer related to the native processes in Alzheimer's Disease which includes

studies on the precise binding patterns *in vivo* by immunohistochemistry in a mouse model and in post mortem brain slices of human AD patients.

7. Abbreviations

(v/v)	Volume per volume
(w/v)	Weight per volume
×g	Earth's gravity
°C	Degree Celsius
2×YT	2×yeast tryptone medium
2×YT-AK	2×yeast tryptone medium with ampicillin and kanamycin
2×YT-GA	2×yeast tryptone medium with glucose and ampicillin
2×YT-T	2×yeast tryptone medium with tetracycline
A	Ampicillin
A_{450}	Absorbance at λ = 450 nm
aa	Amino acid
ab	Antibody
α	Anti
AP	Alcaline phosphatase
AU	Arbitrary units
Aβ	Amyloid-β
BCIP	5-Bromo-4-chloro-3-indolyl phosphate
bp	Base pairs
BSA	Bovine serum albumin
ca.	Circa
CDR	Complementarity determining region
cfu	Colony forming unit
C_H	Constant domain of the antibody's heavy chain
CIP	Calf intestinal phosphatase
C_L	Constant domain of the antibody's light chain
dH_2O	Distilled water
DMEM	Dulbecco's Modified Eagle Medium
DNA	Desoxyribonucleic acid
dNTP	Desoxyribonucleic acid triphosphate
E. coli	Escherichia coli
e.g.	For example (lat. *exempli gratia*)

7. Abbreviations

EDC	1,2-Dichloroethane
EDTA	Ethylenediaminetetraacetic acid
ELISA	Enzyme-linked immunosorbent assay
EtOH	Ethanol
Fab	Fragment antigen binding
FACS	Fluorescence activated cell sorting
Fc	Fragment crystallizable
Fv	Fragment variable
g	Gram
h	Hour
HAL	Human antibody library
HRP	Horseradish peroxidase
i.e.	That is (lat. *id est*)
Ig	Immunoglobulin
IMAC	Immobilized metal ion affinity chromatography
IPTG	Isopropyl β-D-1-thiogalactopyranoside
k_a	Association rate
Kan	Kanamycin
kb	Kilobases
k_d	Dissociation rate
k_D	Binding constant
kDa	Kilodalton
L	Liter
M	Molar concentration (mol/L)
mA	Milliampere
MES	2-(N-morpholino)ethanesulfonic acid
mg	Milligram
µL	Microliter
µM	Micromolar; µmol/L
µm	Micrometer
min	Minute
mL	Milliliter
mM	Millimolar; (mmol/L)
M-PBS(-T)	PBS(-T) with milk powder
MTP	Microtiter plate
MTT	3-(4,5-dimethylthiazol-2-yl)-2,5-diphenyltetrazolium
MW	Molecular weight

NBT	Nitro blue tetrazolium chloride
ng	Nanogram
NHS	N-Hydroxysuccinimide
Ni-NTA	Nitrilotriacetic acid
nm	Nanometer
OD_{600}	Optical density at λ = 600 nm
PAA	Polyacrylamide
PAGE	Polyacrylamide gel electrophoresis
PBS	Phosphate buffered saline
PBS-T	Phosphate buffered saline with Tween20
PCR	Polymerase chain reaction
PEI	Polyethylenimine
pelB	Leader sequence, directs the protein to the periplasm
pHAL35	Phagemid
PI	Propidium iodide
PVDF	Polyvinylidene fluoride
R.U.	Resonance units
rpm	Revolutions per minute
s	Second
scFv	Single chain fragment variable
scFv-Fc	Single chain fragment variable fragment crystallizable fusion
SDS	Sodium dodecyl sulfate
T	Temperature
TAE	Tris Acetate EDTA
TBE	Tris Borate EDTA
TEM	Transmission electron microscopy
TEMED	N,N,N‘,N‘-Tetramethylethaen-1,2-diamine
Tet	Tetracycline
ThT	Thioflavin T
TMB	3,3',5,5'-Tetramethylbenzidine
Tris	2-Amino-2-hydroxymethyl-propane-1,3-diol
U	Unit
V	Volt
V_H	Variable domain of the antibody's heavy chain
V_L	Variable domain of the antibody's light chain

8. List of figures

8. List of figures

9. List of tables

10. Literature

Abbas, A.K. (2007). Cellular and molecular immunology (Philadelphia: Saunders Elsevier).

Alzheimer, A. (1907). Über eine eigenartige Erkrankung der Hirnrinde. Allgemeine Zeitschrift für Psychiatrie und psychisch-gerichtliche Medizin.

Avril, A., Froude, J., Mathieu, J., Pelat, T., and Thullier, P. (2014). Isolation of Antibodies From Non-Human Primates for Clinical Use. Curr. Drug Discov. Technol. *11*, 20–27.

Bacskai, B.J., Kajdasz, S.T., McLellan, M.E., Games, D., Seubert, P., Schenk, D., and Hyman, B.T. (2002). Non-Fc-mediated mechanisms are involved in clearance of amyloid-beta in vivo by immunotherapy. J. Neurosci. Off. J. Soc. Neurosci. *22*, 7873–7878.

Ballard, C., Gauthier, S., Corbett, A., Brayne, C., Aarsland, D., and Jones, E. (2011). Alzheimer's disease. Lancet *377*, 1019–1031.

Barbas, C.F., Kang, A.S., Lerner, R.A., and Benkovic, S.J. (1991). Assembly of combinatorial antibody libraries on phage surfaces: the gene III site. Proc. Natl. Acad. Sci. U. S. A. *88*, 7978–7982.

Bard, F., Barbour, R., Cannon, C., Carretto, R., Fox, M., Games, D., Guido, T., Hoenow, K., Hu, K., Johnson-Wood, K., et al. (2003). Epitope and isotype specificities of antibodies to beta -amyloid peptide for protection against Alzheimer's disease-like neuropathology. Proc. Natl. Acad. Sci. U. S. A. *100*, 2023–2028.

Behring, E. von, and Kitasato, S. (1980). Ueber das Zustandekommen der Diphtherie-Immunität und der Tetanus-Immunität bei Thieren: aus dem Hygienischen Institut des Herrn Geheimerath Koch in Berlin; Behring Kitasato prize 1980 ([S.l.]).

Bereza, M. (2013). Assessment of structural diversity of ß-amyloid with genetically engineered antibody fragments @ DB Thüringen.

Biedler, J.L., Roffler-Tarlov, S., Schachner, M., and Freedman, L.S. (1978). Multiple neurotransmitter synthesis by human neuroblastoma cell lines and clones. Cancer Res. *38*, 3751–3757.

Bird, R.E., Hardman, K.D., Jacobson, J.W., Johnson, S., Kaufman, B.M., Lee, S.M., Lee, T., Pope, S.H., Riordan, G.S., and Whitlow, M. (1988). Single-chain antigen-binding proteins. Science *242*, 423–426.

Bitan, G., Fradinger, E.A., Spring, S.M., and Teplow, D.B. (2005). Neurotoxic protein oligomers--what you see is not always what you get. Amyloid Int. J. Exp. Clin. Investig. Off. J. Int. Soc. Amyloidosis *12*, 88–95.

Breitling, F., and Dübel, S. (1997). Rekombinante Antikörper (Spektrum Akademischer Verlag).

Breitling, F., Dübel, S., Seehaus, T., Klewinghaus, I., and Little, M. (1991). A surface expression vector for antibody screening. Gene *104*, 147–153.

Cattepoel, S., Hanenberg, M., Kulic, L., and Nitsch, R.M. (2011). Chronic Intranasal Treatment with an Anti-Aβ30-42 scFv Antibody Ameliorates Amyloid Pathology in a Transgenic Mouse Model of Alzheimer's Disease. PLoS ONE *6*, e18296.

10. Literature

Chamberlain, A.K., MacPhee, C.E., Zurdo, J., Morozova-Roche, L.A., Hill, H.A., Dobson, C.M., and Davis, J.J. (2000). Ultrastructural organization of amyloid fibrils by atomic force microscopy. Biophys. J. *79*, 3282–3293.

Chasteen, L., Ayriss, J., Pavlik, P., and Bradbury, A.R.M. (2006). Eliminating helper phage from phage display. Nucleic Acids Res. *34*, e145.

Chen, Y.-R., and Glabe, C.G. (2006). Distinct Early Folding and Aggregation Properties of Alzheimer Amyloid-β Peptides Aβ40 and Aβ42 STABLE TRIMER OR TETRAMER FORMATION BY Aβ42. J. Biol. Chem. *281*, 24414–24422.

Clackson, T., Hoogenboom, H.R., Griffiths, A.D., and Winter, G. (1991). Making antibody fragments using phage display libraries. Nature *352*, 624–628.

Cleary, J.P., Walsh, D.M., Hofmeister, J.J., Shankar, G.M., Kuskowski, M.A., Selkoe, D.J., and Ashe, K.H. (2005). Natural oligomers of the amyloid-beta protein specifically disrupt cognitive function. Nat. Neurosci. *8*, 79–84.

D'Herelle, F. (1917). On an invisible microbe antagonistic toward dysenteric bacilli: brief note by Mr. F. D'Herelle, presented by Mr. Roux. 1917. Res. Microbiol. *158*, 553–554.

Dahlgren, K.N. (2002). Oligomeric and Fibrillar Species of Amyloid-beta Peptides Differentially Affect Neuronal Viability. J. Biol. Chem. *277*, 32046–32053.

Dodart, J.-C., Bales, K.R., Gannon, K.S., Greene, S.J., DeMattos, R.B., Mathis, C., DeLong, C.A., Wu, S., Wu, X., Holtzman, D.M., et al. (2002). Immunization reverses memory deficits without reducing brain Abeta burden in Alzheimer's disease model. Nat. Neurosci. *5*, 452–457.

Dübel, S., Stoevesandt, O., Taussig, M.J., and Hust, M. (2010). Generating recombinant antibodies to the complete human proteome. Trends Biotechnol. *28*, 333–339.

Dumoulin, M., and Dobson, C.M. (2004). Probing the origins, diagnosis and treatment of amyloid diseases using antibodies. Biochimie *86*, 589–600.

Durocher, Y., Perret, S., and Kamen, A. (2002). High-level and high-throughput recombinant protein production by transient transfection of suspension-growing human 293-EBNA1 cells. Nucleic Acids Res. *30*, E9.

Edelman, G.M. (1973). Antibody Structure and Molecular Immunology. Science *180*, 830–840.

EL-Manzalawy, Y., Dobbs, D., and Honavar, V. (2008). PREDICTING FLEXIBLE LENGTH LINEAR B-CELL EPITOPES. Comput. Syst. Bioinforma. *7*, 121–132.

Englund, H., Sehlin, D., Johansson, A.-S., Nilsson, L.N.G., Gellerfors, P., Paulie, S., Lannfelt, L., and Pettersson, F.E. (2007). Sensitive ELISA detection of amyloid-β protofibrils in biological samples. J. Neurochem. *103*, 334–345.

Fändrich, M. (2007). On the structural definition of amyloid fibrils and other polypeptide aggregates. Cell. Mol. Life Sci. CMLS *64*, 2066–2078.

Fennell, B.J., McDonnell, B., Tam, A.S.P., Chang, L., Steven, J., Broadbent, I.D., Gao, H., Kieras, E., Alley, J., Luxenberg, D., et al. (2013). CDR-restricted engineering of native human scFvs creates highly stable and soluble bifunctional antibodies for subcutaneous delivery. mAbs *5*, 882–895.

Finder, V.H., and Glockshuber, R. (2007). Amyloid-beta aggregation. Neurodegener. Dis. *4*, 13–27.

Fitzpatrick, A.L., Kuller, L.H., Lopez, O.L., Kawas, C.H., and Jagust, W. (2005). Survival following dementia onset: Alzheimer's disease and vascular dementia. J. Neurol. Sci. *229-230*, 43–49.

Frenkel, D., Katz, O., and Solomon, B. (2000). Immunization against Alzheimer's ?-amyloid plaques via EFRH phage administration. Proc. Natl. Acad. Sci. U. S. A. *97*, 11455–11459.

Garzon-Rodriguez, W., Sepulveda-Becerra, M., Milton, S., and Glabe, C.G. (1997). Soluble Amyloid Aβ-(1–40) Exists as a Stable Dimer at Low Concentrations. J. Biol. Chem. *272*, 21037–21044.

Glabe, C.G., and Kayed, R. (2006). Common structure and toxic function of amyloid oligomers implies a common mechanism of pathogenesis. Neurology *66*, S74–78.

Glenner, G.G., and Wong, C.W. (1984). Alzheimer's disease: initial report of the purification and characterization of a novel cerebrovascular amyloid protein. Biochem. Biophys. Res. Commun. *120*, 885–890.

Goedert, M., Wischik, C.M., Crowther, R.A., Walker, J.E., and Klug, A. (1988). Cloning and sequencing of the cDNA encoding a core protein of the paired helical filament of Alzheimer disease: identification as the microtubule-associated protein tau. Proc. Natl. Acad. Sci. U. S. A. *85*, 4051–4055.

Goletz, S., Christensen, P.A., Kristensen, P., Blohm, D., Tomlinson, I., Winter, G., and Karsten, U. (2002). Selection of large diversities of antiidiotypic antibody fragments by phage display. J. Mol. Biol. *315*, 1087–1097.

Griffiths, A.D., Malmqvist, M., Marks, J.D., Bye, J.M., Embleton, M.J., McCafferty, J., Baier, M., Holliger, K.P., Gorick, B.D., and Hughes-Jones, N.C. (1993). Human anti-self antibodies with high specificity from phage display libraries. EMBO J. *12*, 725–734.

De Haard, H.J., van Neer, N., Reurs, A., Hufton, S.E., Roovers, R.C., Henderikx, P., de Bruïne, A.P., Arends, J.W., and Hoogenboom, H.R. (1999). A large non-immunized human Fab fragment phage library that permits rapid isolation and kinetic analysis of high affinity antibodies. J. Biol. Chem. *274*, 18218–18230.

Haass, C., and Selkoe, D.J. (2007). Soluble protein oligomers in neurodegeneration: lessons from the Alzheimer's amyloid β-peptide. Nat. Rev. Mol. Cell Biol. *8*, 101–112.

Habicht, G., Haupt, C., Friedrich, R.P., Hortschansky, P., Sachse, C., Meinhardt, J., Wieligmann, K., Gellermann, G.P., Brodhun, M., and Götz, J. (2007). Directed selection of a conformational antibody domain that prevents mature amyloid fibril formation by stabilizing Aβ protofibrils. Proc. Natl. Acad. Sci. *104*, 19232–19237.

Haigh, N.G., and Webster, R.E. (1998). The major coat protein of filamentous bacteriophage f1 specifically pairs in the bacterial cytoplasmic membrane. J. Mol. Biol. *279*, 19–29.

Hardy, J.A., and Higgins, G.A. (1992). Alzheimer's disease: the amyloid cascade hypothesis. Science *256*, 184–185.

Harper, J.D., and Lansbury, P.T., Jr (1997). Models of amyloid seeding in Alzheimer's disease and scrapie: mechanistic truths and physiological consequences of the time-dependent solubility of amyloid proteins. Annu. Rev. Biochem. *66*, 385–407.

Harper, J.D., Wong, S.S., Lieber, C.M., and Lansbury, P.T., Jr (1999). Assembly of A beta amyloid protofibrils: an in vitro model for a possible early event in Alzheimer's disease. Biochemistry (Mosc.) *38*, 8972–8980.

Hartley, D.M., Walsh, D.M., Ye, C.P., Diehl, T., Vasquez, S., Vassilev, P.M., Teplow, D.B., and Selkoe, D.J. (1999). Protofibrillar intermediates of amyloid beta-protein induce acute electrophysiological changes and progressive neurotoxicity in cortical neurons. J. Neurosci. Off. J. Soc. Neurosci. *19*, 8876–8884.

Hawkins, R.E., Russell, S.J., and Winter, G. (1992). Selection of phage antibodies by binding affinity. Mimicking affinity maturation. J. Mol. Biol. *226*, 889–896.

10. Literature

Hayashi, N., Welschof, M., Zewe, M., Braunagel, M., Dübel, S., Breitling, F., and Little, M. (1994). Simultaneous mutagenesis of antibody CDR regions by overlap extension and PCR. BioTechniques *17*, 310, 312, 314–315.

Henry, T.J., and Pratt, D. (1969). THE PROTEINS OF BACTERIOPHAGE M13. Proc. Natl. Acad. Sci. U. S. A. *62*, 800–807.

Hilbich, C., Kisters-Woike, B., Reed, J., Masters, C.L., and Beyreuther, K. (1992). Substitutions of hydrophobic amino acids reduce the amyloidogenicity of Alzheimer's disease beta A4 peptides. J. Mol. Biol. *228*, 460–473.

Hillen, H., Barghorn, S., Striebinger, A., Labkovsky, B., Müller, R., Nimmrich, V., Nolte, M.W., Perez-Cruz, C., van der Auwera, I., van Leuven, F., et al. (2010). Generation and therapeutic efficacy of highly oligomer-specific beta-amyloid antibodies. J. Neurosci. Off. J. Soc. Neurosci. *30*, 10369–10379.

Hoet, R.M., Cohen, E.H., Kent, R.B., Rookey, K., Schoonbroodt, S., Hogan, S., Rem, L., Frans, N., Daukandt, M., Pieters, H., et al. (2005). Generation of high-affinity human antibodies by combining donor-derived and synthetic complementarity-determining-region diversity. Nat. Biotechnol. *23*, 344–348.

Hoogenboom, H.R., and Winter, G. (1992). By-passing immunisation. Human antibodies from synthetic repertoires of germline VH gene segments rearranged in vitro. J. Mol. Biol. *227*, 381–388.

Hoogenboom, H.R., Griffiths, A.D., Johnson, K.S., Chiswell, D.J., Hudson, P., and Winter, G. (1991). Multi-subunit proteins on the surface of filamentous phage: methodologies for displaying antibody (Fab) heavy and light chains. Nucleic Acids Res. *19*, 4133–4137.

Hust, M., and Dübel, S. (2005). Phage display vectors for the in vitro generation of human antibody fragments. Methods Mol. Biol. Clifton NJ *295*, 71–96.

Hust, M., Maiss, E., Jacobsen, H.-J., and Reinard, T. (2002). The production of a genus-specific recombinant antibody (scFv) using a recombinant potyvirus protease. J. Virol. Methods *106*, 225–233.

Hust, M., Meyer, T., Voedisch, B., Rülker, T., Thie, H., El-Ghezal, A., Kirsch, M.I., Schütte, M., Helmsing, S., Meier, D., et al. (2011). A human scFv antibody generation pipeline for proteome research. J. Biotechnol. *152*, 159–170.

Huston, J.S., Levinson, D., Mudgett-Hunter, M., Tai, M.S., Novotny, J., Margolies, M.N., Ridge, R.J., Bruccoleri, R.E., Haber, E., and Crea, R. (1988). Protein engineering of antibody binding sites: recovery of specific activity in an anti-digoxin single-chain Fv analogue produced in Escherichia coli. Proc. Natl. Acad. Sci. U. S. A. *85*, 5879–5883.

Ida, N., Hartmann, T., Pantel, J., Schröder, J., Zerfass, R., Förstl, H., Sandbrink, R., Masters, C.L., and Beyreuther, K. (1996). Analysis of heterogeneous A4 peptides in human cerebrospinal fluid and blood by a newly developed sensitive Western blot assay. J. Biol. Chem. *271*, 22908–22914.

Jakob-Roetne, R., and Jacobsen, H. (2009). Alzheimer's disease: from pathology to therapeutic approaches. Angew. Chem. Int. Ed Engl. *48*, 3030–3059.

Jan, A., Gokce, O., Luthi-Carter, R., and Lashuel, H.A. (2008). The Ratio of Monomeric to Aggregated Forms of A?40 and A?42 Is an Important Determinant of Amyloid-? Aggregation, Fibrillogenesis, and Toxicity. J. Biol. Chem. *283*, 28176–28189.

Jan, A., Adolfsson, O., Allaman, I., Buccarello, A.-L., Magistretti, P.J., Pfeifer, A., Muhs, A., and Lashuel, H.A. (2010a). A 42 Neurotoxicity Is Mediated by Ongoing Nucleated Polymerization Process Rather than by Discrete A 42 Species. J. Biol. Chem. *286*, 8585–8596.

Jan, A., Hartley, D.M., and Lashuel, H.A. (2010b). Preparation and characterization of toxic Abeta aggregates for structural and functional studies in Alzheimer's disease research. Nat. Protoc. *5*, 1186–1209.

Jarrett, J.T., Berger, E.P., and Lansbury Jr, P.T. (1993). The carboxy terminus of the. beta. amyloid protein is critical for the seeding of amyloid formation: Implications for the pathogenesis of Alzheimer's disease. Biochemistry (Mosc.) *32*, 4693–4697.

Johnson-Wood, K., Lee, M., Motter, R., Hu, K., Gordon, G., Barbour, R., Khan, K., Gordon, M., Tan, H., Games, D., et al. (1997). Amyloid precursor protein processing and A?42 deposition in a transgenic mouse model of Alzheimer disease. Proc. Natl. Acad. Sci. U. S. A. *94*, 1550–1555.

Kang, M., Kim, S.Y., An, S.S.A., and Ju, Y.R. (2013). Characterizing affinity epitopes between prion protein and ?-amyloid using an epitope mapping immunoassay. Exp. Mol. Med. *45*, e34.

Kayed, R., Head, E., Thompson, J.L., McIntire, T.M., Milton, S.C., Cotman, C.W., and Glabe, C.G. (2003). Common structure of soluble amyloid oligomers implies common mechanism of pathogenesis. Science *300*, 486–489.

Kayed, R., Head, E., Sarsoza, F., Saing, T., Cotman, C.W., Necula, M., Margol, L., Wu, J., Breydo, L., Thompson, J.L., et al. (2007). Fibril specific, conformation dependent antibodies recognize a generic epitope common to amyloid fibrils and fibrillar oligomers that is absent in prefibrillar oligomers. Mol. Neurodegener. *2*, 18.

Klein, W.L. (2002). Aβ toxicity in Alzheimer's disease: globular oligomers (ADDLs) as new vaccine and drug targets. Neurochem. Int. *41*, 345–352.

Klunk, W.E., Jacob, R.F., and Mason, R.P. (1999). Quantifying amyloid beta-peptide (Abeta) aggregation using the Congo red-Abeta (CR-abeta) spectrophotometric assay. Anal. Biochem. *266*, 66–76.

Klunk, W.E., Engler, H., Nordberg, A., Wang, Y., Blomqvist, G., Holt, D.P., Bergström, M., Savitcheva, I., Huang, G., Estrada, S., et al. (2004). Imaging brain amyloid in Alzheimer's disease with Pittsburgh Compound-B. Ann. Neurol. *55*, 306–319.

Knappik, A., Ge, L., Honegger, A., Pack, P., Fischer, M., Wellnhofer, G., Hoess, A., Wölle, J., Plückthun, A., and Virnekäs, B. (2000). Fully synthetic human combinatorial antibody libraries (HuCAL) based on modular consensus frameworks and CDRs randomized with trinucleotides. J. Mol. Biol. *296*, 57–86.

Köhler, G., and Milstein, C. (1975). Continuous cultures of fused cells secreting antibody of predefined specificity. Nature *256*, 495–497.

Kosik, K.S., Joachim, C.L., and Selkoe, D.J. (1986). Microtubule-associated protein tau (tau) is a major antigenic component of paired helical filaments in Alzheimer disease. Proc. Natl. Acad. Sci. U. S. A. *83*, 4044–4048.

Laemmli, U.K. (1970). Cleavage of structural proteins during the assembly of the head of bacteriophage T4. Nature *227*, 680–685.

Lafaye, P., Achour, I., England, P., Duyckaerts, C., and Rougeon, F. (2009). Single-domain antibodies recognize selectively small oligomeric forms of amyloid beta, prevent Abeta-induced neurotoxicity and inhibit fibril formation. Mol. Immunol. *46*, 695–704.

Lambert, M.P., Barlow, A.K., Chromy, B.A., Edwards, C., Freed, R., Liosatos, M., Morgan, T.E., Rozovsky, I., Trommer, B., Viola, K.L., et al. (1998). Diffusible, nonfibrillar ligands derived from Abeta1-42 are potent central nervous system neurotoxins. Proc. Natl. Acad. Sci. U. S. A. *95*, 6448–6453.

10. Literature

Lashuel, H.A. (2005). Membrane permeabilization: a common mechanism in protein-misfolding diseases. Sci. Aging Knowl. Environ. SAGE KE *2005*, pe28.

Lashuel, H.A., Hartley, D., Petre, B.M., Walz, T., and Lansbury, P.T. (2002). Neurodegenerative disease: amyloid pores from pathogenic mutations. Nature *418*, 291–291.

Lashuel, H.A., Hartley, D.M., Petre, B.M., Wall, J.S., Simon, M.N., Walz, T., and Lansbury, P.T. (2003). Mixtures of Wild-type and a Pathogenic (E22G) Form of Aβ40 in Vitro Accumulate Protofibrils, Including Amyloid Pores. J. Mol. Biol. *332*, 795–808.

Lee, M., Bard, F., Johnson-Wood, K., Lee, C., Hu, K., Griffith, S.G., Black, R.S., Schenk, D., and Seubert, P. (2005). Aβ42 immunization in Alzheimer's disease generates Aβ N-terminal antibodies. Ann. Neurol. *58*, 430–435.

Legleiter, J., Czilli, D.L., Gitter, B., DeMattos, R.B., Holtzman, D.M., and Kowalewski, T. (2004). Effect of Different Anti-Aβ Antibodies on Aβ Fibrillogenesis as Assessed by Atomic Force Microscopy. J. Mol. Biol. *335*, 997–1006.

Lemere, C.A., Beierschmitt, A., Iglesias, M., Spooner, E.T., Bloom, J.K., Leverone, J.F., Zheng, J.B., Seabrook, T.J., Louard, D., Li, D., et al. (2004). Alzheimer's Disease A? Vaccine Reduces Central Nervous System A? Levels in a Non-Human Primate, the Caribbean Vervet. Am. J. Pathol. *165*, 283–297.

Lesné, S., Koh, M.T., Kotilinek, L., Kayed, R., Glabe, C.G., Yang, A., Gallagher, M., and Ashe, K.H. (2006). A specific amyloid-β protein assembly in the brain impairs memory. Nature *440*, 352–357.

LeVine, H., 3rd (1999). Quantification of beta-sheet amyloid fibril structures with thioflavin T. Methods Enzymol. *309*, 274–284.

Ling, X., Martins, R.N., Racchi, M., Craft, S., and Helmerhorst, E. (2002). Amyloid beta antagonizes insulin promoted secretion of the amyloid beta protein precursor. J. Alzheimers Dis. JAD *4*, 369–374.

Liu, R., Yuan, B., Emadi, S., Zameer, A., Schulz, P., McAllister, C., Lyubchenko, Y., Goud, G., and Sierks, M.R. (2004). Single Chain Variable Fragments against β-Amyloid (Aβ) Can Inhibit Aβ Aggregation and Prevent Aβ-Induced Neurotoxicity †. Biochemistry (Mosc.) *43*, 6959–6967.

Loo, D.T., Copani, A., Pike, C.J., Whittemore, E.R., Walencewicz, A.J., and Cotman, C.W. (1993). Apoptosis is induced by beta-amyloid in cultured central nervous system neurons. Proc. Natl. Acad. Sci. U. S. A. *90*, 7951–7955.

Mamikonyan, G., Necula, M., Mkrtichyan, M., Ghochikyan, A., Petrushina, I., Movsesyan, N., Mina, E., Kiyatkin, A., Glabe, C.G., Cribbs, D.H., et al. (2007). Anti-A beta 1-11 antibody binds to different beta-amyloid species, inhibits fibril formation, and disaggregates preformed fibrils but not the most toxic oligomers. J. Biol. Chem. *282*, 22376–22386.

Marks, J.D., Hoogenboom, H.R., Bonnert, T.P., McCafferty, J., Griffiths, A.D., and Winter, G. (1991). By-passing immunization. Human antibodies from V-gene libraries displayed on phage. J. Mol. Biol. *222*, 581–597.

Marvin, D.A. (1998). Filamentous phage structure, infection and assembly. Curr. Opin. Struct. Biol. *8*, 150–158.

Mason, R.P., Jacob, R.F., Walter, M.F., Mason, P.E., Avdulov, N.A., Chochina, S.V., Igbavboa, U., and Wood, W.G. (1999). Distribution and fluidizing action of soluble and aggregated amyloid beta-peptide in rat synaptic plasma membranes. J. Biol. Chem. *274*, 18801–18807.

Masters, C.L., Multhaup, G., Simms, G., Pottgiesser, J., Martins, R.N., and Beyreuther, K. (1985). Neuronal origin of a cerebral amyloid: neurofibrillary tangles of Alzheimer's disease contain the same protein as the amyloid of plaque cores and blood vessels. EMBO J. *4*, 2757–2763.

McCafferty, J., Griffiths, A.D., Winter, G., and Chiswell, D.J. (1990). Phage antibodies: filamentous phage displaying antibody variable domains. Nature *348*, 552–554.

McLaurin, J., Cecal, R., Kierstead, M.E., Tian, X., Phinney, A.L., Manea, M., French, J.E., Lambermon, M.H.L., Darabie, A.A., Brown, M.E., et al. (2002). Therapeutically effective antibodies against amyloid-beta peptide target amyloid-beta residues 4-10 and inhibit cytotoxicity and fibrillogenesis. Nat. Med. *8*, 1263–1269.

Meinhardt, J., Sachse, C., Hortschansky, P., Grigorieff, N., and Fändrich, M. (2009). Abeta(1-40) fibril polymorphism implies diverse interaction patterns in amyloid fibrils. J. Mol. Biol. *386*, 869–877.

Moreth, J., Mavoungou, C., and Schindowski, K. (2013). Passive anti-amyloid immunotherapy in Alzheimer's disease: What are the most promising targets? Immun. Ageing A *10*, 18.

Moutel, S., El Marjou, A., Vielemeyer, O., Nizak, C., Benaroch, P., Dübel, S., and Perez, F. (2009). A multi-Fc-species system for recombinant antibody production. BMC Biotechnol. *9*, 14.

Müller-Hill, B., and Beyreuther, K. (1989). Molecular biology of Alzheimer's disease. Annu. Rev. Biochem. *58*, 287–307.

Mullis, K., Faloona, F., Scharf, S., Saiki, R., Horn, G., and Erlich, H. (1992). Specific enzymatic amplification of DNA in vitro: the polymerase chain reaction. 1986. Biotechnol. Read. Mass *24*, 17–27.

Nieba, L., Honegger, A., Krebber, C., and Plückthun, A. (1997). Disrupting the hydrophobic patches at the antibody variable/constant domain interface: improved in vivo folding and physical characterization of an engineered scFv fragment. Protein Eng. *10*, 435–444.

Nisbet, R.M., Nigro, J., Breheney, K., Caine, J., Hattarki, M.K., and Nuttall, S.D. (2013). Central amyloid-β-specific single chain variable fragment ameliorates Aβ aggregation and neurotoxicity. Protein Eng. Des. Sel. PEDS *26*, 571–580.

Noormägi, A., Primar, K., Tõugu, V., and Palumaa, P. (2012). Interference of low-molecular substances with the thioflavin-T fluorescence assay of amyloid fibrils. J. Pept. Sci. *18*, 59–64.

O'Nuallain, B., and Wetzel, R. (2002). Conformational Abs recognizing a generic amyloid fibril epitope. Proc. Natl. Acad. Sci. *99*, 1485–1490.

Okada, T., Ikeda, K., Wakabayashi, M., Ogawa, M., and Matsuzaki, K. (2008). Formation of toxic Abeta(1-40) fibrils on GM1 ganglioside-containing membranes mimicking lipid rafts: polymorphisms in Abeta(1-40) fibrils. J. Mol. Biol. *382*, 1066–1074.

Pini, A., Viti, F., Santucci, A., Carnemolla, B., Zardi, L., Neri, P., and Neri, D. (1998). Design and use of a phage display library. Human antibodies with subnanomolar affinity against a marker of angiogenesis eluted from a two-dimensional gel. J. Biol. Chem. *273*, 21769–21776.

Ray, D.S., Bscheider, H.P., and Hofschneider, P.H. (1966). Replication of the single-stranded DNA of the male-specific bacteriophage M13. Isolation of intracellular forms of phage-specific DNA. J. Mol. Biol. *21*, 473–483.

10. Literature

Rhein, V., Baysang, G., Rao, S., Meier, F., Bonert, A., Müller-Spahn, F., and Eckert, A. (2009). Amyloid-beta leads to impaired cellular respiration, energy production and mitochondrial electron chain complex activities in human neuroblastoma cells. Cell. Mol. Neurobiol. *29*, 1063–1071.

Robert, R., Dolezal, O., Waddington, L., Hattarki, M.K., Cappai, R., Masters, C.L., Hudson, P.J., and Wark, K.L. (2009). Engineered antibody intervention strategies for Alzheimer's disease and related dementias by targeting amyloid and toxic oligomers. Protein Eng. Des. Sel. *22*, 199–208.

Roher, A.E., Chaney, M.O., Kuo, Y.-M., Webster, S.D., Stine, W.B., Haverkamp, L.J., Woods, A.S., Cotter, R.J., Tuohy, J.M., Krafft, G.A., et al. (1996). Morphology and Toxicity of Aβ-(1-42) Dimer Derived from Neuritic and Vascular Amyloid Deposits of Alzheimer's Disease. J. Biol. Chem. *271*, 20631–20635.

Rondot, S., Koch, J., Breitling, F., and Dübel, S. (2001). A helper phage to improve single-chain antibody presentation in phage display. Nat. Biotechnol. *19*, 75–78.

Ross, C.A., and Poirier, M.A. (2005). Opinion: What is the role of protein aggregation in neurodegeneration? Nat. Rev. Mol. Cell Biol. *6*, 891–898.

Rowe, C.C., and Villemagne, V.L. (2011). Brain amyloid imaging. J. Nucl. Med. Off. Publ. Soc. Nucl. Med. *52*, 1733–1740.

Rülker, T., Voß, L., Thullier, P., O' Brien, L.M., Pelat, T., Perkins, S.D., Langermann, C., Schirrmann, T., Dübel, S., Marschall, H.-J., et al. (2012). Isolation and characterisation of a human-like antibody fragment (scFv) that inactivates VEEV in vitro and in vivo. PloS One *7*, e37242.

Sambrook, J., and Russell, D.W. (2001). Molecular Cloning: A Laboratory Manual (CSHL Press).

Schmiedl, A., Breitling, F., Winter, C.H., Queitsch, I., and Dübel, S. (2000). Effects of unpaired cysteines on yield, solubility and activity of different recombinant antibody constructs expressed in E. coli. J. Immunol. Methods *242*, 101–114.

Schofield, D.J., Pope, A.R., Clementel, V., Buckell, J., Chapple, S.D., Clarke, K.F., Conquer, J.S., Crofts, A.M., Crowther, S.R., Dyson, M.R., et al. (2007). Application of phage display to high throughput antibody generation and characterization. Genome Biol. *8*, R254.

Schütte, M., Thullier, P., Pelat, T., Wezler, X., Rosenstock, P., Hinz, D., Kirsch, M.I., Hasenberg, M., Frank, R., Schirrmann, T., et al. (2009). Identification of a putative Crf splice variant and generation of recombinant antibodies for the specific detection of Aspergillus fumigatus. PloS One *4*, e6625.

Selkoe, D.J. (2008). Soluble oligomers of the amyloid β-protein impair synaptic plasticity and behavior. Behav. Brain Res. *192*, 106–113.

Selkoe, D.J., Abraham, C.R., Podlisny, M.B., and Duffy, L.K. (1986). Isolation of low-molecular-weight proteins from amyloid plaque fibers in Alzheimer's disease. J. Neurochem. *46*, 1820–1834.

Singh, H., Ansari, H.R., and Raghava, G.P.S. (2013). Improved method for linear B-cell epitope prediction using antigen's primary sequence. PloS One *8*, e62216.

Sinha, S., Anderson, J.P., Barbour, R., Basi, G.S., Caccavello, R., Davis, D., Doan, M., Dovey, H.F., Frigon, N., Hong, J., et al. (1999). Purification and cloning of amyloid precursor protein beta-secretase from human brain. Nature *402*, 537–540.

Smith, G.P. (1985). Filamentous fusion phage: novel expression vectors that display cloned antigens on the virion surface. Science *228*, 1315–1317.

Solomon, B., Koppel, R., Hanan, E., and Katzav, T. (1996). Monoclonal antibodies inhibit in vitro fibrillar aggregation of the Alzheimer beta-amyloid peptide. Proc. Natl. Acad. Sci. U. S. A. *93*, 452–455.

Solomon, B., Koppel, R., Frankel, D., and Hanan-Aharon, E. (1997). Disaggregation of Alzheimer beta-amyloid by site-directed mAb. Proc. Natl. Acad. Sci. U. S. A. *94*, 4109–4112.

Soltes, G., Hust, M., Ng, K.K.Y., Bansal, A., Field, J., Stewart, D.I.H., Dubel, S., Cha, S., and Wiersma, E.J. (2007). On The Influence Of Vector Design On Antibody Phage Display. J. Biotechnol. *127*, 626–637.

Thie, H., Schirrmann, T., Paschke, M., Dübel, S., and Hust, M. (2008). SRP and Sec pathway leader peptides for antibody phage display and antibody fragment production in E. coli. New Biotechnol. *25*, 49–54.

Tiller, T., Schuster, I., Deppe, D., Siegers, K., Strohner, R., Herrmann, T., Berenguer, M., Poujol, D., Stehle, J., Stark, Y., et al. (2013). A fully synthetic human Fab antibody library based on fixed VH/VL framework pairings with favorable biophysical properties. mAbs *5*, 445–470.

Tran, M.H., Yamada, K., and Nabeshima, T. (2002). Amyloid beta-peptide induces cholinergic dysfunction and cognitive deficits: a minireview. Peptides *23*, 1271–1283.

Vaughan, T.J., Williams, A.J., Pritchard, K., Osbourn, J.K., Pope, A.R., Earnshaw, J.C., McCafferty, J., Hodits, R.A., Wilton, J., and Johnson, K.S. (1996). Human antibodies with sub-nanomolar affinities isolated from a large non-immunized phage display library. Nat. Biotechnol. *14*, 309–314.

Vieira, J., and Messing, J. (1987). Production of single-stranded plasmid DNA. Methods Enzymol. *153*, 3–11.

Walsh, D.M., Lomakin, A., Benedek, G.B., Condron, M.M., and Teplow, D.B. (1997). Amyloid β-protein fibrillogenesis detection of a protofibrillar intermediate. J. Biol. Chem. *272*, 22364–22372.

Walsh, D.M., Hartley, D.M., Kusumoto, Y., Fezoui, Y., Condron, M.M., Lomakin, A., Benedek, G.B., Selkoe, D.J., and Teplow, D.B. (1999). Amyloid beta-protein fibrillogenesis. Structure and biological activity of protofibrillar intermediates. J. Biol. Chem. *274*, 25945–25952.

Walsh, D.M., Klyubin, I., Fadeeva, J.V., Cullen, W.K., Anwyl, R., Wolfe, M.S., Rowan, M.J., and Selkoe, D.J. (2002). Naturally secreted oligomers of amyloid beta protein potently inhibit hippocampal long-term potentiation in vivo. Nature *416*, 535–539.

Wang, X., Zhang, J., Wang, Y., Feng, Y., Zhang, X., Sun, X., Li, J., Du, X., Lambert, M.P., Yang, S., et al. (2009). Conformation-dependent single-chain variable fragment antibodies specifically recognize beta-amyloid oligomers. FEBS Lett. *583*, 579–584.

Wu, T.T., and Kabat, E.A. (1970). An analysis of the sequences of the variable regions of Bence Jones proteins and myeloma light chains and their implications for antibody complementarity. J. Exp. Med. *132*, 211–250.

Yamada, K., Yabuki, C., Seubert, P., Schenk, D., Hori, Y., Ohtsuki, S., Terasaki, T., Hashimoto, T., and Iwatsubo, T. (2009). Aβ Immunotherapy: Intracerebral Sequestration of Aβ by an Anti-Aβ Monoclonal Antibody 266 with High Affinity to Soluble Aβ. J. Neurosci. *29*, 11393–11398.

Yu, Y.-P., Lei, P., Hu, J., Wu, W.-H., Zhao, Y.-F., and Li, Y.-M. (2010). Copper-induced cytotoxicity: reactive oxygen species or islet amyloid polypeptide oligomer formation. Chem. Commun. *46*, 6909–6911.

10. Literature

Zameer, A., Kasturirangan, S., Emadi, S., Nimmagadda, S.V., and Sierks, M.R. (2008). Anti-oligomeric Aβ Single-chain Variable Domain Antibody Blocks Aβ-induced Toxicity Against Human Neuroblastoma Cells. J. Mol. Biol. *384*, 917–928.

Zheng, H., and Koo, E.H. (2006). The amyloid precursor protein: beyond amyloid. Mol. Neurodegener. *1*, 5.

Zovo, K., Helk, E., Karafin, A., Tõugu, V., and Palumaa, P. (2010). Label-Free High-Throughput Screening Assay for Inhibitors of Alzheimer's Amyloid-β Peptide Aggregation Based on MALDI MS. Anal. Chem. *82*, 8558–8565.

A. Appendix

PaD97-D6

M

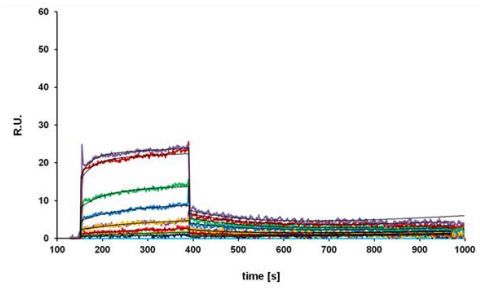

PF

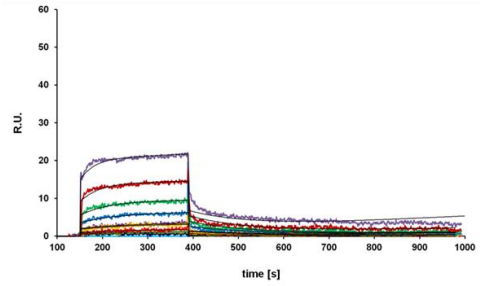

F

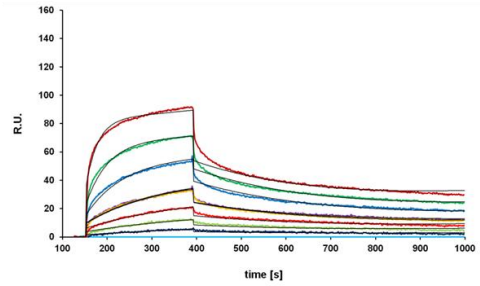

PaD172-F12

M

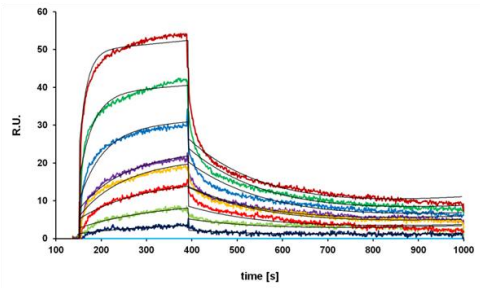

PF

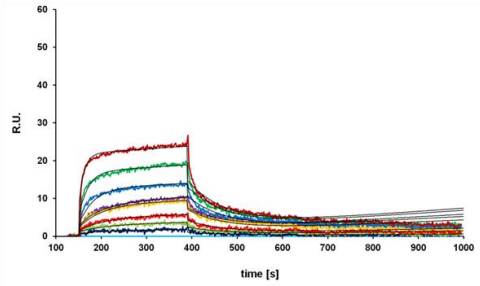

F

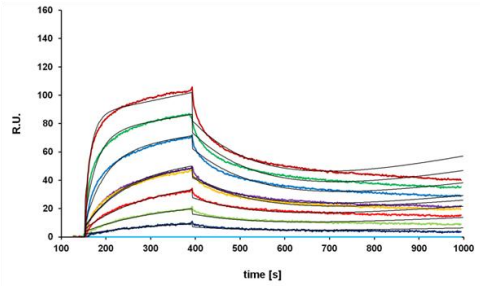

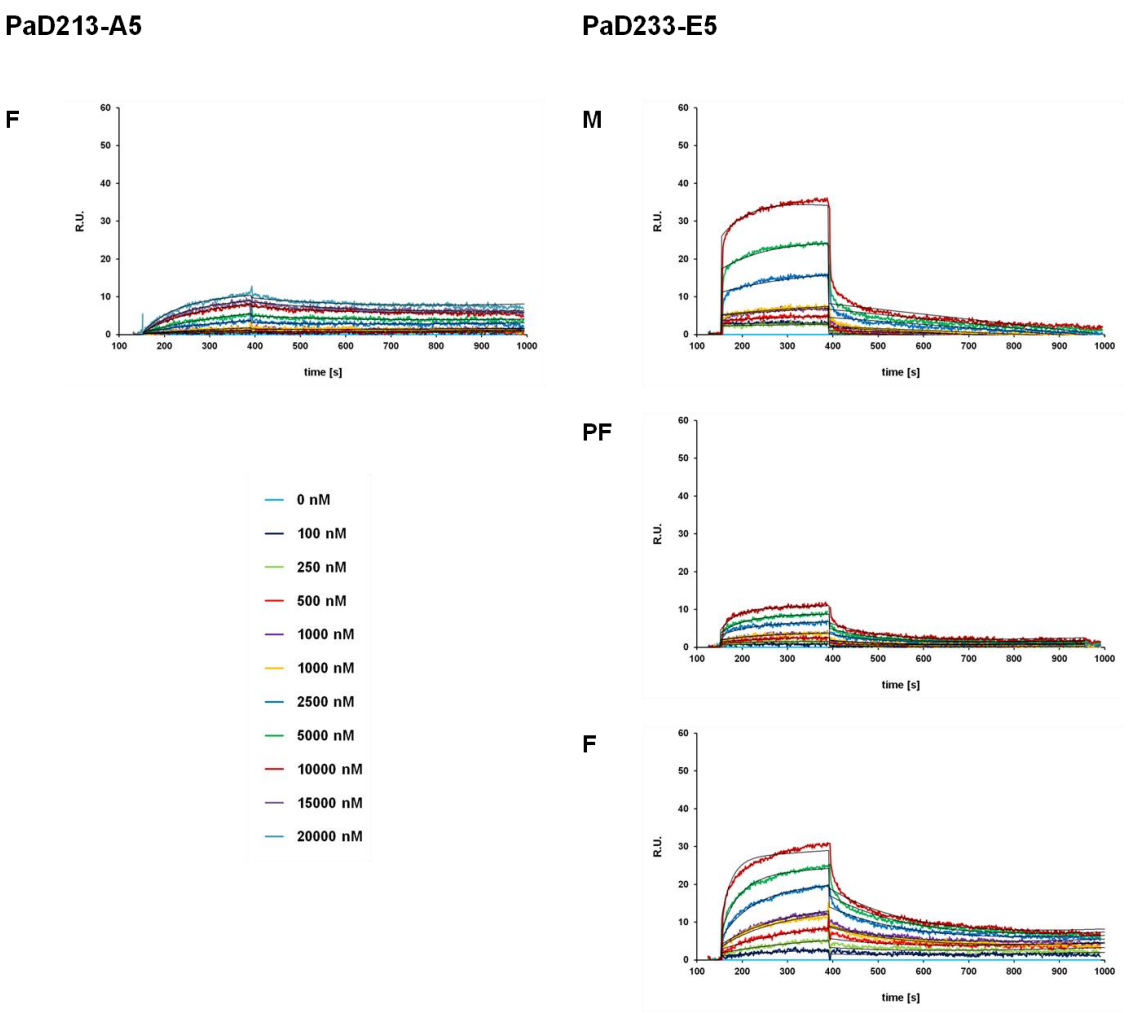

figure A.1: **SPR measurements on various Aβ42 aggregates**
measurements on **(M)** Aβ42 monomers, **(PF)** Aβ42 protofibrils and **(F)** Aβ42 fibrils for PaD97-D6, PaD172-F12 and PaD233-E5, PaD213-A5 only bound to Aβ42 fibrils

Acknowledgments

Many people contributed to the success of this dissertation and I would like to express my gratitude to each and every one of them.

Most of all I want to thank my supervisor **Prof. Stefan Dübel** for giving me the opportunity to work in his group on such a challenging project. He always had time to discuss problems and provided scientific guidance every day.

I kindly thank **PD Dr. Florian Bittner** for being my second examiner on this work.

I want to thank **Prof. Hilal Lashuel** for providing me the opportunity to conduct various experiments in his laboratory in Lausanne.

I thank **PD Dr. Michael Hust** for chairing the defense committee and hosting a weekly "think tank" with me and **Dr. André Frenzel**. André's contribution to this work cannot be stressed enough, not only for the final proofreading but mostly for three years of avid debates and the discussion of experimental strategies.

Everyone in the department of biotechnology contributed to me feeling comfortable and enjoying every day at work. You people made even the toughest day feel like leisure.

My biggest gratitude goes to my **friends and family**, especially to my parents, for their support, their love and caring, and the exquisite culinary provision.

Finally, I thank **Miriam**. You are the single most important person in this world to me and you cannot imagine how significant your contribution to this work was.